



**Savannah River
National Laboratory®**

A U.S. DEPARTMENT OF ENERGY NATIONAL LAB • SAVANNAH RIVER SITE • AIKEN, SC • USA

Design and Materials of Reference Electrodes for Radioactive Waste Tank Service – A Literature Review

K.S. Sykes, J. Jiang, and B. J. Wiersma, SRNL

S. Chawla, N. Sridhar, K. Evans, and J. A. Beavers, DNV

November 2024

SRNL-STI-2024-00539, Revision 0

DISCLAIMER

This work was prepared under an agreement with and funded by the U.S. Government. Neither the U.S. Government or its employees, nor any of its contractors, subcontractors or their employees, makes any express or implied:

- warranty or assumes any legal liability for the accuracy, completeness, or for the use or results of such use of any information, product, or process disclosed; or
- representation that such use or results of such use would not infringe privately owned rights; or
- endorsement or recommendation of any specifically identified commercial product, process, or service.

Any views and opinions of authors expressed in this work do not necessarily state or reflect those of the United States Government, or its contractors, or subcontractors.

Printed in the United States of America

**Prepared for
U.S. Department of Energy**

Keywords: Corrosion, Waste Tank Integrity, Corrosion Monitoring

Retention: Permanent

Tracking Number: 10560

Design and Materials of Reference Electrodes for Radioactive Waste Tank Service – A Literature Review

K. S. Sykes, J. Jiang, and B. J. Wiersma
SRNL

S. Chawla, N. Sridhar, K. Evans, and J.
A. Beavers

DNV

November 2024



Savannah River National Laboratory is operated by Battelle Savannah River Alliance for the U.S. Department of Energy under Contract No. 89303321CEM000080

Reviews and Approvals

AUTHORS:

B. J. Wiersma, SRNL/Advisory Engineer Date
Materials Science and Disposition

S. Chawla, DNV /Principal Engineer Date
Electrochemistry and Alternative Energy

TECHNICAL REVIEWERS:

P.K. Shukla, SRNL/Fellow Engineer Date
Materials Science and Disposition

APPROVAL:

J. Manna, SRNL/Director Date
Materials Technology & Energy Sciences Division

Acknowledgements

The authors acknowledge the U.S. Department of Energy-Environmental Management for the funding and support to conduct this research. The development of more robust reference electrodes for in-situ monitoring of tank corrosion is under the umbrella of a program that was initiated as part of the “R&D Roadmap for Hanford Tank Waste Mission Acceleration” (NNLEMS-2022-00005). The title of the awarded program within the roadmap is, “Integrity Monitoring and Assessment, Prediction, Repair, and Corrosion Control of the Hanford Storage Tanks” (Award #277993). The Principal Investigator for the program is Dr. P.K. Shukla of the Savannah River National Laboratory.

The new reference electrodes will ultimately benefit the Hanford waste tank farm facility. K.D. Boomer of the Chief Technology Office (CTO), Washington River Protection Solutions (WRPS) provided a letter of support for this investigation. J. S. Page, Tank and Pipeline Integrity (TAPI), WRPS, has provided useful reference documents for this review.

Executive Summary

The Hanford site stores approximately 55 million gallons of radioactive and chemically hazardous wastes from the production of weapons materials. The wastes are stored in 177 underground, carbon steel storage tanks, 149 of these are single shell tanks (SSTs) and 28 of these are double shell tanks (DSTs). The DSTs provide critical retrieval and interim storage before the waste is vitrified in the Waste Treatment and Isolation Plant (WTP). The DSTs have been in service for 38 to 56 years and current plans indicate that WTP operations will be completed in 2075. Thus, the tanks will need to remain in service far beyond the initial 40-year life expectancy. For life extension of the tanks, effective corrosion control practices must remain in force. This effort includes direct measurements of the extent of corrosion (e.g., ultrasonic measurements and corrosion coupons) and electrochemical processes (e.g., linear polarization measurements).

Tank corrosion and stress corrosion cracking (SCC) may also be monitored by the use of electrochemical techniques such as measurement of the open circuit potential (OCP) of the tank. Attempts to measure the OCP in waste tanks have been made at both Hanford and SRS. A reference electrode is typically utilized for these measurements. Failures of the reference electrodes in the chemically and radiolytically harsh environments in the tanks have occurred after relatively short term exposures, encumbering long-term surveillance efforts. Therefore, DOE-EM has undertaken a research program to develop reference materials that are capable of surviving the waste tank environment for longer periods of time.

The first phase of this program was to perform a literature review. The purposes of the literature review were two-fold. First, summarize the performance of reference electrodes in both field applications and laboratory testing. From this summary, the types of commercial electrodes that have been utilized, the environments to which they have been exposed, the durability of the electrodes, and failure mechanisms could be categorized, such that weaknesses in materials of construction and electrode design could be defined. Second, identify and recommend materials of construction and electrode designs that will overcome these weaknesses, such that a robust reference electrode is available to provide accurate potential measurements for an extended period of time.

The literature review was organized in the following manner:

Section 1: A discussion of the key corrosion information and performance characteristics that may be gathered from reference electrode data is presented.

Section 2: A summary of the performance of commercial reference electrodes that have been deployed in waste tanks at both Hanford and the Savannah River Site is presented. Additionally, a summary of laboratory studies that investigated the failure mechanisms of the electrodes in the waste environments is discussed.

Section 3: Reference electrodes are made from a variety of materials for a multitude of applications. The literature review highlighted and recommended materials that may survive the harsh chemical and and radioactive environment of the Hanford waste tanks.

Section 4: Reference electrode design was another factor in the failure of commercial electrodes in the waste tanks. The literature presents several alternative designs that will be considered for the development of a new robust reference electrode.

Section 5: Once the materials and design for the reference electrode have been selected and a prototype reference electrode fabricated, a series of tests are necessary to verify functionality. Testing that has been utilized to investigate functionality of commercial reference electrodes were reviewed. Similar tests will be employed for the recommended reference electrode.

This literature review provides the following key observations about the utilization and testing of reference electrodes:

- Measurement of the OCP provides a fundamental basis for predicting long-term performance of a waste tank. This approach provides a conservative estimate of the occurrence of failure modes such as pitting corrosion and SCC.
- Key characteristics of an effective reference electrode system include: lack of sensitivity to redox species, lack of sensitivity to pH, non-polarizability, resistance to chemical species in the waste, low impedance, electrolyte communication, chemical and radiation resistance of the electrode body, and mechanical integrity.
- Long-term (~3 years) testing of commercial Ag/AgCl under laboratory conditions show that the degradation/failure modes could be broadly classified into two types: (1) monotonic positive drift from the initial potential, and (2) sharp drop to negative potentials after a period of relative stability. The degradation was attributable to diffusive intermixing of the internal fills of the Ag/AgCl reference electrodes with the external simulant solutions over time through the porous frit junctions. This process leads to extensive KCl depletion and contamination of the fills, causing loss of potential stability.
- The potential drift trends were correlated to Cl⁻ activity changes in the fill and the effects of various contaminant species originating from the waste simulants.
- Long-term studies on single junction (SJ) Ag/AgCl reference electrodes in actual supernatant waste samples drawn from various DSTs also indicated that degradation of electrodes was found to be primarily due to the intrusion of aggressive chemicals causing clogging, physical and chemical degradation of AgCl, and alteration of the internal electrolyte. Radiation had less impact on electrode degradation compared to the chemicals, though radiolytic species such as H₂O₂ and HNO₃ could possibly have contributed to Ag wire degradation.
- Reference electrodes have been utilized at both Hanford and SRS in the past to make instantaneous measurement and for long term monitoring of the corrosion behavior of tanks. However, reference electrode failures have typically occurred within 2-3 years of installation. Trends in the potential drift that were indicative of failure an electrode during laboratory tests correlate with those observed in the field.
- Electrochemical noise systems, another electrochemical technique, were also deployed in Hanford waste tanks to monitor for localized corrosion and SCC. Although, the technique had modest success, the utilization of the system was discontinued due to many issues related to interpretation of noise signals and interference from a variety of ambient electrical noise.

This literature review provides the following recommendations on materials, design and testing of future reference electrodes:

- Alternate materials of construction for the internal fill of the reference electrode include solid state Ag/AgCl carbon nanotube (CNT) thread reference electrode or a solid state reference electrode using CNT.

- Alternate materials of construction for the reference electrode frit include ion-conducting composite, porous polymer frits, and Teflon frits.
- Alternate materials of construction for the body of the electrode include polymer composites doped with sizeable amounts of high atomic number (high-Z) materials, epoxy resins, non-oxide and oxide ceramics, and carbides of transition metals.
- Additive manufacturing can use several different materials of interest for the development of the reference electrode such as ceramics, metals, and thermoplastics. It can potentially reduce the cost because it can consolidate multiple parts into one and minimize material usage by building objects up rather than cutting, molding, and combining materials.
- Various type of alternative design concepts for reference electrodes have been discussed in the literature to overcome the limitations of traditional reference electrodes. These can be broadly classified into the following categories: reference electrodes with extended diffusion lengths, reference electrodes with improved liquid junction designs, reference electrodes with flowless junction designs, ionic liquid reference electrodes, solid-contact reference electrodes, and Field Effect Transistor (FET) based reference electrodes.
- Reference electrode design development should focus on increasing the lifespan of reference electrodes by increasing the diffusion length of the internal and frit sections. Additive manufacturing may allow more flexibility and reproducibility to accomplish this objective.
- Testing protocols for the accuracy and functionality of the reference electrodes were presented. Electrochemical Impedance Spectroscopy (EIS) has been utilized in previous laboratory studies and may provide a baseline for comparison between the commercial electrodes and the newly developed electrodes.

Table of Contents

1.0 Introduction	1
1.1 Electrochemical Potential and Reference Electrodes	3
1.2 Characteristics of a Reference Electrode System	4
1.2.1 Sensitivity to Redox Species	5
1.2.2 Sensitivity to pH	6
1.2.3 Non-Polarizability	6
1.2.4 Resistance to Other Chemical Species	7
1.2.5 Low Impedance	7
1.2.6 Electrolytic Communication	8
1.2.7 Chemical and Radiation Resistance of Electrode Body	8
1.2.8 Mechanical Integrity	8
2.0 Reference Electrode Performance in DOE-Complex Waste Tanks	8
2.1 Electrode Performance in Waste Tanks in the DOE Complex	9
2.1.1 Early Reference Electrodes at SRS and Hanford	9
2.1.2 Electrochemical Noise Probe at Hanford	14
2.1.3 Multi-Probe Corrosion Monitoring System at Hanford	15
2.1.4 Retractable Corrosion Monitoring Probe System at Hanford	18
2.2 Testing in Simulants at DNV	24
2.3 Testing in Actual Wastes at 222-S	32
3.0 Chemically and Radiation Resistant Materials	37
3.1 Degradation of Ag/AgCl Reference Electrodes	37
3.2 Internal Reference Electrode Materials	38
3.3 Irradiation effects on Ag/AgCl reference electrodes and tank composition	41
3.4 Irradiation penetration factor and radiation shielding	43
3.5 Outer Cover Reference Electrode Materials	44
3.5.1 Irradiation Resistant Materials	44
3.5.2 Alkaline resistant materials	46
3.6 Additive Manufacturing	47
4.0 Design Features	48
4.1 Reference Electrodes with Extended Diffusion Lengths	50
4.2 Reference Electrodes with Improved Liquid Junction Designs	52
4.3 Ionic Liquid Reference Electrodes	56
4.4 Reference Electrodes with Flowless Junction Designs	57

4.5 Solid-Contact Reference Electrodes	59
4.5.1 Electrodes with Solid Fills.....	59
4.5.2 Miniature Screen-Printed Reference Electrodes.....	61
4.5.3 Perovskite-Based Electrodes	62
4.6 Field Effect Transistor (FET) Based Reference Electrodes.....	63
5.0 Verification Protocols	64
5.1 Half-cell Potential Verification	65
5.1.1 Master Reference Electrodes for Verification	65
5.1.2 Quinhydrone Electrode for Verification	65
5.2 Electrochemical Impedance Use for Functional Verification.....	66
5.2.1 High Frequency (HF) Impedance Response	66
5.2.2 Low Frequency (LF) Impedance Response.....	68
6.0 Summary	69

List of Tables

Table 1-1. Criteria for reference electrode performance.	5
Table 2-1. Composition, Temperature and Potential Data for SRS Tanks in the 1970s.....	10
Table 2-2. Composition, Temperature and Potential Data for SRS Tanks in the 1980s ¹²	11
Table 2-3. Description of Reference Electrodes Utilized for MPCMS. ¹⁷	16
Table 2-4. Average life span of reference electrodes attached to an MPCMS	18
Table 2-5. Status of Reference Electrodes in MPCMS Probes in 2019.	18
Table 2-6. Average life span of reference electrodes attached to an RCMP.....	23
Table 2-7. Performance of Reference Electrodes in RCMP.....	24
Table 2-8. Calculated pHs, test temperatures, and some compositional features of the supernatant liquid simulants tested in the DNV reference electrodes studies.....	25
Table 2-9. Main features of the single junction Ag/AgCl reference electrodes tested in DST wastes.	33
Table 3-1. List of radionuclides in tank wastes	42
Table 3-2. Comparison of penetrating power, ionizing power, and shielding of α and β particles, and γ rays.....	43

List of Figures

Figure 1-1. Schematic illustration of conditions for the onset of localized corrosion and SCC and their use in tank integrity prediction.	2
Figure 1-2. Schematic illustration of the change in corrosion potential (OCP) versus time	2
Figure 1-3. A simple schematic of an electrode potential measurement at a metal (M) using a reference electrode (R).	4
Figure 1-4. Effect of ferrous/ferric redox couple at different dilutions on the measured potential on Pt at room temperature	6
Figure 2-1. Reference electrode results in an SRS tank ¹²	11
Figure 2-2. Schematic of PNL Probe ca. 1989. ¹³	13
Figure 2-3. OCP measurements of A537 coupon for probe in Tank AN-107, March 1988. ¹³	13
Figure 2-4. OCP measurements of A537 coupon for probe in Tank AN-107, September 1990. ¹³	14
Figure 2-5. (a) Tank-top Terminal Box, and (b) Reference electrode utilized for MPCMS. ¹⁷	16
Figure 2-6. 241-AN-102 MPCMS Average Monthly Tank and Supernate Tank Material Electrode Potentials from May 2008 to January 2012. ¹⁸	17
Figure 2-7. Photograph of a VLSJ Ag/AgCl reference electrode type that is currently used in Hanford DSTs (manufactured by Van London Co.). ²¹	19
Figure 2-8. Schematic of the internal design of the VLSJ Ag/AgCl electrode currently used in Hanford DST corrosion probes. ²¹	20
Figure 2-9. Four VLSJ Ag/AgCl reference electrodes mounted in RCMP probe head (top) and installation via riser in Tank 241-AP-106 (bottom).	20
Figure 2-10. Corrosion potential data collected from RCMP installed in Tank AW-105 from September 2022 to March 2024 ¹⁷	21
Figure 2-11. Corrosion Potential data collected from RCMP installed in Tank AP-102 from September 2020 to March 2024 ¹⁷	22
Figure 2-12. Corrosion potential data collected from RCMP installed in Tank AW-105 from August 2013 to September 2020 ¹⁷	23
Figure 2-13. Left: Photograph of VLSJ Ag/AgCl reference electrode with compression fitting and wire connection tested at DNV (Ruler scale in cm and inches). Right: Photograph of a PFA test vessel lid showing various Ag/AgCl reference electrodes and tank steel electrodes, prior to insertion in a test vessel for long-term performance testing in a waste simulant.	25
Figure 2-14. Photograph of a DNV test setup for long-term reference electrode study in various DST waste simulants ²²	26
Figure 2-15. Potential trends observed in DNV long-term studies of continuously immersed and retracted VLSJ reference electrodes in various DST supernatant liquid waste simulants. ²³	27
Figure 2-16. Left: High-frequency impedance, nearest 0° phase shift, of VLSJ Ag/AgCl electrodes as a function of time in various DST supernatant liquid waste simulants. Right: Corresponding potential trends of the electrodes over the same exposure period. ¹⁰	29
Figure 2-17. Concentrations of selected analytes measured in the fills of SJ Ag/AgCl electrodes after ~1064 days of immersion in various waste simulants, compared to an Exemplar.	29
Figure 2-18. Left: Photographs of fill samples extracted from an Exemplar VLSJ Ag/AgCl electrode and the AW-101 electrode (after ~1064 days of immersion in waste simulant). Right: FTIR spectra from the two electrode fills.	30
Figure 2-19. SEM secondary electron images of wire elements of SJ Ag/AgCl electrodes; clockwise from top left: Exemplar, AY-101 (2018), SY-103, and AN-102.	31

Figure 2-20. Phase angle (top) and magnitude of impedance (bottom) obtained from EIS of VLSJ Ag/AgCl electrodes after long-term exposures in AY-101 and AW-101 waste simulants, compared to an Exemplar tested in 4M KCl.31

Figure 2-21. Potential change of SJ Ag/AgCl reference electrode in response to incremental intentional contamination of fill solution with AY-101 (2019) waste simulant at room temperature.32

Figure 2-22. Potentials of Ag/AgCl Reference electrodes from Manufacturers (a) A, (b) B, and (c) C collected over different durations in various tank waste samples.34

Figure 2-23. Time-evolution of EIS spectra of electrode from Manufacturer A exposed to Tank AN-106 supernatant waste sample at 35°C.35

Figure 2-24. Left: Radiographs and XMT cross sections of Manufacturer A electrodes after testing in Tank AW-101 supernatant waste. Right: Radiographs of an exemplar electrode from Manufacturer A and an electrode exposed in Tank AN-106 supernatant waste sample at 35°C for 744 days.36

Figure 3-1. Cyclic Voltammetry curves for Ag/AgCl reference electrode over 800 scans in ferrocene (left), FCN reference electrode in ferrocene after 2 weeks of vigorous use (right).³³ ..40

Figure 3-2. The correlation of the stable time with the thickness of the AgCl film. A)5, B)20, C),50, D)100. *The numbers indicate the amount of square wave cycles to thicken the film.³³ ..41

Figure 4-1. Commonly used reference electrode junction designs⁵⁷49

Figure 4-2. Influence of time and the filling solution length on the stability of a reference electrodes OCP.⁶⁰51

Figure 4-3. Reference electrodes design concepts based on long, serpentine fill channels produced by 3D printing and CNC machining (from Duffy et al.⁶⁰).51

Figure 4-4. Experimental results showing change in percent over time with different lengths (left). Change in the OCP over time for the glass tube RE (right).⁶⁰52

Figure 4-5. Left: Operating principle of valve-actuator reference electrode; Middle: Valve-actuator design using shape memory alloy wire; Right: Conceptual design of the valve-actuator integrated reference and pH electrode. From Higuchi et al.⁶³53

Figure 4-6. Structure of microfabricated liquid-junction Ag/AgCl reference electrode developed by Suzuki et al.⁵⁵56

Figure 4-7. Photograph of a commercially available Reflex Ag/AgCl reference electrode.58

Figure 4-8. Left: Schematics of reference electrodes containing solidified KCl fill. Right: Photographs of electrodes prepared using Design (a). From Vonau et al.⁸⁰60

Figure 4-9. Some examples of screen-printed solid-state Ag/AgCl reference electrode configurations developed by various researchers. See Sophocleous⁸⁷ for details and cross-references.61

Figure 4-10. Cyclic voltammograms of a $\text{Na}_{0.9}\text{Mo}_6\text{O}_{17}$ (S 3) and $\text{Li}_x\text{Mo}_{0.95}\text{W}_{0.05}\text{O}_3$ (S 1) in comparison to Pt in 0.1 M FeCl_2 (50 mV/s). From Gabel et al.⁸⁹62

Figure 4-11. Potential of the solid state LLTO reference electrode as a function of time in buffer solutions of different pH at room temperature; and stabilized potentials of two LLTO electrodes as a function of pH. From Lorant et al.⁹⁰63

Figure 4-12. Schematic a chip with and ISFET and REFET. From Comte and Janata⁹¹.....64

Figure 5-1. Results from 2018 study involving long-term exposure of Van London reference electrodes to various tank waste simulants: potentials vs. time (lower plot) and HF impedance vs. time (upper plot).⁹⁴67

Figure 5-2. Impedance spectrum obtained on exemplar Van London reference electrode in 4 M KCl.68

Figure 5-3. Long-term exposure of Van London reference electrode in AW-101 simulant at 35°C: Potential vs. time (left) and impedance spectrum of electrode after 529 days of exposure (right).⁹⁵69

List of Abbreviations

Ag/AgCl	Silver-Silver Chloride
DJE	Double Junction Electrode
DNV	Det Norske Veritas
DOE	Department of Energy
DST	Double Shell Tank
EIS	Electrochemical Impedance Spectroscopy
EM	Environmental Management
EN	Electrochemical Noise
MPCMS	Multi-Probe Corrosion Monitoring System
OCP	Open Circuit Potential
RCMP	Retractable Corrosion Monitoring Probe
SCC	Stress Corrosion Cracking
SCE	Saturated Calomel Electrode
SJE	Single Junction Electrode
SRNL	Savannah River National Laboratory

1.0 Introduction

The Hanford site stores approximately 55 million gallons of radioactive and chemically hazardous wastes from the production of weapons materials. The wastes are stored in 177 underground, carbon steel storage tanks, 149 of these are single shell tanks (SSTs) and 28 of these are double shell tanks (DSTs)¹. The DSTs provide critical retrieval and interim storage before the waste is vitrified in the Waste Treatment and Isolation Plant (WTP). The DSTs have been in service for 38 to 56 years and current plans indicate that WTP operations will be completed in 2075². Thus, the tanks will need to remain in service far beyond the initial 40-year life expectancy. For life extension of the tanks, effective corrosion control practices must remain in force¹.

DOE Order 435.1-1 contains the following corrosion control requirements³:

- Identify corrosion, fatigue and other critical degradation modes.
- Adjust the chemistry of tank waste and implement other necessary corrosion protective measures.
- Identify additional controls necessary to maintain an acceptable operating envelope.

Corrosion control of the waste chemistry in the DSTs relies on ensuring that there is sufficient concentration of chemical species to inhibit the aggressive species that are present. Until the late 1990s corrosion control was accomplished by waste modeling, waste sampling, and corrosion testing in laboratories with tank waste or simulants. However, assumptions regarding how representative the waste samples are result in uncertainties as to the degree of corrosion that may be occurring. The samples also provide a “lagging” indicator as to when corrosion of the tank may have initiated.

An alternative approach to assessing tank corrosion and SCC is the use of electrochemical techniques. Attempts have been made to monitor tank corrosion and SCC using an electrochemical noise technique⁴ but these have not been successful due to many issues related to interpretation of noise signals and interference from a variety of ambient electrical noise. A simpler and more robust approach is to monitor the corrosion potential (E_{corr}) of the tank. The fundamental basis for predicting long-term performance using the tank E_{corr} (also called Open-circuit Potential, OCP) is illustrated schematically in Figure 1-1. The onset of localized corrosion or SCC occurs when the OCP exceeds the repassivation potential for localized corrosion (E_{rp}) or the critical cracking potential for SCC (CCP), respectively, in the same tank waste. This approach ignores the gestation time for initiation and stable growth of localized corrosion or SCC and thus is a conservative estimate for the occurrence of these failure modes. The OCP, E_{rp} , and CCP are measured using laboratory tests in tank waste simulants or real wastes extracted from the tanks. However, the OCP can also be measured directly in the tank. The measurement of OCP in the tank is an attractive method to monitor tank

¹ C. L. Girardot, RPP-7574, Rev. 8, “Double-Shell Tank Integrity Program Plan”, August 10, 2021.

² Parsons, *Final Report: Waste Treatment and Immobilization High Level Waste Treatment Analysis of Alternatives*. Richland: Office of River Protection, 2023.

³ DOE Order 435.1.1

⁴ G. L. Edgemon, *Electrochemical Noise Based Corrosion Monitoring: Hanford Site Program Status*, Corrosion/2005, AMPP, 2005, Paper 05584.

corrosion and SCC integrity because it is less subject to interference from ambient electronic noise and the measurement system is simpler.

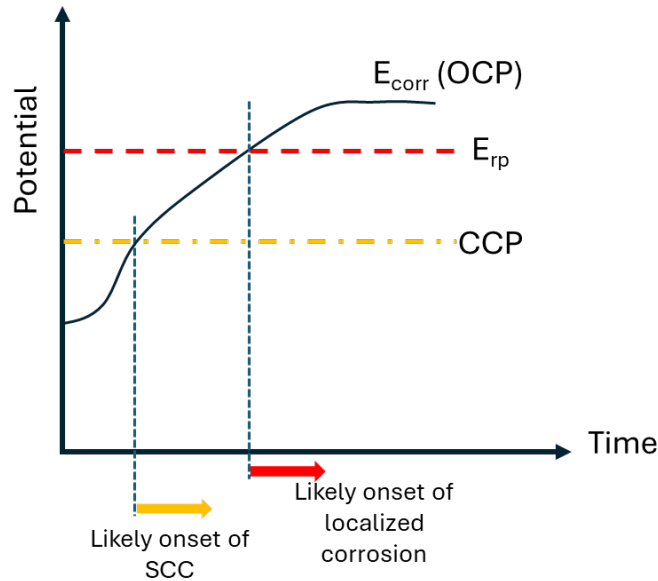


Figure 1-1. Schematic illustration of conditions for the onset of localized corrosion and SCC and their use in tank integrity prediction.

The measurement of OCP involves the use of reference electrodes. The OCP of a metal in an electrolyte is a combination of thermodynamic and kinetic effects of a variety of electrochemical reactions occurring at the interface. This is illustrated in Figure 1-2.

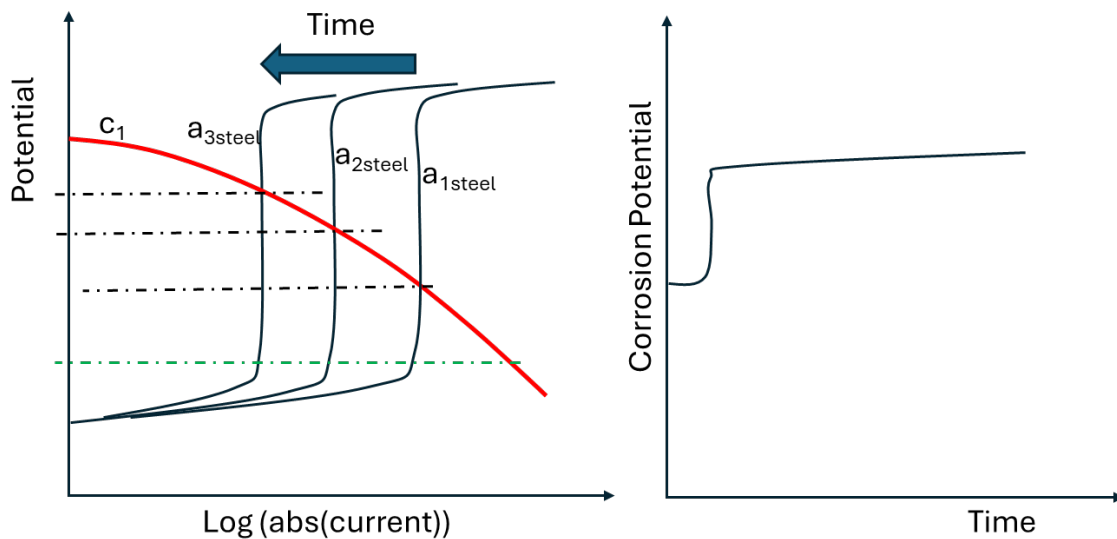


Figure 1-2. Schematic illustration of the change in corrosion potential (OCP) versus time

The anodic currents, shown as “ $a_{1\text{steel}}$ to $a_{3\text{steel}}$ ” are governed by the electrochemical response of the steel to the waste chemistry over time. In Figure 2, the passive current is shown to decrease with time, but this is not necessarily the case for all systems. The cathodic current, shown by c_1 , is governed by the redox reactions occurring in the waste solution. This cathodic current has an opposite sign to the anodic current, but the absolute value of this current is plotted in Figure 1-2. The intersection of the anodic and cathodic currents provides the zero net charge condition representative of OCP (ignoring the ohmic potential drop in the solution). This diagram, called the Evans diagram, shows that the OCP increases with time. However, other electrochemical reactions in a tank may influence changes in OCP over time. Thus, measurement of OCP is important for monitoring the tank performance and relating it to changes in waste chemistry.

1.1 Electrochemical Potential and Reference Electrodes

It is instructive to step back from the complex kinetic processes leading to OCP and consider the thermodynamic aspects of this interface first. The classic definition of chemical potential involves a change in free energy of a chemical species with changes in molar composition at any given temperature and pressure. By this definition, the chemical potential of a single ion cannot be measured, because the addition of only one ionic component is not possible without the charge balancing addition of a counter ion. Thus, the definition of the chemical potential of a single ion, and by extension the activity of a single ion, is only a matter of convenience and cannot be measured directly. Electrochemical potential of a solid (electrode) in equilibrium with an electrolyte is defined as the sum of chemical potential of the electrode in equilibrium with the electrolyte, the chemical potential of the ion of the electrode in the electrolyte, and the electrostatic potential associated with the work involved in bringing a unit charge from infinity to just inside the surface of a solid. However, the work involved in bringing the charge into a solid cannot be measured because the act of bringing the charge through the electrolyte-solid interface will involve changes in surface charges, which cannot be measured. Thus, the electrochemical potential of an electrode/electrolyte interface is indeterminate. A practical approach for determining an electrode potential is to define the potential difference of a system consisting of the electrode/electrolyte interface of interest, a reference system consisting of a reference electrode in a controlled electrolyte, the interface between the two electrolytes, and the external measurement system. Thus, even a thermodynamic definition of an electrode potential involves a reference electrode, with the proviso that any measurement of the voltage difference between the electrode of interest and a reference electrode is performed with minimum of disturbance of the equilibrium of the total system. By convention, the potential of the standard hydrogen electrode (SHE) system, H^+ (activity of $\text{H}^+ = 1$) | H_2 (1 atm. Pressure), is assumed to be 0 V at all temperatures. The SHE is inconvenient in practice as the electrode (typically a platinized Pt) is subject to the influence of redox species in solution and can be poisoned easily by impurities. Thus, practical reference electrode systems are tailored for specific environments and their potentials referenced to the SHE.

It is obvious from the above discussion that the use of a reference electrode system implies that its electrode potential must be insensitive to the act of measurement (even the most sensitive voltage measurement must involve the passage of a small current) and to the composition of the electrolyte in which the measurement is made. In their magisterial work on reference

electrodes, Ives and Janz⁵ state the issue thus: “ If an electrode does not work properly, its failure to do so presents a physicochemical problem outside the scope of thermodynamics. It must be examined in such terms as the chemical purity and physical states of the essential phases and interfaces”. This perspective will be explored in subsequent sections.

1.2 Characteristics of a Reference Electrode System

A simple schematic of an electrode potential measurement is shown in Figure 1-3.

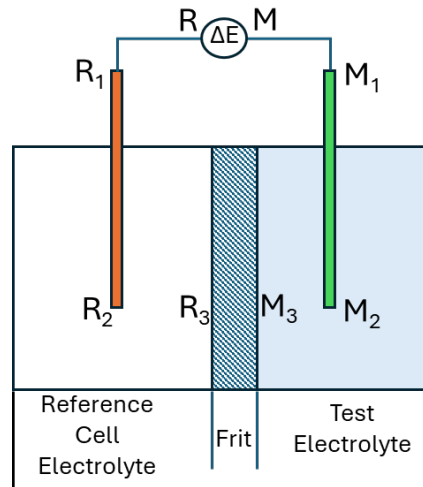


Figure 1-3. A simple schematic of an electrode potential measurement at a metal (M) using a reference electrode (R).

This simple cell consists of an electrode of interest, M, reference electrode, R, the test solution containing M, a reference solution containing R, a membrane or frit that separates the two solutions, and the external circuits consisting of wires and a high input impedance voltmeter. In reality, this arrangement may be more complex consisting of other intermediate solutions between the reference electrode and the test electrode and other barriers to protect the reference cell. The measured potential difference consists of several voltage drops:

$$\Delta E_{measured} = (E_M - E_R) + i \times \{ (Z_{R_1-R}) + (Z_{M_1-M}) + (Z_{M_1-M_2}) + (Z_{M_2-M_3}) + (Z_{M_3-R_3}) + (Z_{R_3-R_2}) + (Z_{R_2-R_1}) \} \quad (1)$$

The Z_{R_1-R} , etc. refer to the complex impedances of various parts of this system. The current drawn by the measuring system is given by:

$$i = \Delta E_{measured} / Z_{voltmeter} \quad (2)$$

Thus, the actual potential difference is related to the measured potential difference by:

$$(E_M - E_R) = \Delta E_{measured} \times \left[1 - \frac{\{ (Z_{R_1-R}) + (Z_{M_1-M}) + (Z_{M_1-M_2}) + (Z_{M_2-M_3}) + (Z_{M_3-R_3}) + (Z_{R_3-R_2}) + (Z_{R_2-R_1}) \}}{Z_{voltmeter}} \right] \quad (3)$$

⁵ D.J.G. Ives and G.J. Janz, Reference Electrodes – Theory and Practice, 1961, Academic Press, Inc. (reprinted in 1996 by NACE International, Inc.).

Where, $Z_{voltage}$ is the input impedance of the voltage measuring instrument. If the voltage measurement system has a high input impedance compared to the impedances of the various interfaces, the desired potential, $(E_M - E_R)$ is not significantly different from the measured voltage. Thus, a large input impedance voltmeter is critical for accurate potential measurements. However, if blockage of the frit or electrolyte communication within the reference electrode system occurs, then its impedance may increase sufficiently to affect the measured potential difference. Additionally, air pockets or other discontinuities in the electrolytic communication between interfaces may cause increased measurement noise due to electromagnetic interference and small changes in the actual OCP may not be easy to resolve.

A second important aspect of the OCP measurement is the changes in the reference potential, E_R . As mentioned in the previous section, the E_R is affected by: (1) the presence of redox species in the system that may influence the reference electrode potential, (2) the electrochemical polarization of the reference electrode due to the current drawn by the measurement system, and (3) the change in potential due to changes in species involved in the equilibrium reaction of the reference electrode. The general criteria for good reference electrode performance are shown in Table 1-1.

1.2.1 Sensitivity to Redox Species

All reference electrodes operate on the basis of heterogeneous redox equilibria. The hydrogen electrode uses the H^+/H_2 redox system as its basis, but this reaction occurs at the surface of a solid catalyst metal (e.g., Pt). If there are other redox species in solution, such as O_2 and Fe^{3+} , they also set up redox equilibria at the Pt surface and the resulting potential will be dictated by the kinetics of the reaction with higher redox potential reaction. This is illustrated for Fe^{3+}/Fe^{2+} redox reactions at different dilutions in a solution of 4% NaCl on Pt (Figure 1-4).

Table 1-1. Criteria for reference electrode performance.

Criterion	Performance issue
Lack of Sensitivity to Contamination with Other Redox Species	The reference electrode potential is typically increased by redox species in solution
Lack of Electrochemical and Chemical Sensitivity to pH (buffering, precipitation)	Change in solution pH alters the redox reactions at the electrode. Extreme pH values affect the speciation in the reference electrode and electrode surface
Non-polarizability	The potential should not be affected by current passed
Resistance to Other Chemical Species	The chemistry of buffer solution may change or electrode surface may change
Low impedance	High impedance will alter measured potential and induce electronic noise
Electrolyte Communication	Plugging will reduce electrolyte communication and increase impedance. Loss of internal electrolyte will result in dry out and failure of the electrode. Free communication with external electrolyte will alter chemistry.
Chemical and Radiation Resistance of Electrode Body	The body of the electrode may be adversely affected. Radiolytic products may alter electrochemical reactions
Mechanical Integrity	The body of the electrode may fail

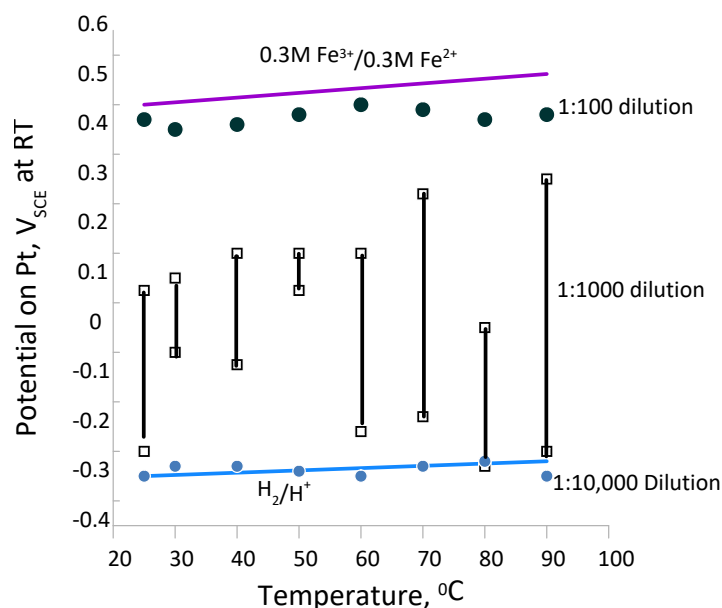


Figure 1-4. Effect of ferrous/ferric redox couple at different dilutions on the measured potential on Pt at room temperature⁶

Only at very low concentrations of impurities (less than about $3 \times 10^{-5} \text{M Fe}^{3+}/\text{Fe}^{2+}$) does the potential correspond to the H^+/H_2 reaction. Similar effects were found on other corrosion resistant alloys, such as Alloy 22⁴, which have been used as pseudo-reference electrodes. Redox species can be present in the test solutions or enter into solutions from corrosion reactions, radiolysis, or exposure to air. Most primary reference electrodes are insensitive to other redox reactions in the system, provided they do not alter the chemistry of the reference electrode.

1.2.2 Sensitivity to pH

The hydrogen and Quinone electrodes are examples of reference electrodes that are extremely sensitive to pH because they operate on the basis of H^+ reduction reactions. However, metal oxide electrodes, such as Ir/IrO₂ and W/WO₃ electrodes and glass electrode are also sensitive to pH and are used as pH electrodes. These electrodes can be used as reference electrodes when the surrounding solution is pH-buffered.

1.2.3 Non-Polarizability

Ideal reference electrodes operate under essentially equilibrium conditions. This means that their potential does not change significantly upon passage of a small current across their interface. For example, in the case of the hydrogen electrode, Pt has a large exchange current density that enables it to undergo very little polarization upon passage of a small current.

⁶ J. Kolts and N. Sridhar: 'Temperature Effects in Localized Corrosion', Corrosion of Nickel-Base Alloys, Cincinnati, Ohio, 1984, ASM International, 191-197.

Similarly, Ag/AgCl electrode operates under near equilibrium conditions between Ag and AgCl, whereby a small anodic current dissolves a small concentration of Ag that then precipitates as a AgCl salt film, whereas a small cathodic current dissolves AgCl to replate Ag. Thus, this electrode is essentially a non-polarizable electrode. However, when the AgCl layer completely dissolves and bare Ag wire is exposed to solution, significant anodic polarization can occur. When passive metals are used as reference electrodes, even a small anodic current can increase the potential significantly (see Figure 1-2). In the case of valve metals such as Ti and Zr, the resulting oxide films can be either semi-conductive or insulating, resulting in large ohmic potential drops in the film. Such electrodes are highly polarizable and are poor reference electrodes.

1.2.4 Resistance to Other Chemical Species

Many anionic species can attack the reference electrodes and change the surface equilibria. For example, exposure of Ag/AgCl electrode to highly alkaline solution can result in the conversion of AgCl to Ag₂O, resulting in significant change in the reference potential. Some species such as sulfur or sulfides can also form sulfides or poison the surface catalytic reactions, as in the case of Pt used in the Hydrogen electrode. The ability of some teals to form sulfides can be used in some systems, as in the case of the Ag/Ag₂S electrode.

Radiolytically generated free radicals may also affect chemical reactions and must be evaluated. Early studies of reference electrode performance in radiation environment used high energy radiation from a linear accelerator simulating that in the core of a nuclear reactor⁷. Danielson⁸ evaluated the effect of gamma irradiation on the performance of reference electrodes using a Co⁶⁰ source to generate Gamma radiation around a non-radioactive waste simulant consisting of a mixture of 3.0 molal NaOH, 0.5 molal NaNO₂, and 1.0 molal NaNO₃ at ambient temperature. The study showed that the performance of Ag/AgCl and Saturated Calomel Electrodes (SCE) did not degrade up to a total fluence of 9.4x10⁸ Rads. Marsh et al.⁹ evaluated the effect of Gamma radiation from Co⁶⁰ source on SCE at an absorbed dose rate of 2x10³ Sv/h for 100 hours and found no effect on Saturated Calomel Electrode (SCE) potential in comparison to another SCE that was shielded from radiation using 10 cm of lead (Pb).

1.2.5 Low Impedance

The impedance is affected by the semi-permeable membrane or frit used at the interface between the reference electrode solution and test solution. If this frit is blocked, the effective diffusivity of ionic species is reduced. The effective diffusivity is given by

$$D_{eff} = D \times \rho \times (1 - \tau) \quad (4)$$

Where, ρ is the porosity and τ is the tortuosity. If the porosity is low and tortuosity is high, then the effective diffusivity becomes low and increases the impedance. In solid-state or gel

⁷ D.F. Taylor, *Response of Electrochemical Sensors to Ionizing Radiation in High-Temperature Aqueous Environments*. Corrosion, 1991, **47**(2): 115–122.

⁸ M. J. Danielson, *Effect of Gamma Radiation on Stability of Silver-Silver Chloride and Mercury-Calomel Commercial Reference Electrodes*, Corrosion, 1995, **51**(6): 450–455.

⁹ G.P. Marsh, K.J. Taylor, G. Bryan, and S.E. Worthington, *The influence of radiation on the corrosion of stainless steel*. Corrosion Science, 1986. **26**(11): 971-982.

electrodes, the impedance is also affected by changes in the gel layer or polymer fill. In the case of reference electrodes used in non-aqueous systems, the impedance may also be affected by the reference fill solutions. In such cases, suitable supporting electrolytes must be used to reduce electrolyte impedance. Another source of high impedance is poor electrical connections (e.g., corroded contacts) and long electrical leads to the measurement system. Long leads also introduce electromagnetic noise in the system and should be minimized if at all possible. As shown in Eq. 3, the impedance of the reference electrode plays an important role mainly when a low-input impedance measurement system is used. Unfortunately, this may often be the case in field measurements.

1.2.6 Electrolytic Communication

Electrolyte (ionic and gaseous) communication is essential for the functioning of the reference electrode. However, if the communication is free flowing, the reference electrode compartment solution is replaced by the external test solution and the reference electrode potential drifts significantly. Typically, multiple junctions may be used to increase the diffusion path. However, if there is significant impediment to flow of species, the interface impedance will increase altering the measured potential (Eq. 3).

1.2.7 Chemical and Radiation Resistance of Electrode Body

Many reference electrode bodies are made of polymers that can be affected by certain chemical species, such as hydroxide or oxidizing compounds. Radiation can also affect the integrity of the reference electrode body through change in glass transition temperature, crazing, or softening. Finally, chemicals and radiation can affect elastomeric seals through volumetric swelling or embrittlement resulting in leakage.

1.2.8 Mechanical Integrity

The mechanical robustness of reference electrodes is key for field application, where they can be seldom handled with the same gentleness as in the laboratory. Often shear forces from moving liquids or from solids entrained in liquids can crack or erode the reference electrode body or the tip.

2.0 Reference Electrode Performance in DOE-Complex Waste Tanks

Electrochemical techniques have been utilized to monitor corrosion in waste tanks at both Hanford and the Savannah River Site (SRS). The performance of these corrosion monitoring systems was reviewed and is presented. As will be discussed, these systems frequently fail after relatively short-term exposure to the chemically and radioactively harsh environments of the waste tanks. Recently, there has been extensive laboratory testing to understand the failure modes of the reference electrodes in both simulated and actual waste environments. This testing was also reviewed below.

2.1 Electrode Performance in Waste Tanks in the DOE Complex

2.1.1 Early Reference Electrodes at SRS and Hanford

Prior to 1996, the use of reference electrodes within the DOE complex to measure the tank potential was limited. SRS in the 1970's utilized a saturated calomel electrode (SCE) to measure the tank potential in four waste tanks to determine if at the current waste compositions and temperatures these tanks were susceptible to SCC. Similar tanks had previously experienced SCC in supernates with these compositions¹⁰. Tank potentials were measured by immersing both a working SCE and an inactive SCE (emptied of electrolyte to measure any spurious signal from strong electrical fields) in the waste supernate and attaching the tank lead to a cooling coil supply line that was welded to the tank. Potentials were measured at various locations in the tank by connecting the tank lead to five different cooling coils (some extending into both supernate and sludge and some into supernate only). The largest range of potentials in any tank was 5 mV. The potentials were monitored for approximately 30 days.

Table 2-1 shows the composition, temperature and potential data obtained during the month-long exposure. In general, the data followed expected trends (i.e., higher pH wastes resulted in more negative (active) potentials)¹¹. On the other hand, the effect of an oxidizing species, such as mercury, is also exhibited as potentials of tanks that contained mercury were more positive (noble). Although two of the tanks had experienced cracking previously, it was concluded that the measurements demonstrated that the tanks were in a passive condition. However, it is now recognized that SCC typically occurs under passive conditions, where the passive film breaks down locally. The tank potential measurements in the table also suggest that the potentials were similar to those observed in actual wastes and simulants with carbon steel coupons, which were performed in the laboratory. Differences were attributed to the use of fresh coupon surfaces in the laboratory versus the thick oxide that likely exists on the tank walls.

In the 1980's, SRS demonstrated feed preparation processes for the waste vitrification facility in two of the waste tanks¹². The degradation concern in this case was pitting in dilute wastes due to chlorides either at the liquid air interface or at the interface between liquid and solid waste layers. The method for determining tank potential was similar to that used in the 1970s, except that a sleeve-type, double junction Ag/AgCl (DJE) was deployed in addition to an SCE. The sleeve type junction was considered to be more resistant to pluggage by slurries than the normal frit junctions. The double junctions allowed the outer junction to be filled with sodium rather than potassium chloride solutions, which may have resulted in precipitation in the tetraphenylborate waste. The additional concerns of localized redox and aggressive species required multiple probes, movement of the probes through the depth of the tank contents and a means of determining probe elevation. In addition to the reference electrode probe, pH, Eh and chloride laboratory probes were attached to 50 ft. waterproof leads. Probes that contained fill

¹⁰ R. S. Ondrejcin, S.P. Rideout, J. A. Donovan, *Control of Stress Corrosion Cracking in Storage Tanks Containing Radioactive Waste*, Nuclear Technology, 1979, **44**(2): 297-306.

¹¹ N. Sridhar, J.A. Beavers, B.C. Rollins, S. Chawla, K. Evans and X. Li, *Stress Corrosion, Cracking and Localized Corrosion of Carbon Steel in Nitrate Solutions*, Corrosion, 2016, **72** (7): 927-942.

¹² D. F. Bickford, J. W. Congdon, and S. B. Oblath, "Corrosion of Radioactive Waste Tanks Containing Washed Sludge and Precipitates", *Materials Performance*, 1988, **27**(5), 16-21.

solutions were completely filled, and vent holes were closed with polyvinylchloride electrical tape and sealed with silicon rubber. ASTM A537 carbon steel coupons, the tank material of construction, were attached to waterproof leads and the coupon junctions were potted in silicone rubber.

Table 2-1. Composition, Temperature and Potential Data for SRS Tanks in the 1970s.

	Tank Designation			
	F-4	F-8	H-11	H-15
Nitrate (M)	2.4	1.7	3.5	3.6
Nitrite (M)	3.1	0.5	0.8	1.1
Hydroxide (M)	2.8	1.1	0.79	1
Chloride (M)	0.032	0.03	0.03	0.016
Sulfate (M)	0.032	0.18	0.03	0.05
Carbonate (M)	0.18	0.1	0.1	0.1
Mercury (ppm)	12	40	240	100
Supernate Temperature (°C)	56	40	49	48
Tank Leakage	No	No	Yes	Yes
Tank Potential (mV vs. SCE)	-440	-0.12	-0.085	-0.065
Carbon steel coupon potential in simulant (mV vs. SCE, 2 mo.)	-460	NA	-140	NA

The probes were calibrated in the field immediately prior to use. They were then bundled together with PVC electrical tape inside 2-inch diameter by 1.5-ft long, schedule 40 PVC pipe. The pipe was attached to a 50-ft steel tape measure, which permitted determination of the relative elevation of the probes in the tanks. Probe readings were taken at various elevations. After the tanks had been scanned in this manner, periodic readings were taken at constant elevations to determine the drift of tank potentials and changes in the passive films on the coupons during aging. Aged coupons were shorted to the tanks through a nanoammeter to determine the risk of galvanic corrosion. An example of the reference electrode data is shown in Figure 2-1.

As shown in the figure, the tank contained approximately 4 feet of waste, and it contained both sludge solids and a clear solution. The tank potential did not vary with elevation or the presence of solids. However, the potentials of the carbon steel (Fe) coupons did change depending on the elevation and presence of the solids. These potentials were similar to those observed in both actual wastes and simulants, which suggested minimal effect of irradiation.

The potentials were monitored for 40 days in two tanks. The composition, temperature and potential for each tank are shown in Table 2-2. In general, the data again followed expected trends (i.e., higher pH results in more negative potentials). However, the presence of mercury in the solids phase may also have contributed to the more noble potential observed in Tank H-42. Based on these results and laboratory tests it was concluded that this test demonstrated that the tanks were in a passive condition.

Both SRS tests provided “snapshots” of the tank conditions and, in neither case, was deterioration of the reference electrode probe noted. The probes were not intended for long-term trending purposes and, thus, no precautions were taken to improve the design or materials for the electrodes.

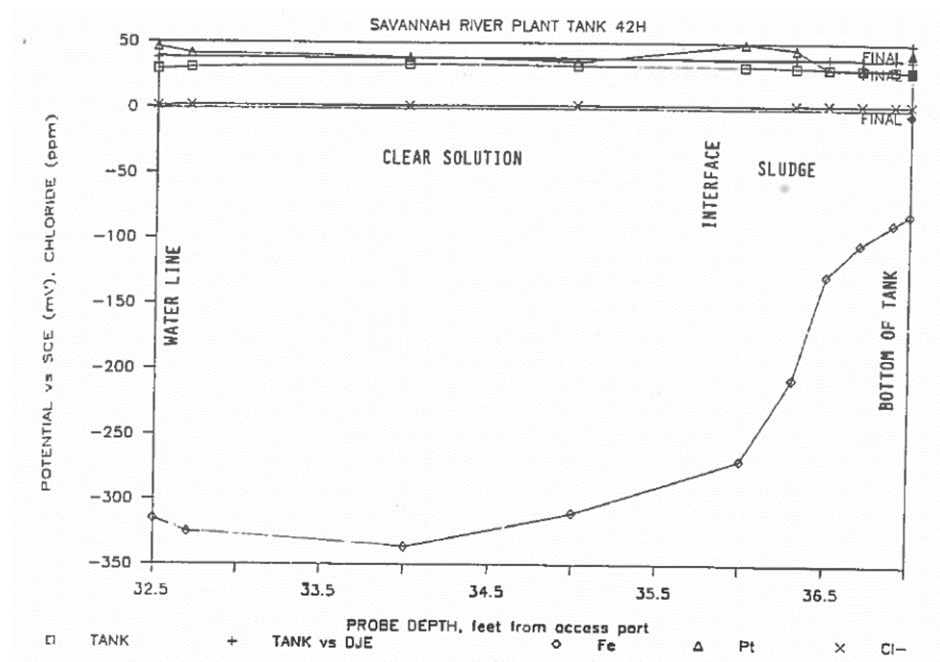


Figure 2-1. Reference electrode results in an SRS tank¹²

Table 2-2. Composition, Temperature and Potential Data for SRS Tanks in the 1980s¹²

	Tank Designation	
	H-42	H-48
Nitrate (M)	0.0014	0.09
Nitrite (M)	0.026	0.24
Hydroxide (pH)	9.5	11.5
Chloride (M)	0.0001	0.0004
Sulfate (M)	0.0003	0.009
Carbonate (M)	0.064	0.29
Supernate Temperature (°C)	< 40	< 40
HgO (wt% in solids)	0.53	0
Tank Potential (mV vs. SCE)	40	-290

The reference electrodes in the tanks are challenging to deploy and extract, as demonstrated by these early attempts. The difficulties encountered with radiological exposure and disposal constraints make long-term performance of a reference electrodes desirable. Furthermore, the

long-term potential of the tank may drift with time depending on the waste simulant. This was evident in many of the waste simulant tests in the laboratory. The actual in-tank potential of the tank steel is the net result of the drifts in the corrosion potential of the tank steel and the reference electrode. Therefore, it is imperative to determine the drift in the reference electrode potential to determine whether the corrosion potential of the tank is attaining values that may necessitate corrective actions.

At the Hanford site, longer term monitoring was attempted early on. A corrosion monitoring probe, designed by Pacific Northwest Laboratories (PNL), was also installed in Tank AN-107 between 1987-1990¹³. At the time, the waste chemistry was outside the corrosion control specification (i.e., pH 10.8). Laboratory polarization scans performed in simulants and actual AN-107 waste indicated that the tank potential was near the active/passive transition, which could lead to failure by SCC. The purpose of the probe was to measure the potential and polarization resistance to assess the general corrosion rate. The probe consisted of a reference electrode, working electrodes fabricated from A537 carbon steel, and a thermocouple (see Figure 2-2). An Ag/AgCl electrode (with a teflon tip) was used as the reference electrode. The body of the probe was made of "Scotchcast", a 3M resin. A PVC tube was used for the outer wall and probe mold. Stainless steel shot was placed in the probe body to increase the overall weight and overcome buoyancy forces. A stainless-steel aircraft cable was attached to maneuver the probe. A standard shielded cable was used for electrical connections. The anticipated life of the probe was 90 days; however, the probe functioned for approximately 3 years.

Figure 2-3 shows the potential measurements approximately 6 months after the probe had been inserted into the tank. Neglecting the time when the probe lead was cut, the tank wall potential was approximately -0.300 V vs. Ag/AgCl, while the A537 samples were at -0.44 V vs. Ag/AgCl. The potential was very stable over a seven-day period. Figure 2-4 shows the potential measurements after 3 years of exposure. The tank potential at this time was also around -0.300 V; however, the potential of the A537 coupon had increased to approximately -0.325 V. The increase was attributed to the build-up of oxide film on the surface of the sample. For both electrodes, the potential was relatively stable. After 1990, the data from the electrode was not utilized as much. The reasons are not clear for the suspension of measurements, and there are no indications that it was due to probe failure. However, the data from the polarization resistance electrode, as expected, indicated a low corrosion rate. There was a desire to develop techniques that provided information on localized corrosion mechanism (e.g., pitting). Thus, the focus turned to techniques, such as electrochemical noise.

¹³ J. I. Mickalonis, SRT-MTS-92-3022, *Trip Report: Informational Meetings on the PNNL Probe for Corrosion Monitoring*, 1992.

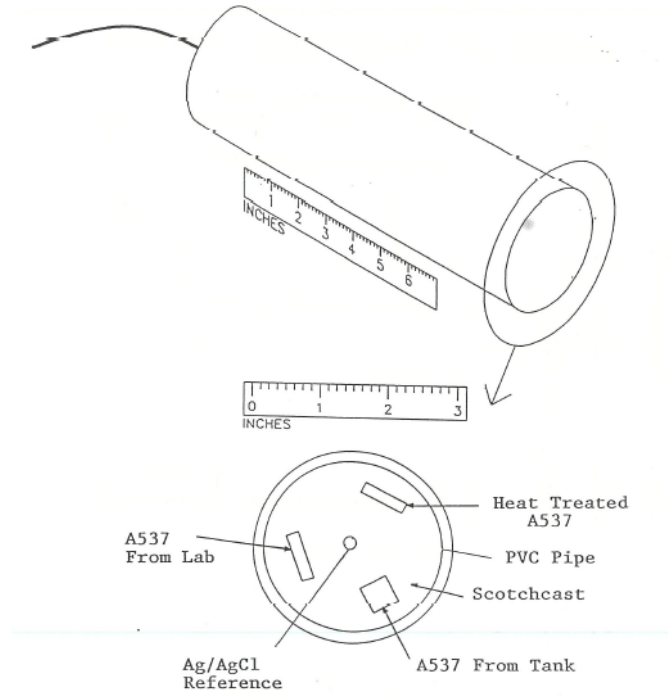


Figure 2-2. Schematic of PNL Probe ca. 1989.¹³

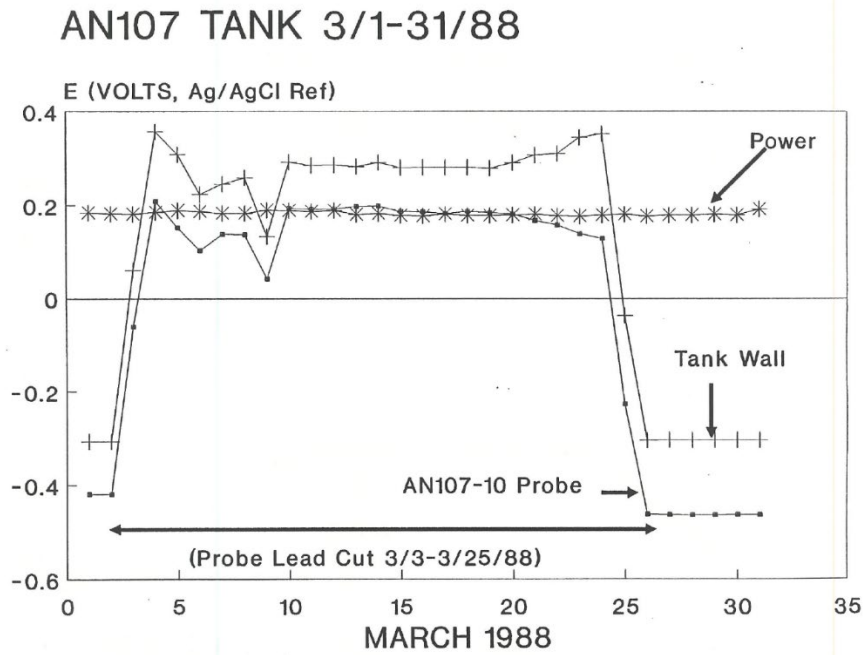


Figure 2-3. OCP measurements of A537 coupon for probe in Tank AN-107, March 1988.¹³

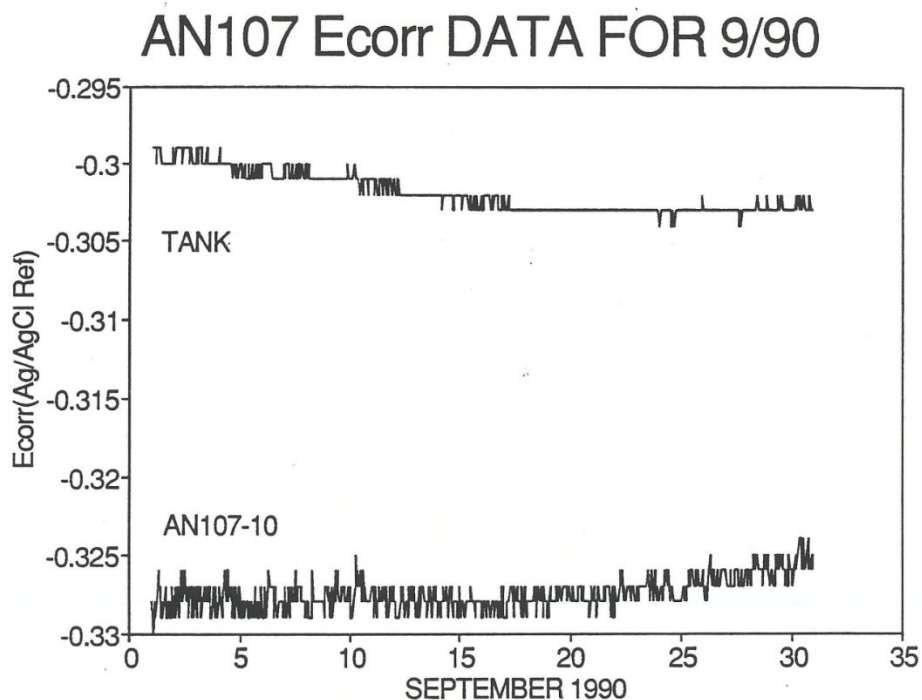


Figure 2-4. OCP measurements of A537 coupon for probe in Tank AN-107, September 1990.¹³

2.1.2 Electrochemical Noise Probe at Hanford

Beginning in 1995 corrosion monitoring in DST began a new phase, that is an emphasis on electrochemical noise (EN) systems¹⁴. There were three primary reasons for the new approach.

- Previous corrosion monitoring systems had utilized general corrosion techniques such as electrical resistance (ER) and linear polarization resistance (LPR). The results merely demonstrated the expected low general corrosion rates for carbon steel in high pH solution. This did not address primary degradation mechanisms of concern, which were localized corrosion mechanisms such as pitting and stress corrosion cracking.
- Previous monitoring systems did monitor the potential, however, there was not an extensive database that provided information on the critical potentials for cracking and pitting, which could be compared to the potential measurement. Given that the wide variety of waste chemistry, there was the possibility that meaningful comparisons could not be made even if the potential was measured.
- Previous monitoring systems did not emphasize long-term monitoring. There was a concern regarding the durability of the systems at that time.

EN was seen as an opportunity to provide information on the localized corrosion behavior of the tanks. Given that EN utilized electrodes made from carbon steel, the stability of a reference electrode in the waste environment was not as great of a concern.

¹⁴ G. L. Edgemon, V. S. Anda, M. M. Dahl, and K. D. Boomer, *The Evolution of Corrosion Monitoring in Hanford High-Level Waste Tanks*, Journal of Nuclear Materials Management, July 2013, **41** (4), 48-60.

The EN systems were implemented from 1997 through 2005. However, due to many issues related to interpretation of the signals and interference from other electrical noise signals the monitoring system did not provide information that was actionable (i.e., actions such as when to add chemicals such as hydroxide). As stated previously, EN instrumentation does not directly measure corrosion occurring on the internal surfaces of the tank or monitor the open circuit potential of the tank wall. Tank wall corrosion must be inferred from the measurements made on the EN electrodes.

2.1.3 Multi-Probe Corrosion Monitoring System at Hanford

In 2004, a group of corrosion and nuclear waste chemistry experts from industry, academia, and other DOE Sites, evaluated proposed initiatives to optimize the waste chemistry specification requirements for a small set of DSTs with waste chemistries that were particularly difficult to adjust¹⁵. This panel was referred to as the Expert Panel Oversight Committee (EPOC). The experts concluded that optimized waste chemistry control limits could likely be established by conducting laboratory tests to determine the range of corrosion potentials conducive to SCC for a given DST waste type, then monitoring the corrosion potential of the associated DST(s) with relatively simple in-tank corrosion monitoring systems¹⁵. Thus, one of the weaknesses of previous potential monitoring attempts was addressed.

In 2005 and 2006, researchers performing laboratory corrosion testing, identified the relationship between corrosion potential and the initiation of pitting and SCC in the DST 241-AN-102 and DST 241-AN-107 waste types¹⁶. Once the range of potentials for pitting and SCC were defined in the laboratory testing for the DST 241-AN-102 and 241-AN-107 waste types, focus shifted to measuring the corrosion potential of those tanks. In 2007, the functions and requirements were completed for the first new corrosion monitoring system associated with this program, known as the Multi-Probe Corrosion Monitoring System (MPCMS). The first MPCMS was installed in 241-AN-102 in May 2008. In addition to these DST, probes were planned for Tank AY-102, AY-101, and AW-104. These DST represented a wide variety of chemistries present in the tank farm.

Figure 2-5 shows the reference electrode configuration and tank-top terminal box for the MPCMS. The reference electrodes that were utilized in the MPCMS are described in Table 2-3¹⁷. The anticipated life expectancy of the probe was 10 years¹⁸. All three electrodes were installed on

¹⁵ M.T. Terry, RPP-RPT-22126, *Expert Panel Workshop for Hanford Site Double-Shell Tank Waste Chemistry Optimization*, January 1, 2004.

¹⁶ C.S. Brossia, F. Gui, C. Scott, RPP-RPT-31680, *Final Report, Hanford Tanks 241-AN-107 and 241-AN-102: Effect of Chemistry and Other Variables on Corrosion and Stress Corrosion Cracking*, October 30, 2006.

¹⁷ S. Philo, RPP-RPT-44463 Rev.0, *Effects of Temperature and Contamination on MPCMS Electrodes I 241-AY-101 and 241-AN-107 Tank Waste Simulants*, March 26, 2010.

¹⁸ M. M. Dahl and R. J. Crosswhite, RPP-RPT-51766, Rev. 41, *Corrosion Probe Monitoring Systems: January through March 2024 Quarterly Report*, May 2024. (Note: Multiple revisions of this report were reviewed and provided information for this report)

Tanks AN-102 and AY-102. The Ag/AgCl reference electrode proved to be the most robust electrode. The SCEs failed after between 33-55 months of use, while the Cu/CuSO₄ electrodes failed after 24-48 months. Therefore, in the remaining three tanks (AN-107, AW-104, and AY-101) only Ag/AgCl electrodes were installed.

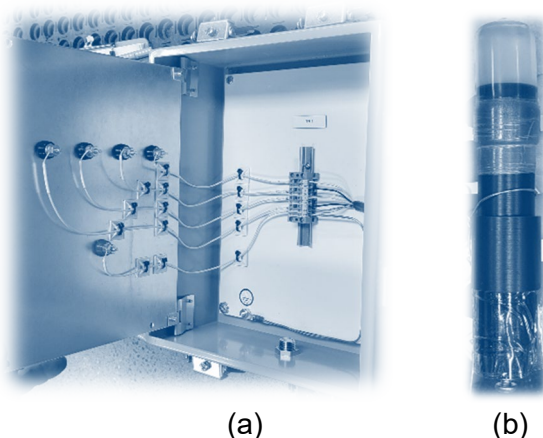


Figure 2-5. (a) Tank-top Terminal Box, and (b) Reference electrode utilized for MPCMS.¹⁷

Table 2-3. Description of Reference Electrodes Utilized for MPCMS.¹⁷

Reference Electrode	Description
Schiff Associates® Model RE-AGAGCL-65 MPCMS-Style Ag/AgCl Reference Electrode.	A specifically-designed Ag/AgCl electrode for the MPCMS application with a Kynar body and porous Kynar frit (for radiation resistance), uses a 1 M potassium chloride filling solution
Schiff Associates Model RE-HGHGCL-65 MPCMS-Style SCE.	A specifically-designed SCE for the MPCMS application with a Kynar body and porous Kynar frit (for radiation resistance)
Schiff Associates Model RE-SCUCUSO4-65 MPCMS-Style Cu/CuSO ₄ Reference Electrode.	A specifically-designed Cu/CuSO ₄ electrode for the MPCMS application with a Kynar body and porous Kynar frit (for radiation resistance), uses a saturated copper sulfate filling solution

An example of the data that has been obtained in Tank AN-102 is shown in Figure 2-6. The data shown includes the tank potential vs. a Ag/AgCl electrode and two tank material electrodes that are mounted on the MCPMS mast. The potentials shown in the figure are adjusted to the SCE reference electrode scale. The temperature of the supernate is also shown in the figure. As

expected, the potential oscillated inversely with the change in temperature. The two tank material electrodes produced similar values, while the tank potential was typically 5-10 mV more positive than the tank materials. During first four years after installation, the potential drifted in the positive direction by approximately 20 mV, however, there was no indication of a failure of the electrode.

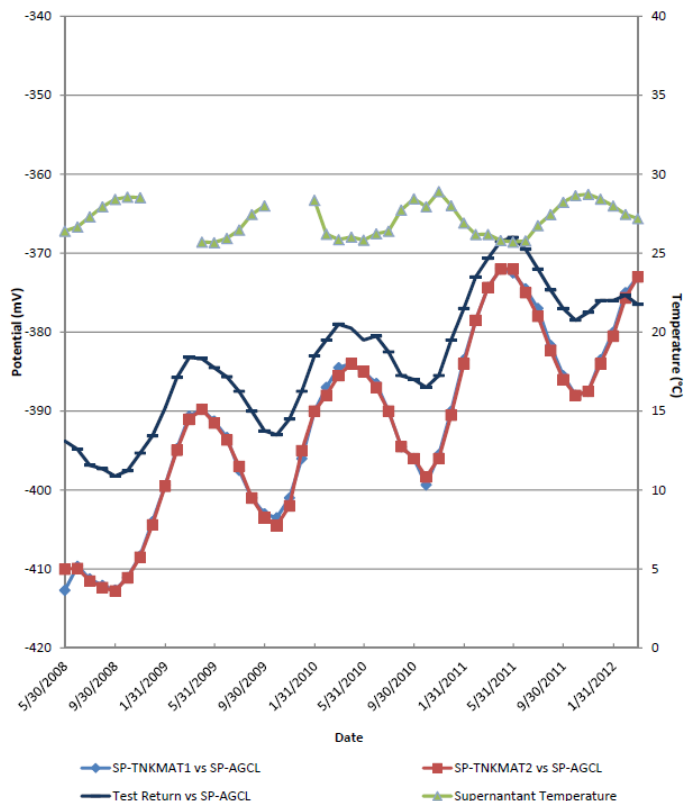


Figure 2-6. 241-AN-102 MPCMS Average Monthly Tank and Supernate Tank Material Electrode Potentials from May 2008 to January 2012.¹⁸

This was the last operable electrode in Tank AN-102 as most of the reference electrodes in this tank failed within 3 years. Table 2-4 shows the average lifespan of a reference electrode as a function of the type of electrode and the tank. The data from the remaining four tanks indicate that reference electrodes tended to fail in approximately 3 years or less. The two longest lasting electrodes were in the supernate that had a relatively low hydroxide concentration (0.5 to 0.6 M) and contained significant quantities of organics. The performance of the Ag/AgCl electrode in Tank AN-102 was significantly better than the SCE and CuSO₄ electrodes. Based on this result, only Ag/AgCl reference electrodes were installed in tanks AN-107, AW-104 and AY-101.

Table 2-4. Average life span of reference electrodes attached to an MPCMS

	Tank	Average Lifetime Ag/AgCl (months)	Average Lifetime SCE (months)	Average Lifetime CuSO ₄ (months)
MPCMS	AN-102	158	44	36
	AN-107	138 (6**)	NA	NA
	AY-102*	32	26	36
	AW-104	6	NA	NA
	AY-101	30	NA	NA

*Status when tank leakage detected in August 2012. Only 39 months of operation.

**Lifetime of electrode in the sludge solids; Other lifetime was in the supernate

Table 2-5 shows the condition of the reference electrodes in 2019, approximately 10 years after installation. Recall that 10 years was the desired lifetime for these reference electrodes. Discounting the performance of the electrodes in Tank AY-102 (because of the tank failure in 2012), only 2 of the 20 original reference electrodes remained operational in 2019.

Table 2-5. Status of Reference Electrodes in MPCMS Probes in 2019.

	Tank	Installation Date	Operational	Suspect	Failed	Total
MPCMS	AN-102	May-08	1	0	5	6
	AN-107	Jun-10	1	0	3	4
	AY-102*	Mar-09	2	0	4	6
	AW-104	Jul-10	0	0	4	4
	AY-101	Apr-09	0	0	6	6
Total			4	0	22	26

* Status when tank leakage detected in August 2012. Only 39 months of operation.

2.1.4 Retractable Corrosion Monitoring Probe System at Hanford

A significant problem with the MPCMS, was that once installed in a DST it was challenging to troubleshoot, inspect, repair, or replace any of the in-tank electrodes or other waste-contacting components. In 2011, MPCMS designers and equipment engineers began to make changes in the design of the deployment system. In 2012, a set of design requirements for a new Retractable Corrosion Monitoring Probe (RCMP) were issued¹⁹.

¹⁹ C. A. Sumner, RPP-SPEC-49792, *Procurement Specification for the 241-AW-105 Retractable Corrosion Monitoring Probe Assembly*, May 17, 2012.

As with the MPCMS, the primary purpose of the RCMP is to facilitate the measurement of the DST corrosion potentials. However, instead of using a large, fixed, in-tank probe to hold electrodes at various elevations in the DST, the RCMP assembly consists of a small replaceable cable reel assembly and associated housing. The entire assembly is approximately 3 ft. x 3 ft. x 2 ft. and can be carried and installed by hand. The cable reel assembly consists of a simple reel wound with cable leading to a probe head containing the required electrodes. The probe head can be raised and lowered in the tank via the cable reel assembly.

The primary reference electrode currently used for potential monitoring in DSTs in the RCMP system is a single-junction Ag/AgCl type manufactured by Van London Co²⁰. A photograph of the electrode is shown in Figure 2-7. The body and frit of the Van London reference electrode are made of Kynar (PVDF or Polyvinylidene fluoride), an inert thermoplastic fluoropolymer with a combination of thermal, alkali, and radiation resistance. The Van London single junction (VLSJ) electrode contains a fill of 4-M KCl and is identical to the reference electrode type currently installed in DSTs that are outfitted with RCMPs.



Figure 2-7. Photograph of a VLSJ Ag/AgCl reference electrode type that is currently used in Hanford DSTs (manufactured by Van London Co.).²¹

A schematic of the internal design of the VLSJ Ag/AgCl electrode currently used in Hanford DST corrosion probes is shown in Figure 2-8. The Kynar body of the electrode is approximately 4 inches long and 0.75 inches in diameter at the largest section. The internal element is made from a 0.01-inch diameter, fine Ag wire that is connected to a stainless-steel screw terminal in the end cap for electrical connection. The Ag wire extends into the middle of the electrode cavity and is sealed into the inner diameter of the body with polymeric sealing pads. The end of the Ag wire inside the electrode cavity is coated with an AgCl layer that is approximately 0.5-inch long and has an average thickness of about 0.008 inches. The electrode cavity is filled with a 4-M KCl gel of proprietary composition. The other end of the electrode body is sealed with an end cap that contains a cylindrical porous frit made of natural Kynar. The porous frit provides a low-resistance liquid junction between the electrode and the external waste solution, while restricting intermixing and cross contamination of the electrode fill with the waste.

²⁰ Van London Co., 10540 Rockley Rd, Houston, TX 77099. Part No. VL8604201.

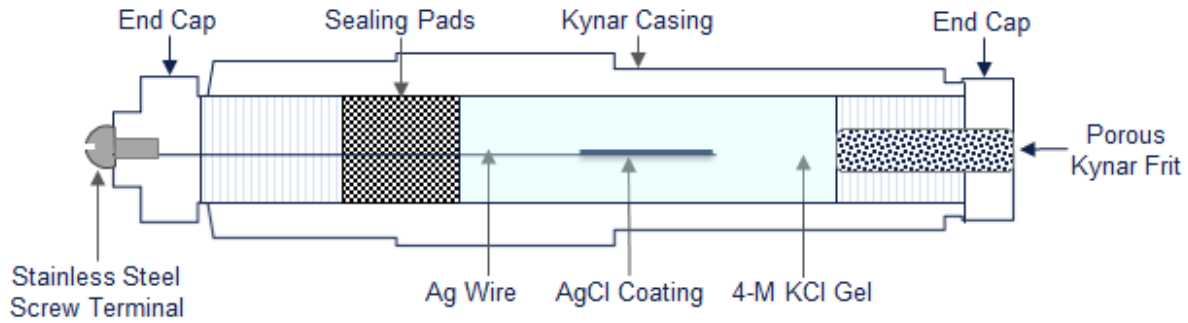


Figure 2-8. Schematic of the internal design of the VLSJ Ag/AgCl electrode currently used in Hanford DST corrosion probes.

Up to four electrodes of this Van London design can be mounted and potted into the head of the Retractable Corrosion Monitoring Probe (RCMP) for installation in the tank, as shown in the photographs in Figure 2-9.

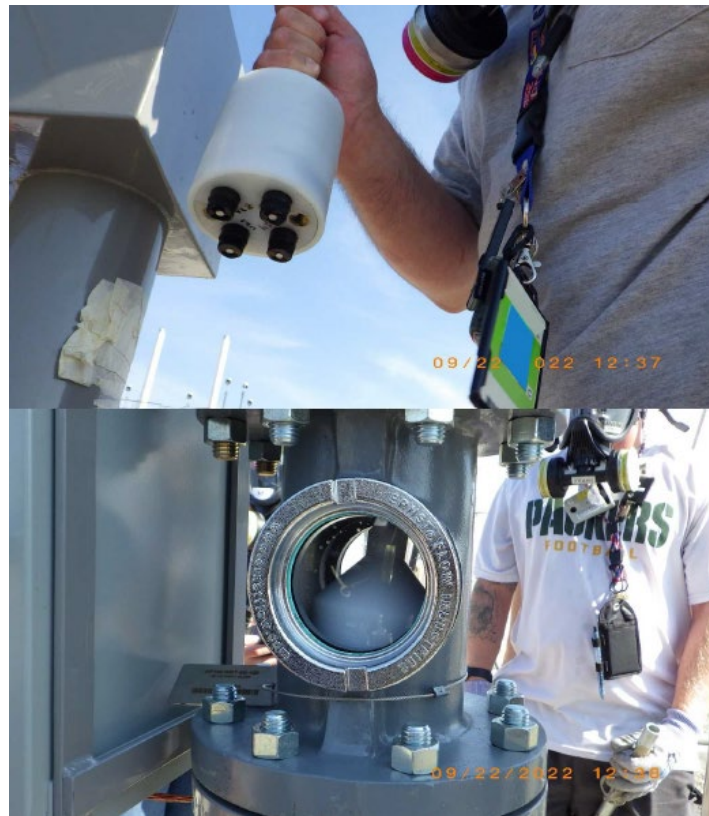


Figure 2-9. Four VLSJ Ag/AgCl reference electrodes mounted in RCMP probe head (top) and installation via riser in Tank 241-AP-106 (bottom)²¹.

²¹ M.J. Feldmann, RPP-RPT-63666, Rev.0, *Construction Acceptance Test Report for the 241-AP-106 Retractable Corrosion Monitoring Probe (RCMP)*, Prepared by Sargent & Lundy for Washington River Protection Solutions, LLC, October 2022.

An example of the data that has been obtained in Tank AW-105 is shown in Figure 2-10. Note that only the tank potential is measured (i.e., there are no tank material coupons with this arrangement). The potentials shown in the figure are adjusted to the SCE reference electrode scale. The temperature of the supernate is also shown in the figure. The potential has been relatively stable for nearly 18 months and the two reference electrodes are in good agreement. However, two of the four reference electrodes in this tank failed after 15 months.

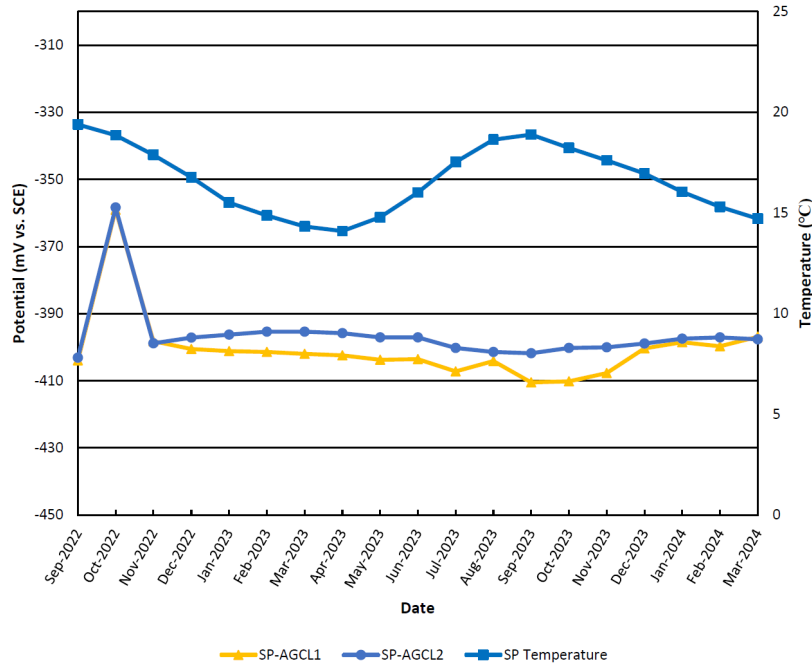


Figure 2-10. Corrosion potential data collected from RCMP installed in Tank AW-105 from September 2022 to March 2024¹⁷.

Figure 2-11 presents the potential data from Tank AP-102. All four of the original reference electrodes had either failed or were suspect within 15 months of being installed. In this situation failure was detected by a sharp 400 mV increase in the potential that occurred within a three-to-six month period. If this were true, the tank potential would be in a range where the steel would be susceptible to localized corrosion or SCC.



Figure 2-11. Corrosion Potential data collected from RCMP installed in Tank AP-102 from September 2020 to March 2024¹⁷.

Figure 2-12 presents the potential data from Tank AW-105. Both of the original reference electrodes had either failed or were suspect within 9 months of being installed. In this situation, failure was a bit more subtle. The tank potential had drifted slowly in the negative direction approximately 80 mV. Between 2013 and 2020, the potential had drifted in the negative direction approximately 150 mV. If this were accurate, this indicates that the tank wall may be experiencing active corrosion. Four new reference electrodes were installed in 2022. Already, two of the reference electrodes have failed within 15 months.

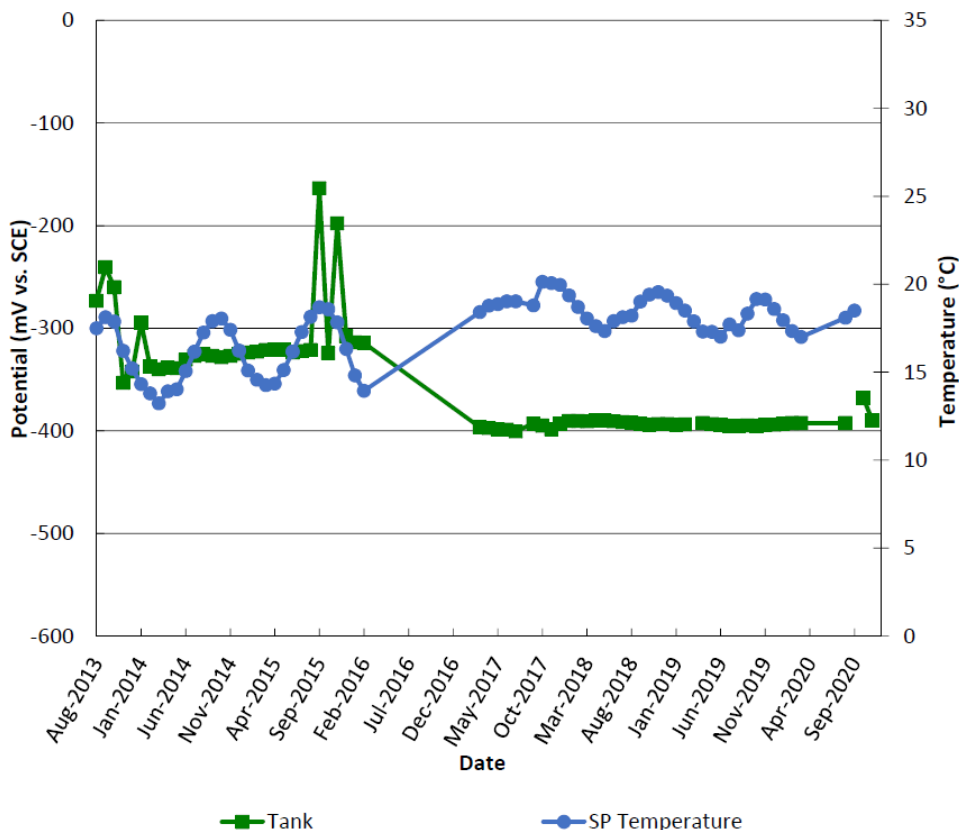


Figure 2-12. Corrosion potential data collected from RCMP installed in Tank AW-105 from August 2013 to September 2020¹⁷.

Table 2-6 shows the average lifespan of a Ag/AgCl reference electrode that has been installed in a DST. With the exception of Tank SY-101, the reference electrodes tended to fail in approximately 2 years or less. The hydroxide concentration in the supernate in Tank SY-101 is also relatively low (i.e., between 0.5 to 1 M). The performance of the Ag/AgCl electrode in Tank AN-102 was significantly better than the SCE and CuSO₄ electrodes. Based on this result, only Ag/AgCl reference electrodes were installed in Tanks AN-107, AW-104 and AY-101.

Table 2-6. Average life span of reference electrodes attached to an RCMP.

	Tank	Average Lifetime Ag/AgCl (months)
RCMP	AW-105 #1	9
	AW-105 #2	15
	SY-101	66
	AY-101	19
	AP-102	13
	AP-106	NA
	AZ-101	11

Table 2-7 shows the condition of the reference electrodes in 2024, approximately 2-11 years after installation. Excluding Tank SY-101, 14 of the 22 reference electrodes have failed or are suspect within two years of installation.

Table 2-7. Performance of Reference Electrodes in RCMP.

	Tank	Installation Dates	Operational	Suspect	Failed	Total
RCMP	AW-105 #1	Aug-13*	0	1	1	2
	AW-105 #2	Sep-22	2	0	2	4
	SY-101	Jul-14	0	1	2	3
	AY-101	Sep-19	2	0	2	4
	AP-102	Sep-20	0	2	2	4
	AP-106	Sep-22	4	0	0	4
	AZ-101	Oct-20	0	3	1	4
			8	7	10	25

2.2 Testing in Simulants at DNV

Accurate measurements of tank-wall potentials are important, especially in mission-critical tanks (e.g., AP farm tanks related to DFLAW, 242-A Evaporator feed tank, etc.), where the impacts of waste transfers and other operations are to be monitored. Starting in FY2018, DNV performed long-term testing and evaluation of various types of commercial primary reference electrodes, including the VLSJ Ag/AgCl electrodes, in nonradioactive simulants of the supernatant liquid waste in various tanks to better predict field performance in the DST environments.

The wastes stored in the Hanford DSTs are highly alkaline in nature and span a wide range of chemistries. To test the long-term performance of the reference electrodes, nonradioactive simulants of the supernatant liquids stored in various DSTs were formulated. Table 2-8 shows the calculated pHs, test temperatures, and some compositional features of the simulants tested. The OH⁻ concentrations of the simulants ranged from 0.53 M to 5.76 M and the sodium concentrations ranged from 3.66M to 12.4 M. Metal analytes with reported concentrations exceeding 5×10^{-4} M were included in the simulant formulations.

For testing, a stainless-steel reducing union with PTFE ferrules was used to seal around the PTFE tube and the electrode body, shielding the electrical connection from the test environment (Figure 2-13). The tests were performed in 1-L vessels made of chemically resistant perfluoroalkoxy (PFA) polymer. Many simulants were tested at room temperature while a few, such as the AW-101, AW-105, and AZ-101 simulants, were tested at elevated temperatures corresponding to in-tank waste temperatures. For elevated temperature tests, the test vessel was equipped with a heating tape, temperature controller, and thermocouple to provide controlled heating. Various electrode types, including the incumbent VLSJ Ag/AgCl type, were exposed to each waste simulant (Figure 2-13).

Table 2-8. Calculated pHs, test temperatures, and some compositional features of the supernatant liquid simulants tested in the DNV reference electrodes studies.

Tank Simulant ID (Year of Formulation)	pH at 25°C	Test Temp (°C)	Waste Features
AY-101 (2018)	13.6	RT	No TIC
AY-101 (2019)	13.9	RT	High TIC
AP-102 (2019)	14.1	RT	High TIC
AZ-101 (2019)	14.3	70	High temperature
AN-102 (2018)	14.4	RT	High TIC, TOC, complexants, heavy metals
AW-105 (2018)	14.8	RT	High fluoride
AW-105 (2019)	14.5	35	Full TOC makeup
SY-103 (2018)	15.3	RT	High aluminum, nitrite, nitrate
AW-101 (2018), 35C	15.6	35	High aluminum, nitrite, nitrate, hydroxide

RT: Room Temperature
TIC: Total Inorganic Carbon
TOC: Total Organic Carbon

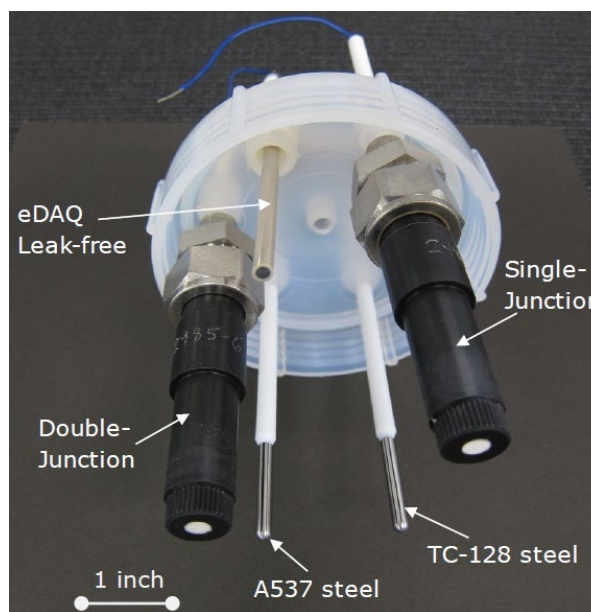
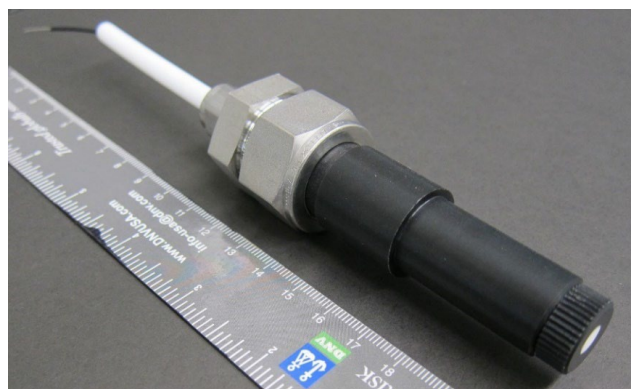


Figure 2-13. Left: Photograph of VLSJ Ag/AgCl reference electrode with compression fitting and wire connection tested at DNV (Ruler scale in cm and inches). Right: Photograph of a PFA test vessel lid showing various Ag/AgCl reference electrodes and tank steel electrodes, prior to insertion in a test vessel for long-term performance testing in a waste simulant²².

A photograph of the test setup is shown in Figure 2-14. Each test vessel was filled with approximately 800 mL of waste simulant to fully immerse the electrodes. PTFE tubes containing

²² S. Chawla, et al., RPP-RPT-63781, Rev. 0, FY2021 DST Chemistry Testing Report, Prepared by DNV GL USA, Inc. for Washington River Protection Solutions, LLC, May 2022.

the electrical leads from the electrodes were inserted through ports in the PFA lid of the vessel and sealed with compression fittings. One port in the lid was used for inserting a Pt-Nb counter electrode for periodic impedance measurements. Another capped port was reserved for inserting a laboratory reference electrode or Luggin probe to make electrochemical measurements on the test reference electrodes.



Figure 2-14. Photograph of a DNV test setup for long-term reference electrode study in various DST waste simulants²².

A standard laboratory SCE was used as the reference electrode for potential measurements. To avoid contamination of the laboratory SCE and damage to its glass body and frit from the high-pH simulants, the laboratory SCE was not kept continuously immersed but inserted in the test cells only when potential or electrochemical impedance spectroscopy (EIS) measurements were to be made. Before and after each use, the potential of the laboratory SCE was verified against a master SCE, which was maintained in a saturated KCl solution.

For the simulants tested at elevated temperatures, a Luggin capillary filled with the simulant was used. Potential measurements were made against the laboratory SCE maintained at room temperature during measurements. A potentiostat in a 2-electrode configuration was used for EIS, with the test reference electrode as the working electrode. The EIS measurements were performed under potential control using a sinusoidal AC voltage perturbation of $5 \text{ mV}_{\text{rms}}$ around the open-circuit potential of the test electrode. Impedance measurements were carried out in the 5 kHz to 100 Hz frequency range. The high-frequency impedance nearest 0° phase shift was recorded as the electrolytic impedance. This term represents the combined resistive impedances from the test reference electrode fill, porous frit junction, laboratory reference-electrode fill and frit junction, and waste simulant solution. Some EIS scans were performed over a wider frequency range of 10 kHz to 2 MHz using a $3.5 \text{ mV}_{\text{rms}}$ sine wave excitation. The low-frequency response in these scans was used to study interfacial changes on the Ag/AgCl wire elements of electrodes that exhibited either a large positive drift or a large negative potential drop.

Long-term tests of VLSJ Ag/AgCl reference electrodes were carried out over periods ranging to about 3 years. Figure 2-15 summarizes the potential trends that were observed for continuously immersed and retracted (i.e., periodically immersed, either weekly (“w”) or monthly (“m”)) electrodes as a function of time in various waste simulants.²³

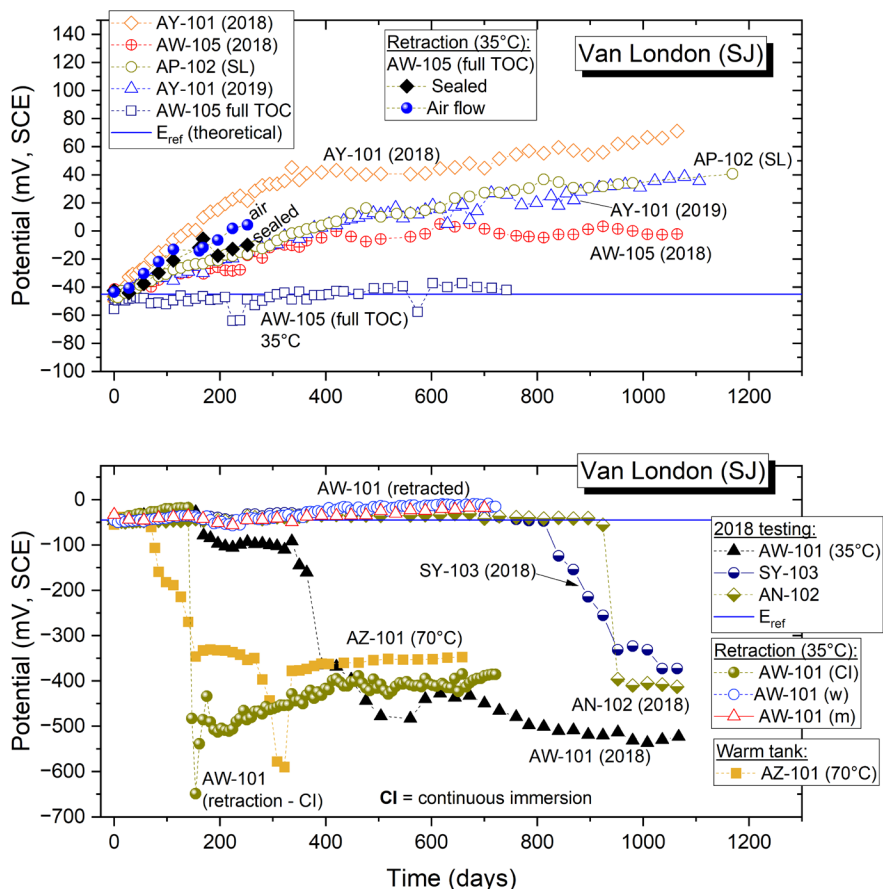


Figure 2-15. Potential trends observed in DNV long-term studies of continuously immersed and retracted VLSJ reference electrodes in various DST supernatant liquid waste simulants.²³

From the potential trends, the degradation/failure modes for Ag/AgCl electrodes could be broadly classified into two types: (1) monotonic positive drift from the initial potential, and (2) sharp drop to negative potentials after a period of relative stability. The degradation was attributable to diffusive intermixing of the internal fills of the Ag/AgCl reference electrodes with the external simulant solutions over time through the porous frit junctions leads to extensive KCl depletion and contamination of the fills, causing loss of potential stability. All of the simulants in which the reference electrodes exhibited positive drifts had pHs, calculated using OLI software, that were below about 14.8. On the other hand, the simulants in which the electrodes exhibited a sharp potential drop either had pHs greater than 14.9 (AW-101 and SY-103) or a high temperature (AZ-101, 70°C). The period of relative stability prior to the sharp potential drop was

²³ K. Evans, et al., *In-Tank Corrosion Probes: DNV laboratory evaluations of reference electrodes, Presentation at the Tank Integrity Expert Panel Corrosion Subgroup Meeting, Denver, CO, March 2023.*

shorter at higher pH or higher temperature. The exception to these trends was the AN-102 simulant, which had a pH of 14.4, exhibited a relatively stable potential over about 900 days and then exhibited a large potential drop.

During the long-term tests, EIS measurements were also periodically performed on the electrodes. The EIS measurements were performed under potential control using a sinusoidal AC voltage perturbation of 5 mV_{rms} around the open-circuit potential of the test electrode in a frequency range of 5 kHz to 100 Hz. Figure 2-16 shows the high-frequency impedance, nearest 0° phase shift, of VLSJ Ag/AgCl electrodes as a function of time in various DST supernatant liquid waste simulants. This term represents the combined resistive impedances from the test reference electrode fill, porous frit junction, laboratory reference-electrode fill and frit junction, and waste simulant solution. The high-frequency impedances of the electrodes tested in the SY-103, AN-102, and AW-101 simulants exhibited some increase with time compared to their initial values but, in general, the impedances of all of the electrodes remained low (<600 Ω). Furthermore, no correlation was observed between the large potential drops that were observed for the SY-103, AN-102, and AW-101 electrodes (Figure 2-16) and the changes in their high-frequency impedances.

After completion of the long-term exposures to various waste simulants, various methods were used to analyze some of the tested SJ Ag/AgCl electrodes and compare them with a fresh, unused electrode (“Exemplar”) of the same type to understand the reasons for degradation. These methods included visual examination to identify physical damage, and internal investigations, after cutting the electrodes open, by chemical analysis and FTIR spectroscopy of the fill, and Raman spectroscopy and scanning electron microscopy (SEM) with energy dispersive x-ray spectroscopy (EDS) of the Ag/AgCl wire elements.²⁴

No damage was observed on the PVDF bodies of the electrodes after the long-term exposures. However, the fills in all the electrodes had transformed from colorless gels into light brown, viscous liquids or jelly-like, wet semi-solids. Chemical analysis of electrode fills (Figure 2-17) revealed significant depletions in the K⁺ and Cl⁻ concentrations of all of the tested SJ Ag/AgCl electrodes compared to the Exemplar. Significant contamination by Na⁺, OH⁻, NO₃⁻, and NO₂⁻ ions was observed due to intrusion from the respective waste simulants through the electrode frits. The pHs of the fills had increased to 13 or higher compared to about 6 in the Exemplar.

Samples of fills extracted from the SJ Ag/AgCl Exemplar and AW-101 electrodes were analyzed by FTIR. The IR spectrum of the Exemplar gel showed two major absorbance bands close to those of water, indicating the presence of water-related O-H stretch and H₂O molecule bending vibrations. After subtracting the water spectrum, the Exemplar fill's IR peaks closely matched those of sodium carboxymethylcellulose (NaCMC), a common hydrogel former used to reduce ionic mobility and leakage in reference electrode fills. The AW-101 fill showed significant changes including the absence of the O-H stretch band, indicating water loss, and heavy nitrate and nitrite contamination from the AW-101 waste simulant (Figure 2-18). It is possible that structural changes such as cross-linking also occurred in the NaCMC structure.

²⁴ S, Chawla, K. Evans, S. Feng, and N. Sridhar, *Long-Term Performance of Reference Electrodes in Alkaline Radioactive Waste Storage Environments*, Corrosion, 2024, **80**(5): 472-488.

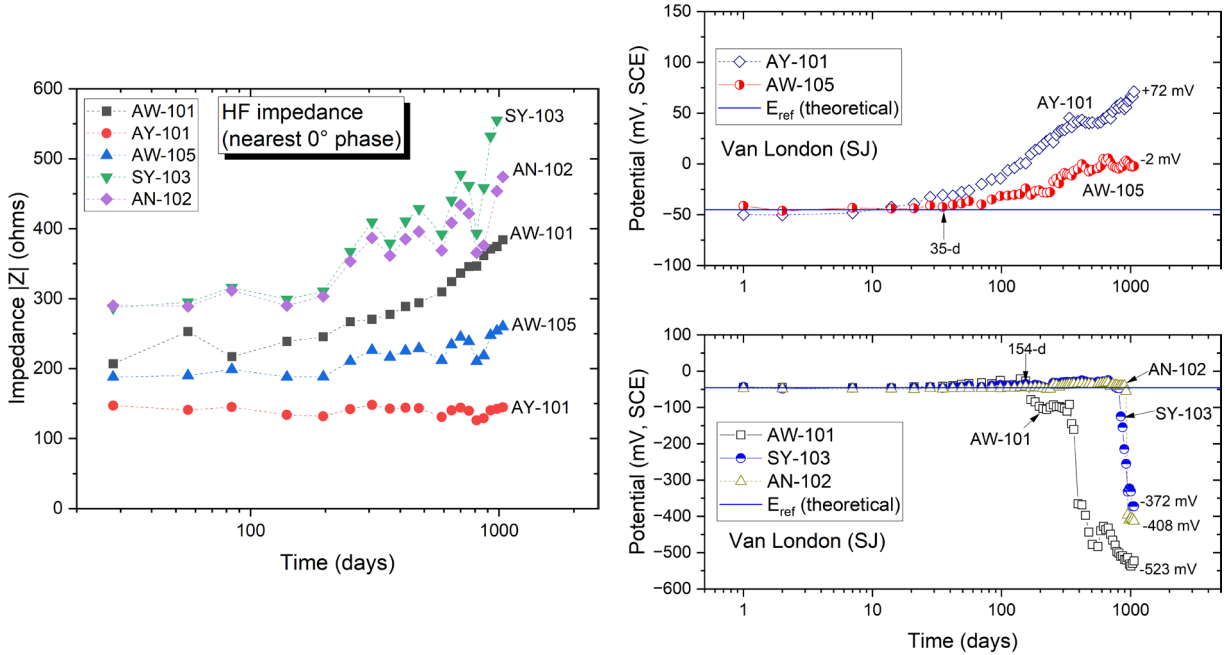


Figure 2-16. Left: High-frequency impedance, nearest 0° phase shift, of VLSJ Ag/AgCl electrodes as a function of time in various DST supernatant liquid waste simulants. Right: Corresponding potential trends of the electrodes over the same exposure period.²³

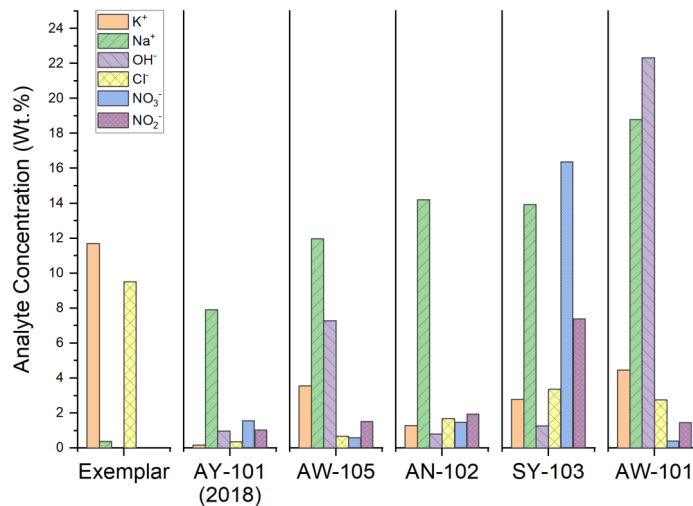


Figure 2-17. Concentrations of selected analytes measured in the fills of SJ Ag/AgCl electrodes after ~1064 days of immersion in various waste simulants, compared to an Exemplar.

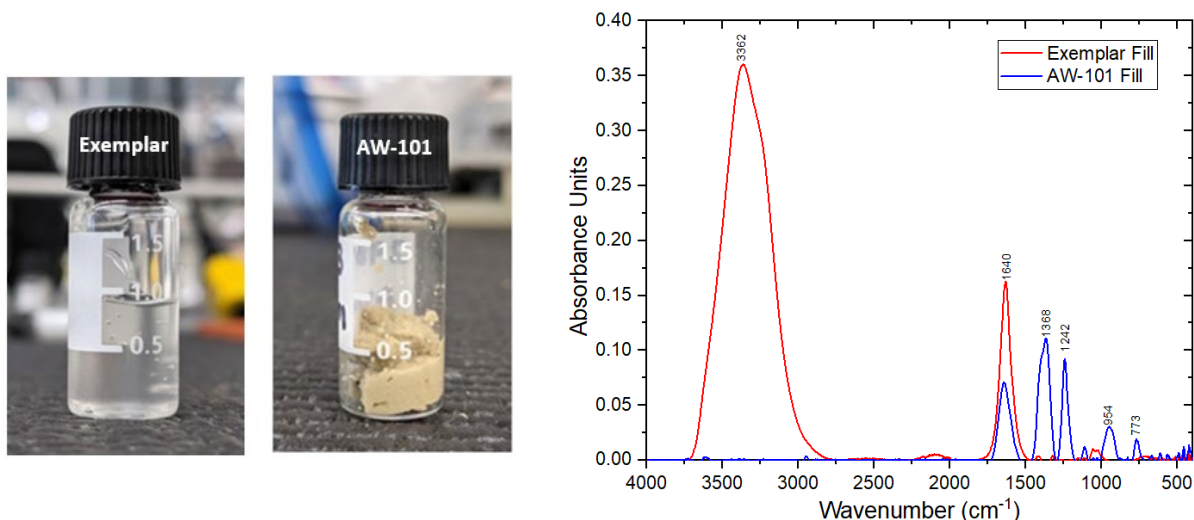


Figure 2-18. Left: Photographs of fill samples extracted from an Exemplar VLSJ Ag/AgCl electrode and the AW-101 electrode (after ~1064 days of immersion in waste simulant). Right: FTIR spectra from the two electrode fills.

An SEM examination of SJ Ag/AgCl wire elements showed varying degrees of chemical attack on the AgCl layers due to waste simulant intrusion, with specific observations for different electrodes (Figure 2-19). The SEM images revealed that the AgCl layers on electrodes tested in AN-102 and SY-103 simulants experienced deep intercrystalline attack; whereas the electrode tested in AY-101 simulant showed only superficial surface roughening. The AgCl coating on the AW-101 wire was the thinnest amongst all the wires. Except for two large (~2-mm) accretions, the coated region on the AW-101 wire was uniformly thin and smooth. EDS analysis indicated that the AgCl layers on the examined electrodes contained high concentrations of elements like C, N, O, F, Na, Al, and K, originating from waste simulants, with significant deviations in Ag/Cl ratios compared to the Exemplar electrode.

Full spectrum EIS scans, in a wider frequency range of 10 kHz to 2 MHz and using a 3.5 mV_{rms} sine wave excitation, were performed on two VLSJ Ag/AgCl reference electrodes and compared to an Exemplar to study their potential trends and frequency responses (see Figure 2-20). The first electrode, exposed to AY-101 simulant, showed a positive monotonic drift of 76 mV over 918 days, while the second electrode, exposed to AW-101 simulant, exhibited a large negative potential drop of about 377 mV over 529 days. The low-frequency impedance, which is representative of the polarization resistance, was slightly higher for the positively drifted electrode (AY-101) and more than an order of magnitude higher for the negatively drifted electrode (AW-101) compared to the Exemplar, as shown in Figure 2-20. The large increase in low-frequency impedance in the AW-101 electrode was attributable to loss of the AgCl layer due to chemical attack by the intruded waste. Significant differences in phase shift were observed below 1 Hz, with the negatively drifted electrode (AW-101) showing higher phase angles. At frequencies above 1 kHz, the impedance magnitudes of both drifted electrodes were only slightly higher than the Exemplar, and the phase angles were close to 0°, indicating resistive response.

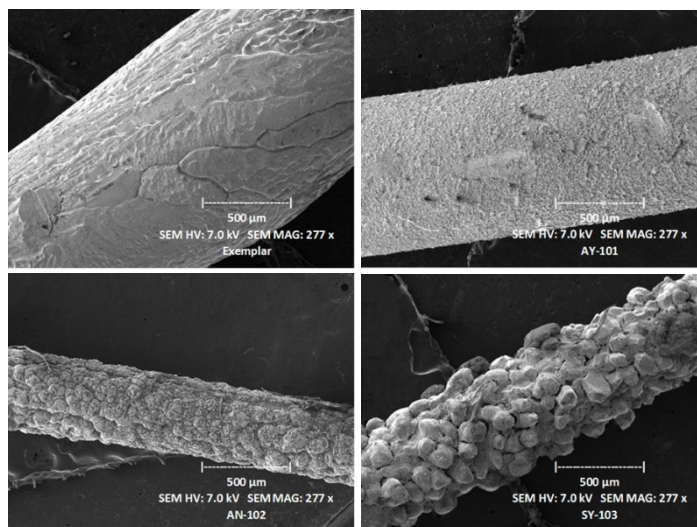


Figure 2-19. SEM secondary electron images of wire elements of SJ Ag/AgCl electrodes; clockwise from top left: Exemplar, AY-101 (2018), SY-103, and AN-102.

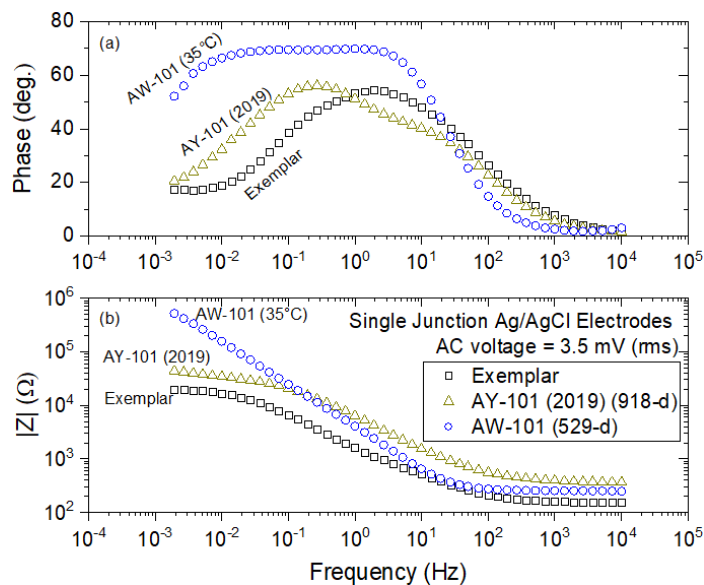


Figure 2-20. Phase angle (top) and magnitude of impedance (bottom) obtained from EIS of VLSJ Ag/AgCl electrodes after long-term exposures in AY-101 and AW-101 waste simulants, compared to an Exemplar tested in 4M KCl.

The potential response of a fresh SJ Ag/AgCl electrode to intentional contamination with AY-101 (2019) simulant showed a positive drift in potential over 11 contamination steps, with a final drift of about 60 mV (Figure 2-21). This behavior was similar to that observed in long-term natural contamination.

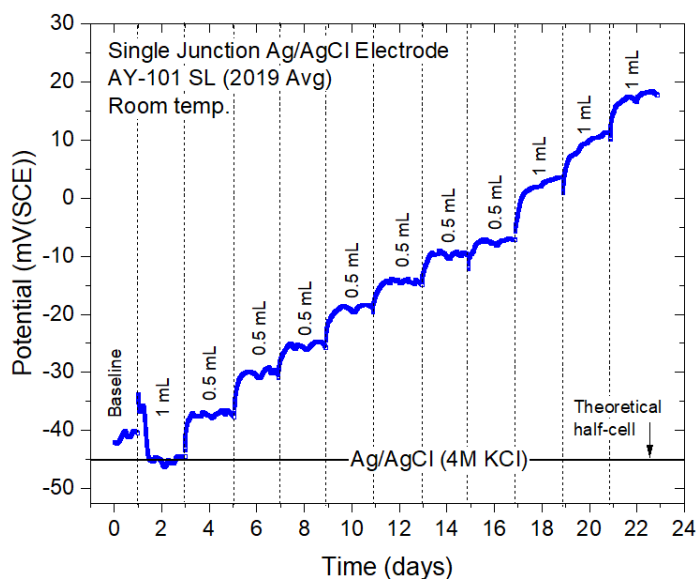


Figure 2-21. Potential change of SJ Ag/AgCl reference electrode in response to incremental intentional contamination of fill solution with AY-101 (2019) waste simulant at room temperature.

In summary, the long-term testing of VLSJ Ag/AgCl reference electrodes in various DST waste simulants showed the following:

- Over time, the porous frit junctions caused extensive KCl depletion and contamination of the electrode fill, resulting in a loss of potential stability.
- The main degradation modes for the reference electrodes were monotonic, positive potential drift, and sharp drops to negative potentials.
- Electrode failure by large potential drop occurred in waste simulants with very high pHs. This type of failure was accompanied by a large increase in polarization resistance and attack and thinning of the AgCl layer by the intruded waste simulant.

2.3 Testing in Actual Wastes at 222-S

A long-term study on Ag/AgCl reference electrodes in radioactive supernatant waste samples drawn from various DSTs was performed in hot cells at the Hanford 222-S Laboratories.²⁵ Three different Ag/AgCl reference electrode designs from Manufacturers A, B, and C were tested, each with distinct materials and geometries. The main features of the electrodes from the three manufacturers are summarized in Table 2-9. The electrodes from Manufacturer A (Van

²⁵ S. Feng, S. Chawla, D. Frye, K. Evans, and N. Sridhar, *Long-Term Performance of Ag/AgCl Reference Electrodes for Corrosion Potential Monitoring in Radioactive Tank Waste at the Hanford Site*, *Corrosion*, 2024, **80**(6): 660-672.

London Co.) contained a gel fill and were the same type currently deployed in Hanford DSTs. The electrodes from Manufacturer B (eDAQ Inc) contained a liquid fill, and the electrodes from Manufacturer C (BORIN Manufacturing) contained a wet solid fill.

Table 2-9. Main features of the single junction Ag/AgCl reference electrodes tested in DST wastes.

Manufacturer		A	B	C
Size	Diameter (cm)	1.9	0.5	3.1
	Length (cm)	10	13	21
Body material		PVDF ^(A)	PEEK ^(A)	ABS ^(A)
Junction	Material	Porous PVDF	Polymer	Ceramic
	Surface Area (cm ²)	0.28	0.13	6.02
Electrolyte		4 M KCl in aqueous gel	3.4 M KCl in water	NaCl loaded in solid fill
Measured potential of as-received electrodes at 25°C (mV _{SCE})		-41±3	-27±3	-49±5
^(A) PVDF: Polyvinylidene fluoride; PEEK: Polyether ether ketone; and ABS: Acrylonitrile butadiene styrene				

The reference electrodes were tested in supernatant from various tanks, including AN-106, AP-102, AW-101, AW-105, AY-101, and AZ-101, under different temperatures and radiation levels. The Ag/AgCl reference electrodes from different manufacturers were tested in 500-mL glass jars containing tank waste supernatants at temperatures representative of the tank conditions, primarily at 35°C and ambient hot cell temperature. Weekly measurements involved monitoring potentials of Ag/AgCl reference electrodes and tank liner carbon steel against a laboratory SCE using a Luggin tube. EIS was used to characterize changes in electrolytic resistivity and polarization processes of Ag/AgCl reference electrodes due to exposure to tank wastes, with measurements performed bi-weekly. Dose rates were measured and calculated for the test cells and actual tanks, with the highest dose rate inside the test cell observed in the AZ-101 waste due to a high Cs-137 concentration. Failed electrodes were analyzed using x-ray microtomography (XMT), SEM/EDS, and Raman spectroscopy to examine conditions and changes in the electrodes.

Ag/AgCl electrodes from Manufacturer A showed a general increase in potential over time, with significant drops indicating failure, especially in AW-101, AN-106, and AP-102 tank wastes (Figure 2-22). Electrodes from Manufacturer B also failed, exhibiting sudden potential drops in various tank wastes, with the most significant drop being 900 mV in AW-105. Electrodes from Manufacturer C were more stable compared to A and B, with only minor fluctuations and potentials remaining close to the initial values.

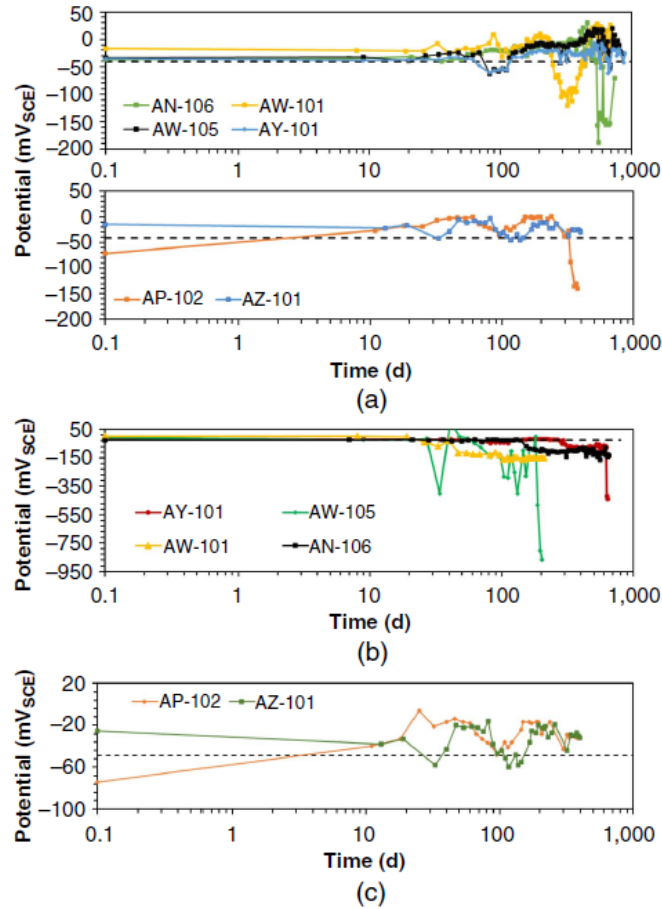


Figure 2-22. Potentials of Ag/AgCl Reference electrodes from Manufacturers (a) A, (b) B, and (c) C collected over different durations in various tank waste samples.

Impedance measurements (Figure 2-23) indicated that the polarization resistance (R_p) increased significantly over time, correlating with potential changes, especially for electrodes exposed to AN-106, AW-101, and AP-102.

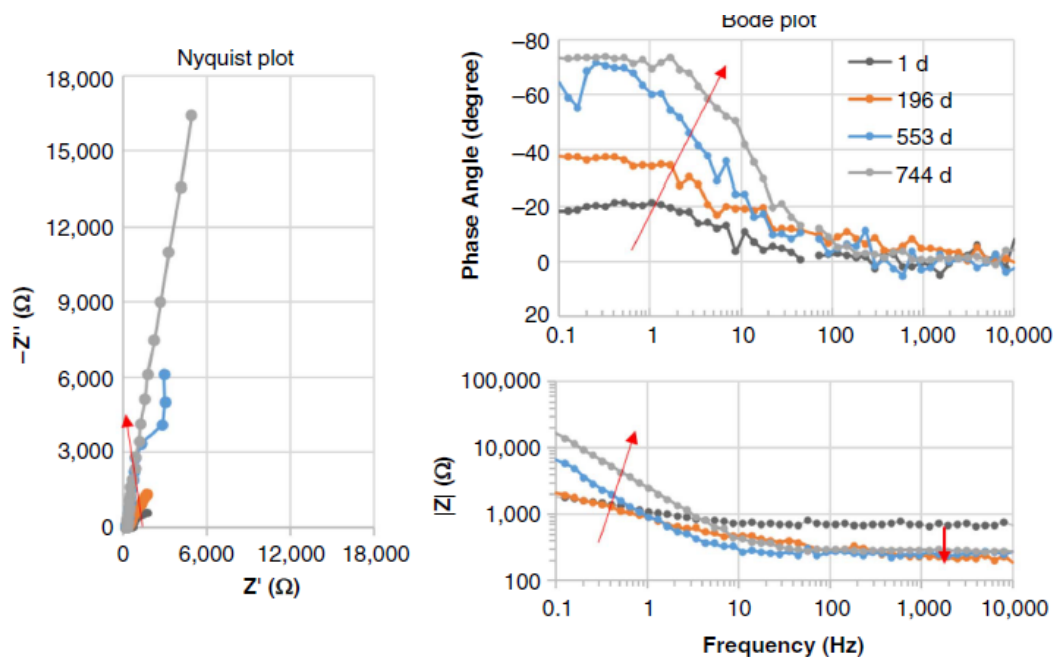


Figure 2-23. Time-evolution of EIS spectra of electrode from Manufacturer A exposed to Tank AN-106 supernatant waste sample at 35°C.

Radiography and computed tomography scans (Figure 2-24) showed significant degradation inside the electrode from Manufacturer A, including thinned Ag wires, loose AgCl layers, and clogged frit materials. Electrodes remained radioactive even after cleaning, indicating tank waste intrusion into the electrode body.

SEM/EDS analysis revealed the formation of new compounds on Ag wires, including elements like C, O, Na, Al, and Si, indicating chemical reactions with tank waste. Analysis of the frit junction materials showed clogging by materials from tank waste, with elements like Na, Al, and Si being predominant. Raman spectroscopy showed peaks indicating the presence of Ag-Cl bonding and new chemical phases formed during tank waste exposure.

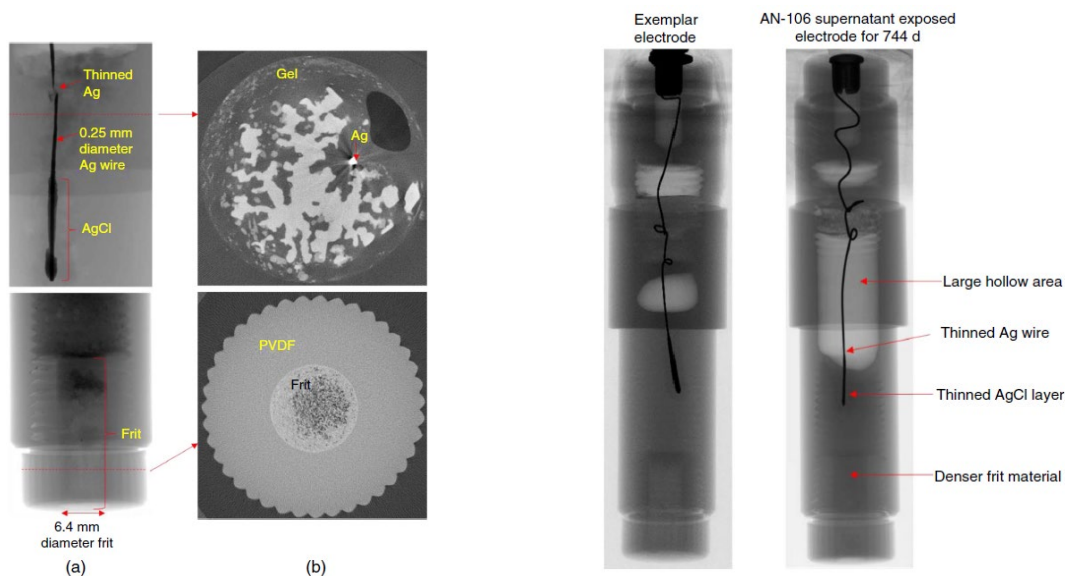


Figure 2-24. Left: Radiographs and XMT cross sections of Manufacturer A electrodes after testing in Tank AW-101 supernatant waste. Right: Radiographs of an exemplar electrode from Manufacturer A and an electrode exposed in Tank AN-106 supernatant waste sample at 35°C for 744 days.

In summary, the long-term testing of the reference electrodes in radioactive waste samples from various DSTs showed the following:

- The primary degradation mechanisms included the intrusion of aggressive chemicals through porous frit materials, leading to clogging, physical and chemical degradation of the AgCl, and alteration of the internal electrolyte. The chemical composition of the tank waste, including the presence of aggressive anions, significantly influenced the degradation and performance of the electrodes.
- Radiolytic species such as H_2O_2 and HNO_3 may have contributed to the degradation of the Ag wire, but chemical effects were more significant than radiation in long-term performance.
- Gradual potential drift, electrolyte resistance decrease, and increased polarization resistance indicated degradation, while a sudden potential drop of over 100 mV signified electrode failure.
- Electrode design and environmental conditions significantly affect the performance and failure probability of Ag/AgCl electrodes, with chemicals having a stronger impact than radiation.
- The studies concluded that electrode design and environmental conditions significantly affect performance, with solid-state electrodes showing the most promise for future deployment.

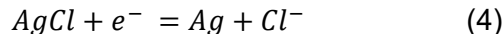
3.0 Chemically and Radiation Resistant Materials

The previous sections have demonstrated that the commercial electrodes, particularly the internal junction materials, are susceptible to contamination and degradation due to the waste chemistry. Radiolysis may also factor into the degradation of the Ag wire. In this section, candidate materials for the reference electrode that are chemically robust and radiation resistant are considered.

3.1 Degradation of Ag/AgCl Reference Electrodes

When a conventional Ag/AgCl reference electrode is deployed in a tank supernatant, significant contamination by Na^+ , OH^- , NO_3^- , and NO_2^- ions may occur due to intrusion from the waste supernatant through the electrode frit. In addition to various ions, organics ligands are also likely to diffuse through the frit into the electrode chamber, contributing to the contamination. The potential of the reference electrode is strongly dependent upon the microenvironment for the Cl^- -containing solution (usually potassium chloride or sodium chloride to minimize the liquid junction potential) in contact with Ag/AgCl. Contact of this electrode solution with the external environment occurs through an ion conducting bridge (porous membrane or frit). Dilution of the Cl^- solution or contamination with an incompatible external environment can cause large shifts in the generated reference electrode potential.

In the tank supernatant, OH^- , NO_3^- , NO_2^- and CO_3^{2-} ions are considered dominant. The potential response of the OH^- concentration can be estimated as follows²⁶. The redox half-cell reaction of the Ag/AgCl reference electrode is:



The potential of the Ag/AgCl reference electrode is governed by the activity of Cl^- ions in the fill and is given by the Nernst Equation:

$$E = E^o - \frac{2.303RT}{F} \log a_{\text{Cl}^-} \quad (5)$$

Changes in Cl^- ion activity and the chemical environment around the Ag/AgCl element inside the reference electrode shift the electrode potential. The results showed significant contamination and KCl depletion in the fills that was attributable to long exposure time, large concentration gradients of chemical species across the frit, and various other physicochemical factors.

Metathesis reactions can occur on the AgCl surface when Cl^- ions are exchanged with other anions present in the waste, forming sparingly soluble silver compounds that alter the electrode's response. The formation and solubility products of these silver compounds, along with the activities of the anions, influence the electrode potential. The potential response of the electrode due to foreign ion contamination was analyzed in terms of the Nikolskii-Eisenman Equation:

²⁶ S, Chawla, K. Evans, S. Feng, and N. Sridhar, *Long-Term Performance of Reference Electrodes in Alkaline Radioactive Waste Storage Environments*, Corrosion, 2024, **80**(5): 472-488.

$$E_{obs} = E^o + \frac{2.303RT}{z_i F} \log \left(a_i + \sum_{j \neq i} K_{i-j} a_j^{z_i/z_j} \right) \quad (6)$$

where E_{obs} , is the electrode potential; E^o is a term that includes all potential contributions that are independent of ionic activities, a ; subscripts i and j represent the primary (analyte) ion (i.e., Cl^- for the Ag/AgCl electrode) and an interferant ion, respectively; z is the ionic charge; and K_{i-j} is the potentiometric selectivity coefficient, which determines the effect of the interferant ion. Potentiometric selectivity coefficients quantify the effects of interferant ions on the potential response of ion-selective electrodes, including the Ag/AgCl electrode. The Nikolskii-Eisenman Equation is empirical in nature and assumes a Nernstian potential response to the primary ion as well as the interferant ions, with K_{i-j} being a weighting factor for the latter. When no interferants are present or the selectivity coefficients of the interferants' activities are very low, the Nikolskii-Eisenman Equation (Equation 6), reduces to the Nernst Equation (Equation 5) for the primary ion. Hydroxide ion was identified as a dominant interferant for the Ag/AgCl electrode in alkaline media, forming insoluble AgOH and potentially transforming into more stable Ag(I) oxide. A selectivity coefficient for hydroxide ion, $K_{\text{Cl-OH}}$, was estimated from the intentional contamination study and used to calculate the long-term potential drifts for various combinations of Cl^- and OH^- activities in the fills of contaminated Ag/AgCl reference electrodes.

The organic species are also likely to interact with these Ag species and affect the solubility of Ag/AgCl in the supernatant. These organic species can pose challenges when designing a reference electrode to minimize the internal contamination and interaction with the Ag species. To maximize the performance reference electrodes, careful consideration of materials for the internal and outer components are a necessity.

3.2 Internal Reference Electrode Materials

The degradation of the internal materials of Ag/AgCl reference electrodes provides a challenging obstacle to overcome in complex sample matrixes such as tank waste. Throughout this section, several materials will be reviewed to maximize the performance of the internal components of the Ag/AgCl reference electrodes to allow for accurate, reliable, and continuous measurements.

Several documents from DNV and Hanford indicate that the failure of the reference electrode has been thought to be due to containments attached to the silver wire, or the silver wire deteriorating over time.²⁷ Upon development of a degradation resistant reference electrode the material of the wire should be considered to decrease the amount of degradation. In a patent Alvarez et al., developed and demonstrated the use of a solid state Ag/AgCl carbon nanotubes (CNT) thread reference electrode. A bare CNT thread was plated with 0.3 M AgNO_3 in 1M NH_3 to form Ag on the CNT and then AgCl was formed on the surface using FeCl_3 . They found during the testing that the Ag/AgCl coated CNTS are comparable to the commercial Ag/AgCl reference electrodes. While they did not include long term stability tests, the physical and chemical characteristics of carbon nanotubes could provide interesting results when

²⁷ K. Evans, S. Chawla, K. Sherer, B. Rollins, and J. Beavers. DNV. *In-Tank Corrosion Probes: DNV Laboratory Evaluations of Reference Electrodes*. March 2023.

incorporated into reference electrodes.²⁸ In another example employing carbon nanotubes, Rius et al., developed a solid-state reference electrode using carbon nanotubes as the transducer layer between a polyacrylate membrane to entrap the Ag/AgCl system.²⁹ They found that the performance of the solid-state reference electrode was best (insensitivity to changes in KCl, NaCl, NaNO₃ and pH) with photo-nBA reference membrane single walled carbon nanotubes. Generally, carbon nanotubes have been shown to exhibit carrier mobility, chemical stability, and offer chemical functionalization for tunability for various applications. Therefore, employing carbon nanotubes to be used for some of the internal components of the reference electrode could offer higher chemical resistance in the event the tank waste leaches into the compartments.

Moreover, because of the tank waste supernatant's intrusion through the frit, the frit of the reference electrode can be the largest limitation of the accuracy and viability provided by the reference electrode. For example, the Van London reference electrodes currently employed in waste tanks to monitor the potential have a porous frit type and the junction material is Kynar with a fill solution of 4 M KCl gel. After forensic investigation of the Van London reference electrodes, DNV found that several of them have failed due to the intrusion of tank waste through the porous frit junction by analyzing the gel filling and silver wire. Both the gel filling solution and the silver wire were affected by the tank waste and led to the failure of the electrodes.³⁰ Therefore, the search for alternative materials for the frit/junction type are vital to the development of a stable and accurate reference electrode.

Bühlmann et al. performed several studies on various porous glass frits and porous polymer frits. They found that, while increasing the pore size of the glass frits, the sample dependence of the potential decreases. While this improves the performance of the electrode, the disadvantage of the larger pores allows for intermixing of the solution with the internal solution due to higher flow rates through the frit. In comparison to porous glass frits, they looked at porous polymer frits. They used porous polyethylene and Teflon frits and found that they had more stable potentials over time; however, because the pores are larger, they still cause internal contamination of the reference solution.³¹ In an example by Rafea et al., to alleviate cross contamination from the frit, mesoporous borosilicate glass-ceramic compositions were used as frits in reference electrodes. They found that the mesoporous glass-ceramic frit-based reference electrodes exhibited a lower flow rate compared to available microporous frit based reference electrodes such as Teflon, KT-glass, and polyethylene. The average pore size for the mesoporous glass-ceramic frits were around 2.2 nm while other reference electrode frits such as Teflon, KT-glass and polyethylene had pore sizes of 1 µm, 0.5 -1 µm, and 10 µm, respectively. Teflon, KT-glass, and polyethylene also had a significantly larger documented

²⁸ U.S. Pat. Appl. 2017; US 20170363563 A1 20171221 Carbon nanotube based reference electrodes and all-carbon electrode assemblies for sensing and electrochemical characterization 2. N. T. Alvarez; D. Zhao; W. Heineman; V. Shanov; D. Siebold

²⁹ F. Xavier Rius-Ruiz, A. Kisiel, A. Michalska, K. Maksymiuk, J. Riu, and F. Xavier Rius, Solid-state reference electrodes based on carbon nanotubes and polyacrylate membranes, *Analytical and Bioanalytical Chemistry*, 2011, **399**: 3613-3622

³⁰ S. Feng. *Tank Deployable Reference Electrode Testing at 222-S Laboratory*. TIEP Corrosion Subgroup Meeting. March 23, 2023.

³¹ M. P. S. Mousavi, S. A. Saba, E. L. Anderson, M. A. Hillmyer, and P. Bühlmann, *Avoiding Errors in Electrochemical Measurements: Effect of Frit Material on the Performance of Reference Electrodes with Porous Frit Junctions*, *Analytical Chemistry*, 2016, **88**: 8706-8713

potential drift of 200 $\mu\text{V}/\text{h}$ compared to $-2.4 \mu\text{V}/\text{h}$ from the mesoporous glass-ceramic reference electrodes.³²

Additionally, inorganic glass composites with good ionic conduction have been studied as solid electrolytes in electrochemical systems. Two interesting materials $\text{Na}_{1+x}\text{Zr}_2\text{Si}_x\text{P}_{3-x}\text{O}_{12}$ (NASICON) and $\text{Na}_2\text{Zn}_2\text{TeO}_6$ (NETO). An extensive literature study of doped $\text{Na}_{1+x}\text{Zr}_2\text{Si}_x\text{P}_{3-x}\text{O}_{12}$ shows that the materials exhibit highest conductivities when containing 3–3.5 sodium ions per formula unit, M cation with an ionic radius close to $r = 0.72 \text{ \AA}$ as well as silicon ions substituting phosphorous ions. The ion-conductivity of $\text{Na}_2\text{Zn}_2\text{TeO}_6$ is a novel solid sodium-ion conductor. For likely deployment in the waste tanks, the long-term stability of these ion-conducting composites needs to be evaluated.

In another instance involving stability of reference electrodes, Shen and coworkers studied the degradation of Ag/AgCl reference electrodes in choline chloride based deep eutectic solvents, and developed a Pt $[\text{Fe}(\text{CN})_6]^{3-}/[\text{Fe}(\text{CN})_6]^{4-}$ reference electrode to combat the challenges.³³ In many studies, the Ag/AgCl reference electrode has been found to be incompatible with deep eutectic solvents because of the anhydrous nature and high concentration of chloride ions. To demonstrate the instability of the Ag/AgCl reference electrode, they performed a cyclic voltammetry study over 800 cycles, 14 hours, and exhibited a dramatic shift of the redox potential of ferrocene. Ferrocene is a common internal standard to test redox potentials. As shown in Figure 3-1, the shift of the potential is attributed to the shift of the reference potential of the Ag/AgCl reference electrode due to the degradation. After two weeks of heavy usage of the FCN reference electrode it was used in a cyclic voltammetry study to determine the stability of the redox potential of ferrocene (Figure 3, right).

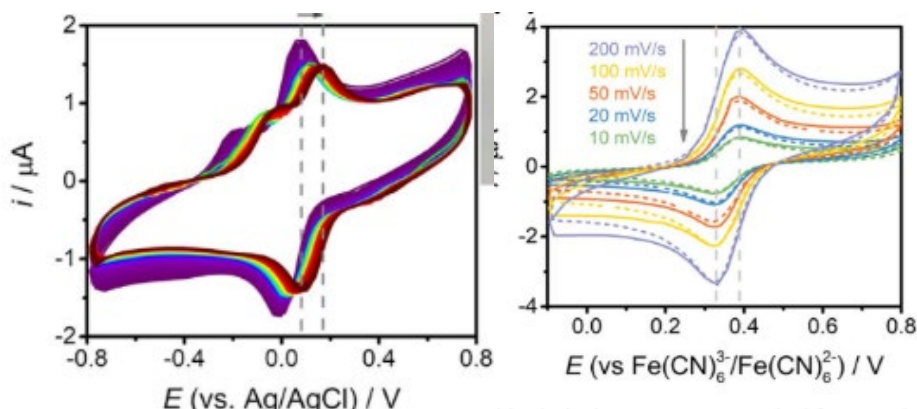


Figure 3-1. Cyclic Voltammetry curves for Ag/AgCl reference electrode over 800 scans in ferrocene (left), FCN reference electrode in ferrocene after 2 weeks of vigorous use (right).³³

It is thought that the FCN reference electrode would be highly stable for this particular system because the high viscosity of ethaline leads to low diffusivity of $[\text{Fe}(\text{CN})_6]^{3-}/[\text{Fe}(\text{CN})_6]^{4-}$ and minimizes the diffusion of ions across the porous frit.³³ While the degradation of the Ag/AgCl is notable, the reason for the degradation is something that Shen and coworkers wanted to

³² I. H. A. Badr and O. A. S. Rafeaa, *Evaluation of mesoporous borosilicate glass-ceramic composites as frits in reference electrodes*, Royal Society of Chemistry, 2022, **12**: 28878-28885

³³ X. Shen, et.al., *Evaluating and Developing a Reliable Reference Electrode for Choline Chloride Based Deep Eutectic Solvents*, Journal of the Electrochemical Society, May 2020, **167**(8).

investigate further. They found a correlation between the stable time (t_s) and the film thickness of the AgCl film (Figure 3-2). This suggests that over time the AgCl is constantly being lost from the Ag wire.³³ Since there were no documented solids, it was thought the AgCl was dissolving in the ethaline. Many previous studies have suggested the AgCl dissolving from the Ag wire to form other complexes, such as dissolving in concentrated hydrochloric acid or in non-aqueous solutions dissolving in acetonitrile containing high concentrations of chloride.³³ Seemingly, the Ag/AgCl reference electrode can be problematic with the AgCl becoming unstable and dissolving over time in a variety of solutions.

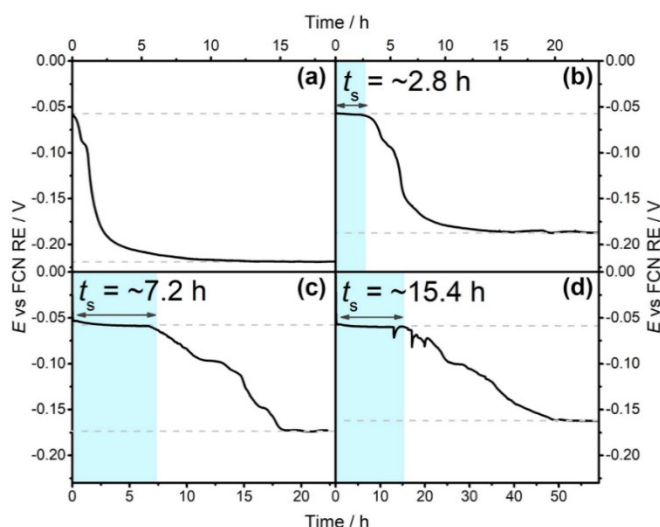


Figure 3-2. The correlation of the stable time with the thickness of the AgCl film. A)5, B)20, C)50, D)100. *The numbers indicate the amount of square wave cycles to thicken the film.³³

While the longevity of this study³³ is still not where the reference electrode for the waste tank systems should be, it gives more thought to controlling and tuning the reference electrodes for a given application. More specifically, controlling the film thickness of the AgCl offers tuneability and the idea of using the viscosity of the solution to minimize the diffusion of ions through the frit is a creative way to use the contents to their advantage.

Overall, by optimizing the materials for the internal components of the reference electrode, the aim is to lessen the cross contamination from the tank waste and the internal components of the reference electrode. By achieving this, the reference electrode will be more robust in a high activity environment and have longer lifetime stability.

3.3 Irradiation effects on Ag/AgCl reference electrodes and tank composition

While maximizing the internal components of the reference electrode by material selection and optimization, another challenging aspect of designing a reference electrode for tank waste is the irradiation effects on Ag/AgCl reference electrodes.

Radiation creates high-energy, transient redox species that may cause the RE potential to drift from the thermodynamic value when they recombine upon the electrode surface. Radiolysis of water generates active species such as hydrated electrons and hydroxyl radicals as follows³⁴:



Hydrated electrons directly reduce Ag^+ precursor to Ag^0 nuclei (Reaction V), which progressively coalesce into clusters. To prevent hydroxyl radicals from oxidizing nascent Ag^0 clusters, scavengers such as alcohols are usually added prior to the irradiation process to react with the hydroxyl radicals. This results in the formation of hydroxyalkyl radicals, which, in turn, react with other molecules in solution to produce new radicals for the reduction of Ag^+ to Ag^0 .³⁵ Reactions (I)~(V) indicate that the chemicals and radioactivity in the tank supernatant can cause the degradation of Ag/AgCl reference electrodes, characteristic of the electrode potential shift and the changes of the electrode structures.

In Hanford waste supernatants, numerous chemicals and radionuclides have been detected.³⁶ The major non-radioactive chemicals include but are not limited to: NaOH , NaNO_2 , NaNO_3 , NaF , NaCl , NH_4Cl , HCOONa , NaAc , Na_2CO_3 , acetonitrile, uranium, lead, chromium, benzene, butanol, Hg, biphenyls, trichlorophenol, Na_4EDTA . Major radionuclides are listed in Table 3-1.³⁷

Table 3-1. List of radionuclides in tank wastes

Radionuclides	Type of Radioactivity	Half-life
Hydrogen-3 (tritium) (^3T)	β decay	12.3 years
Carbon-14 (^{14}C)	β decay	5730 years
Strontium-90 (^{90}Sr)	β decay	29 years
Technetium-99 (^{99}Tc)	β decay	210000 years
Iodine-129 (^{129}I)	β, γ decay	16 million years
Cesium-137 (^{137}Cs)	β, γ decay	30 years
Uranium isotopes (^{233}U , ^{234}U , ^{235}U , ^{238}U)	α decay	703.8 million years for ^{235}U
Neptunium-237 (^{237}Np)	α, γ decay	2144000 years
Plutonium isotopes (^{239}Pu , ^{240}Pu , ^{241}Pu)	α decay	24,100 years for ^{239}Pu
Americium (^{241}Am)	α, γ decay	432 years

³⁴ P. Uttayarat, J. Eamsiri, T. Tangthong, P. Suwanmala, *Radiolytic Synthesis of Colloidal Silver Nanoparticles for Antibacterial Wound Dressings*, *Advances in Materials Science and Engineering*, Advances in Materials Science and Engineering, **2015**: 376082.

³⁵ B. Soroushian, I. Lampre, J. Belloni, M. Mostafavi, *Radiolysis of silver ion solutions in ethylene glycol: solvated electron and radical sea venging yields*, *Radiation Physics and Chemistry*, 2005, **72**(2-3): 111-118.

³⁶ J. Marcial, B. Riley, A. Kruger, C. Lonergan, J. Vienna, *Hanford low-activity waste vitrification: A review*, *Journal of Hazardous Materials*, 2024, **461**: 132437.

³⁷ M. J. Kupfer, A. L. Boldt, K. N. Hodgson, L. W. Shelton, B. C. Simpson, R. A. Watrous, M. D. LeClair, G. L. Borsheim, R. T. Winward, B. A. Higley, R. M. Orme; N. G. Colton, S. Lambert, D. Place, W. W. Schulz, HNF-SD-WM-TI-740, *Standard Inventories of Chemicals and Radionuclides in Hanford Site Tank Wastes*, February 1999.

3.4 Irradiation penetration factor and radiation shielding

Ionizing radiation is electromagnetic radiation that carries higher energy than nonionizing radiation; ionizing radiation radionuclides are capable of ejecting electrons from atoms and produce negatively charged free electrons and positively charged ionized atoms. Ionizing radiation consists of any types of photons (X- and γ -rays) or particles (alpha, beta, and neutrons). The three most common types of radiation are³⁸:

- Alpha – A particle consisting of two protons and two neutrons emitted from the nucleus of an atom. These charged particles lose their energy very rapidly in matter and are easily shielded by small amounts of material, such as a sheet of paper or the surface layer of skin. Alpha particles are only hazardous when they are internally deposited.
- Beta – An electron emitted from the nucleus of an atom. These charged particles lose their energy rapidly in matter, although less so than alpha radiation. Beta radiation is easily shielded by thin layers of metal or plastic. Beta particles are generally only hazardous when they are internally deposited.
- Gamma – Electromagnetic radiation, or photons, emitted from the nucleus of an atom. Gamma radiation is best shielded by thick layers of lead or steel. Gamma energy may cause an external or internal radiation hazard. (X-rays are similar to gamma radiation but originate from the outer shell of the atom instead of the nucleus.)

The more material the radiation can pass through, the greater the penetration power and the more dangerous they are. In general, the greater mass presents the greater the ionizing power and the lower the penetration power.

Shielding has merits such as it has independent efficacy in safe working conditions over the time of exposure and distance that require continued managerial regulation. Thus, an appropriate shielding against nuclear radiation is constantly in demand for a secure life and a healthy environment as the radiation uses are consistently viable in various human activities. A good radiation shield is one that can attenuate, absorb, or block the maximum part of incident gamma radiation. The nature and mechanism of interaction between gamma rays and materials is a critical issue to study to determine the ability of these radiations to diffuse and crack in the medium that according to the mechanism of interaction helps to choose the more applicable radiation shield.

Table 3-2. Comparison of penetrating power, ionizing power, and shielding of α and β particles, and γ rays.

Particle	Symbol	Mass	Penetrating power	Ionizing power	Example shielding
Alpha	α	4 amu	Very Low	Very High	Paper skin
Beta	β	1/2000 amu	Intermediate	Intermediate	Aluminum
Gamma	γ	0	Very High	Very Low	2 inches lead

³⁸ J. Shultis, R. Faw, *Radiation Shielding and Radiological Protection* in Dan Gabriel Cacuci (ed.), *Handbook of Nuclear Engineering*, Springer Science, 2010, 1311-1448.

The radiation protection efficiency (RPE) of a material is an important parameter to know material's shielding ability and is determined as follows³⁹:

$$\text{RPE} = (1 - I/I_0) \times 100 \quad (15)$$

where I_0 and I are the un-attenuated and attenuated photon intensities respectively. Their relation follows the Lambert–Beer law as follows:

$$\ln(I/I_0) = (\mu/\rho) \times \rho t \quad (16)$$

where t (cm) is the sample thickness, μ (cm^{-1}) is the linear attenuation coefficient, and ρ (g/cm^3) is a measured density of the sample. The mass attenuation coefficient (μ/ρ) for any chemical compound or mixture of elements is given by

$$(\mu/\rho)_c = \sum_i w_i (\mu/\rho)_i \quad (17)$$

where w_i is the weight fraction and $(\mu/\rho)_i$ is the mass attenuation coefficient of the i th constituent element.

3.5 Outer Cover Reference Electrode Materials

The outer cover materials for the reference electrode provide a protective barrier of the internal components from the tank waste. As previously mentioned, the internal components of the reference electrode can fail if the tank waste leaches into the internal compartment, causing a failure of the Ag wire, frit, and/or contaminate the filling solution. Additionally, the outer cover materials can provide protection against radiation as a shield and protection against high alkaline solutions. Here, several irradiation resistant materials and alkaline resistant materials are discussed to be used for the outer cover of the reference electrode.

3.5.1 Irradiation Resistant Materials

Many types of materials have been used as radiation shielding barriers to keep a safe environment for everyday practice in all radiation facilities.⁴⁰ Customarily, lead, multiple layers of single slabs of pure elements such as barium (Ba), lead (Pb), copper (Cu), iron (Fe), and concrete are reliable, efficient, materials. However, lead and concrete are discarded from consideration; concrete, due to its heterogeneous nature and moisture variation, to predict radiation protection, and lead due to insidious hazards to human health and the environment. On the other hand, polymer and its composites offer promising suitable alternative candidates to lead and concrete in the field of radiation shielding due to its lightweight, durability, flexibility along with superior physical, mechanical, optical, and radiation resistance properties. Besides, polymers can easily be doped with sizeable amounts of high atomic number (high-Z) materials to form their composites that are more competent radiation shields.

Polymers in the form of bonded molecules are proposed in the radiation shielding industry due to their significant properties such as elasticity, compatibility, low cost, and low density, which nominate them as good candidates for radiation attenuation. Furthermore, polymers are materials containing elements with a low atomic number such as carbon (C), hydrogen (H),

³⁹ Y. Harima, *An approximation of gamma-ray buildup factors by modified geometrical progression*, Nucl. Sci. Eng, 1983, **83**(2): 484-491.

⁴⁰ Y. Wu, Z. Wang, *Progress in Ionizing Radiation Shielding Materials*, Adv. Eng. Mater., **2024**:2400855.

oxygen (O), and nitrogen (N). In polymers, radiation resistance depends on the oxygen concentration present in the material. Organic polymer materials are characterized by low density, corrosion resistance, and a low dielectric constant, which allow their application in many fields containing radiation hazard. The interaction of a polymer material with radiation determines their applicability in radiation environments. Usually, materials having dense structures are better in radiation resistance due to a high degree of symmetry.⁴¹

For example, Kacal et al., studied various polymers and their gamma radiation attenuation. They found that polyacrylonitrile, natural rubber, and polyvinylidene chloride have the highest attenuation coefficient values of the polymers tested.⁴² Similar results were found by Mann et al., that polyvinylidene chloride (PCV) has the highest attenuation to gamma radiation. Among the other polymers tested, PCV has the highest equivalent atomic number of the polymers tested, which is directly related to the attenuation of gamma radiation indicating it is the best at shielding.⁴³ To improve the polymer performance, different fillers can be added to form a polymer composite. Polymer composites are convenient because they retain the characteristics of the polymer in addition to the filler. When forming a polymer composite to be radiation resistant, it is important to think of the type of radiation that should be shielded (Table 3-2), the rate of the adsorbed dose, and size of the material.

Epoxy resins are a class of reactive prepolymers and polymers that contain epoxide groups.⁴⁴ They can react with hardeners or curing agents, form a strong, durable substance used in a variety of commercial and industrial applications. Because they have many desirable properties, including high strength, low cost, flexibility, low toxicity, good chemical resistance, low shrinkage, and good adhesive strength, they have recently been used in radiation shielding. Epoxy resins are often used as a matrix for composite materials that can be used to shield against X-rays, gamma rays, and neutrons. The properties of epoxy resins can be further improved by adding micro- and nanoparticles to the matrix. For example, bismuth oxide (Bi_2O_3) nanoparticles are often used in radiation shielding because they are effective at absorbing radiation. Al-Dhuhabat et al., studied the shielding capabilities of pure epoxy, aluminum oxide epoxy, and ferric oxide epoxy. The epoxy composites showed higher shielding capabilities than the epoxy alone. While the polymer composite with inorganic materials provides enhanced performance, polymer composites using nanofillers have a stronger molecular interaction via chemical bonding, thus leading to further enhancement in terms of overall stability.⁴⁵

⁴¹ C. More, Z. Alsayed, M. S. Badawi, A. Thabet, P. Pawar, *Polymeric composite materials for radiation shielding: a review*, Environmental Chemistry Letters, 2021 **19**(2):2057–2090.

⁴² M.R. Kaçal, F. Akman, M.I. Sayyed, F. Akman, *Evaluation of gamma-ray and neutron attenuation properties of some polymers*, Nuclear Engineering and Technology, 2019, **51**(3):818-8124.

⁴³ K. S. Mann, A. R., M. S. Heer, *Shielding behaviors of some polymer and plastic materials for gamma-rays*, Radiation Physics and Chemistry, 2015, **106**(1): 247-254.

⁴⁴ N. Moonkum, C. Pilapong, K. Daowtak, G. Tochaikul, *Radiation Protection Device Composite of Epoxy Resin and Iodine Contrast Media for Low-Dose Radiation Protection in Diagnostic Radiology*, Polymers, 2023, **15**(2): 430 (1-10).

⁴⁵ M.J.R. Aldhuhabata, M. S. Amanaa, N.a J. Jubiera, A.A. Salimb, *Improved gamma radiation shielding traits of epoxy composites: Evaluation of mass attenuation coefficient, effective atomic and electron number*, Radiation Physics and Chemistry, 2021, 179(2): 109183.

To improve the polymer performance and characteristics, a stiff material called filler can be added to the polymer matrix to form a polymer composite.⁴⁶ The combination between filler and polymer matrix provokes the formation of a mixture that influences the polymer–composite properties by retaining the properties of both the filler and the polymer. The composite materials are named according to the re-inforcement and the matrix material constituting them. There are many types of matrix materials such as metal matrix composites, polymer matrix composites, ceramic matrix composites, and epoxy resin matrix composites. The availability of radiation shielding materials that can be molded into specific shapes and used even at high temperatures is quite significant for medical and industrial procedures.

Investigators working in the field of radiation protection have focused and reported numerous polymer matrices that can be used as gamma-ray shields like high-density polyethylene (HDPE) composite loaded with tungsten (W), molybdenum sulfide (MoS_2), and boron carbide (B_4C); micro- and nanosized tungsten oxide (WO_3) dispersed emulsion polyvinyl chloride (EPVC) polymer composites; lead oxide filled isophthalic resin polymer composites; silicone rubber composites containing bismuth content; polymer bricks; polyester composites re-inforced with zinc; composites of high-density polyethylene with zinc oxide; lead oxide; $\text{Gd}_2\text{O}_3/\text{PEEK}$ composites; and ultra-high-molecular-weight polyethylene (UHMWPE) composites containing varying contents of surface-treated samarium oxide (Sm_2O_3) or gadolinium oxide (Gd_2O_3) particles as dual thermal neutron- and gamma-shielding materials.⁴⁷

3.5.2 Alkaline resistant materials

Non-oxide and oxide ceramics (SiC , YSZ, Li_2ZrO_3 , LiAlO_2 , and SrZrO_3) are generally stable in hydroxide media at low and elevated temperatures.⁴⁸ However, SiC , YSZ, Li_2ZrO_3 and LiAlO_2 may undergo structural and chemical changes due to dissolution of the ceramic particles in the hydroxide media followed by precipitation. The SrZrO_3 powder is both chemically and structurally stable. They are considered as promising separator materials in molten hydroxide for intermediate temperature water electrolysis system. Several metal oxides such as CeO_2 and TiO_2 also exhibit good alkaline stability.

Additionally, several engineering plastics exhibit high resistance to concentrated acids and alkalis.⁴⁹ Fluoropolymers are a distinct class of per- and polyfluoroalkyl substances (PFAS), high molecular weight (MW) polymers with fluorine attached to their carbon-only backbone. Fluoropolymers possess a unique combination of properties and unmatched functional performance critical to the products and manufacturing processes they enable and are irreplaceable in many uses. Fluoropolymers are thermally, biologically, and chemically stable, negligibly soluble in water, nonmobile, nonbioavailable, nonbioaccumulative, and nontoxic.

⁴⁶ S. Nambiar, J. Yeow, *Polymer-Composite Materials for Radiation Protection*, ACS applied materials & interfaces, 2012, **4**(11): 5717-5726.

⁴⁷ P. Zhang, C. Jia, J. Li, W. Wang, *Shielding composites for neutron and gamma-radiation with $\text{Gd}_2\text{O}_3/\text{W}$ core-shell structured particles*, Materials Letters, 2020, **276**(10):128082.

⁴⁸ M. Anisur, A. Aphale, M. Reisert, P. Dubey, S. Heo, J. Hong, K. Patil, H. Xu, C. Yuh, P. Singh, *Stability of ceramic matrix materials in molten hydroxide under oxidizing and reducing conditions*, Inter. J. Hydrogen Energy, 2021, **46**(28): 14898-14912.

⁴⁹ J. Sheng, *Critical review of alkaline-polymer flooding*, J Petrol Explor Prod Technol, 2017, **7**(1):147–153.

Fluoropolymers have been widely used in different chemical applications including alkaline-chlorine processes.

Polyether ether ketone (PEEK) material, has excellent alkali resistance and can be used in environments with a pH of 14. Its excellent chemical stability, mechanical properties and processing properties make it an ideal material for the manufacture of high corrosion resistance, high strength, and high durability equipment. PEEK is a thermoplastic special engineering plastic, has excellent chemical resistance, high temperature resistance and oxidation resistance. It can be used at high temperatures and pressures for long periods of time and has excellent mechanical and electrical properties.

Polyvinylidene fluoride (PVDF) is a semi-crystalline thermoplastic fluoropolymer. It is readily melt-processible. It can be fabricated by injection and compression molding. It combines high mechanical strength with good processability. Because of its good alkali resistance, PVDF membranes have been examined to extend membrane life and expand membrane applications in alkaline environments.

UHMW (ultrahigh molecular weight polyethylene) is a low-cost, versatile plastic with resistance to a broad range of chemicals, including concentrated acids and alkalis as well as many organic solvents. Its high molecular weight makes it extremely tough, with excellent resistance to abrasion and impact.

Zirfon® is a porous composite separator material composed of a polysulfone matrix and ZrO₂ which is present as a powder.⁵⁰ The manufacturing is based on the film-casting technique. The separator is very stable in concentrated KOH solutions at elevated temperatures. The ZIRFON PERL UTP 500 membrane is composed of an open mesh polyphenylene sulfide fabric which is symmetrically coated with a mixture of a polymer and zirconium oxide.

Another class of alkaline resistant materials are superhard materials.⁵¹ These include but are not limited to carbon allotropes, with the hardest possible material being diamond, followed by carbon nitrides, cubic boron nitride, boron allotropes, and borides, nitrides, and carbides of transition metals as such chromium, rhenium, molybdenum, tungsten. Some of these carbides (WC) and nitrides (TiN) are widely used in machining tools and mining.

3.6 Additive Manufacturing

Additive manufacturing (AM) has several advantageous properties when developing a reference electrode.⁵² For example, additive manufacturing can potentially reduce the cost because it can consolidate multiple parts into one and minimize material usage by building objects up rather than cutting, molding, and combining materials. AM offers an ease of modifying the designs to fit the experimental needs and can rapidly produce the designs accurately and precisely. Additionally, additive manufacturing can use several different materials of interest for the

⁵⁰ D. Henkensmeier, W. Cho, P. Jannasch, J. Stojadinovic, Q. Li, D. Aili, J. Oluf Jensen, *Separators and Membranes for Advanced Alkaline Water Electrolysis*, Chem. Rev., 2024, **124**(10):6393–6443.

⁵¹ J. Haines, J. Léger, G. Bocquillon, *Synthesis and Design of Superhard Materials*, Annual Review of Materials Research, 2001, **31**:1-23.

⁵² M. Whittingham, R. Crapnell, E. Rothwell, N. Hurst, C. Banks, *Additive manufacturing for electrochemical labs: An overview and tutorial note on the production of cells, electrodes and accessories*, Talanta Open, 2021, **4**:100051.

development of the reference electrode such as ceramics, metals, and thermoplastics.⁵³ For example, Lewenstam et al., developed a solid-state reference electrode using a polymer/inorganic salt composite with an Ag/AgCl wire embedded in the polymeric matrix as the reference element.⁵⁴ The reference electrode was found to be insensitive to several changes to pH, concentration, and mobility of ions. The stability of the reference electrode was found to be exceptional with a shift of +/- 0.5 mV and lasted for greater than two months. The solid-state composite reference electrode was mechanically robust and was simple to manufacture. In another example, Girault et al., performed a large-scale fabrication of a solid-state reference electrode on a flexible substrate by using inkjet printing to print the silver patterns on a flexible PET substrate and then chemically transform it into Ag/AgCl electrodes. The method proved to be low cost, simple, and effective, showing exceptional reproducibility using large scale production.⁵⁵ Moreover, Kochan et al., developed the fabrication of a solid contact reference electrode by 3D printing using a PVC based composite. They discussed the benefits of the reproducibility and accuracy of the manufacturing process using 3D printing. The fabrication can be integrated and controlled from a PC screen, which eliminates any lab errors when fabricating the reference electrode by injection molding or other fabrication methods.⁵⁶

Overall, additive manufacturing provides an ease of fabrication, greater accuracy and precision, cheaper cost, and less material usage when considering the development of a reference electrode for tank waste. The flexibility of design and material usage with additive manufacturing could provide a unique way to fabricate a reference electrode to maximize the performance while minimizing slight changes in the fabrication if it is developed in a lab based environment.

4.0 Design Features

Traditional reference electrode designs consist of a reference element immersed in a reservoir of electrolyte or fill with a known ionic activity, housed within a casing. The internal electrolyte can be in the form of liquid, gel, semisolid, or solid and has three main functions: (1) provide a known ionic activity of a redox species, (2) support ion-to-electron transduction via a redox reaction on the surface of the reference element, and (3) support a small ionic current flow across a salt bridge or liquid junction with the external environment, preferably through anion and cation species with similar mobilities to minimize junction potentials.

The casing of the electrode isolates the internal electrolyte from the external environment. The junction between the internal electrolyte and the external environment provides ionic communication, thus completing the electrochemical circuit. To minimize intermixing between the internal and external solutions, the junction in traditional reference electrode designs typically consists of a microcapillary, ground sleeve, frit or porous plug, or sealed fiber wick in

⁵³ N. Dossi, R. Toniolo, F. Terzi, F. Impellizzieri, G. Bontempelli, *Pencil leads doped with electrochemically deposited Ag and AgCl for drawing reference electrodes on paper-based electrochemical devices*. *Electrochimica Acta*, 2014, **146**(11): 518-524

⁵⁴ Z. Mousavi, K. Granholm, T. Sokalski and A. Lewenstam, *An analytical quality solid-state composite reference electrode*, *Analyst*, 2013. **138**(18): 5216-5220

⁵⁵ A. Bananezhada, M. Jovičb, L. F. Villalobosc, K. V. Agrawalc, M. R. Ganjalialia, H. H. Girault, *Large-scale fabrication of flexible solid-state reference electrodes*, *Journal of Electroanalytical Chemistry*, 2019, **847**(8): 113241

⁵⁶ A. Lewenstama, B. Bartoszewicz, J. Migdalskia, A. Kochanb, *Solid contact reference electrode with a PVC-based composite electroactive element fabricated by 3D printing*, *Electrochemistry Communications*, 2019, **109**(10): 106613

the casing (see Figure 4-1⁵⁷). While traditional reference electrodes are suitable for many applications, they have significant drawbacks. These include electrolyte leakage, contamination of the external environment, and intrusion of the external environments into the electrolyte. Electrode contamination in long-term exposures affects the ionic activity of the redox species in the internal electrolyte, introduces extraneous species, which disturbs the equilibrium on the reference element and causes changes in the electrode potential. Furthermore, certain intrusive species can react with the internal element through metathesis, complexation, or dissolution reactions and alter the electrode response.

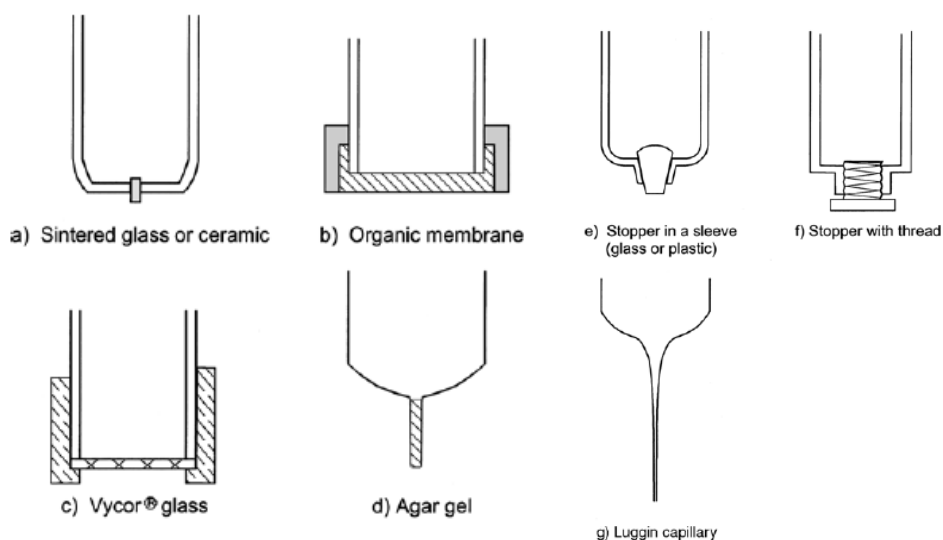


Figure 4-1. Commonly used reference electrode junction designs. From Kahlert⁵⁷.

Guth et al.⁵⁸ summarized the improvements in classical rod-shaped reference electrode design and the evolution of planar and solid-state designs for potentiometry. Troudt et al.⁵⁹ reviewed recent advancements in reference electrodes for electrochemistry, emphasizing the need for improved stability, reproducibility, and compatibility with modern electrochemical sensors.

Various type of alternative design concepts for reference electrodes are discussed in the literature to overcome the limitations of traditional reference electrodes. These can be broadly classified into the following categories:

1. Reference electrodes with extended diffusion lengths
2. Reference electrodes with improved liquid junction designs
3. Reference electrodes with flowless junction designs
4. Ionic liquid reference electrodes

⁵⁷ H. Kahlert, *Electroanalytical Methods: Guide to Experiments and Applications*, 2010, Eds: F. Scholz, et al. Springer, Berlin, Heidelberg. 291-308.

⁵⁸ U. Guth, F. Gerlach, M. Decker, W. Oelbner, and W. Vonau, *Solid-state reference electrodes for potentiometric sensors*, *J Solid State Electrochem.*, 2009, **13**:27–39.

⁵⁹ B. K. Troudt, C.R. Rousseau, X.I.N. Dong, et al., *Recent progress in the development of improved reference electrodes for electrochemistry*. *Anal. Sci.*, 2022, **38**: 71–83.
<https://doi.org/10.2116/analsci.21SAR11>

5. Solid-contact reference electrodes
6. Field Effect Transistor (FET) based reference electrodes

4.1 Reference Electrodes with Extended Diffusion Lengths

Duffy and coworkers⁶⁰ explored the idea of enhancing the lifespan of reference electrodes by increasing the diffusion length. Their work includes a mathematical model, experimental validation, and practical applications using 3D printing and CNC machining. The stability of reference electrodes is determined by the open circuit potential (OCP), which is related to the concentration of redox-active species and can be quantified using the Nernst equation. Deviation of the OCP from its initial value in an environment can be indicative of concentration changes in the redox-active species due to diffusion. The authors modeled the lifetime of the reference electrode based on a 1D representation of Fick's law of diffusion and developed reference electrodes based on this model. The OCP is directly related to the concentration of redox active species, thus the Nernst equation can be employed. [1]

$$C(x, t) = \frac{C_0 - C_\infty}{\sqrt{\pi t}} H(x, t) + C_\infty \quad (18)$$

$$E_{OCP} = E_{RE}(t) - E_{Test} = -2.303 \frac{RT}{nF} \log_{10} \left[\frac{C(0,t)}{C_\infty} \right] \quad (19)$$

Duffy and coworkers used the Nernst Equation (Eqn. 2) to compare the OCP of a reference electrode to an identical electrode in a test solution to demonstrate how the reference electrode changes regarding diffusion. $C(0,t)$ should remain constant one the reference electrode is immersed in the test solution until the electrolytes diffusion reaches the reference couple. Here, the reference electrode lifetime, $t_{lifetime}$, is quantified at some point where the OCP deviates significantly from the initial value.⁶⁰

$$P = \frac{E_{OCP}(t_{lifetime})}{E_{OCP}(0)} = \log_{10} \left[\frac{C(0,t_{lifetime})}{C_\infty} \right] / \log_{10} \frac{C_0}{C_\infty} \quad (20)$$

$$C(0, t_{lifetime}) = \frac{C_0}{C_\infty}^P C_\infty \quad (21)$$

By using equation 18, equation 20 can be solved for $t_{lifetime}$ using the design parameters and the solution to the 1D diffusion problem given in equation 1. Using a percentage is more accurate than doing so with only shifts in the potential. A change in percent will be more easily noticed in similar concentration reservoirs than a 10 mV shift.

By using a mathematical analysis, they were able to observe a large change on the stability of the reference electrode based on the filling solutions length (Figure 4-2). They demonstrate that the diffusion front takes longer to reach the reference couple once the distance is increased and that the rate of diffusion is slowed down.

⁶⁰ . S. Duffy, D. M. Hall, and S. N. Lvov, *Increasing the lifespan of reference electrodes by increasing the diffusion length*, *Electrochimica Acta*, 2023, **438**: 141562.

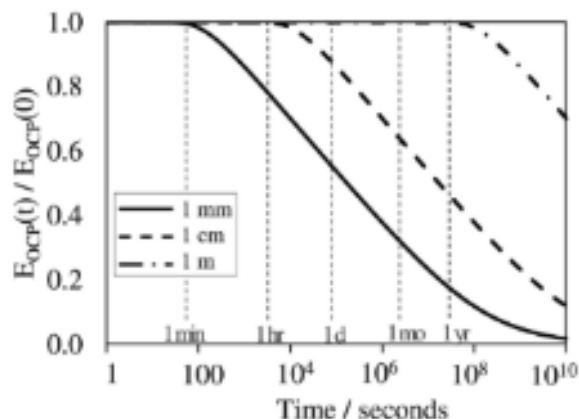


Figure 4-2. Influence of time and the filling solution length on the stability of a reference electrodes OCP.⁶⁰

Additionally, their lifetime model predictions were confirmed experimentally. Reference electrode housings with long, serpentine, and narrow filling solution channels, made by 3D printing and CNC machining, were used to produce small reference electrodes with enhanced lifetimes; these electrodes outperformed conventional designs (see Figure 4-3). Housings with serpentine cavities 2 mm x 2 mm in cross-section and up to 75 cm long were produced by the 3D printing process. A small Ag/AgCl couple element was introduced through an opening in the top end of the channel and the bottom end of the channel formed the junction with external solution. The channel was filled with an agar gel containing 1-mol/Kg KCl + saturated AgCl salt. Their study suggested that increasing the length of the filling solution channel is more effective than changing the diffusion coefficient of the filling solution material for extending the lifespan of reference electrodes.

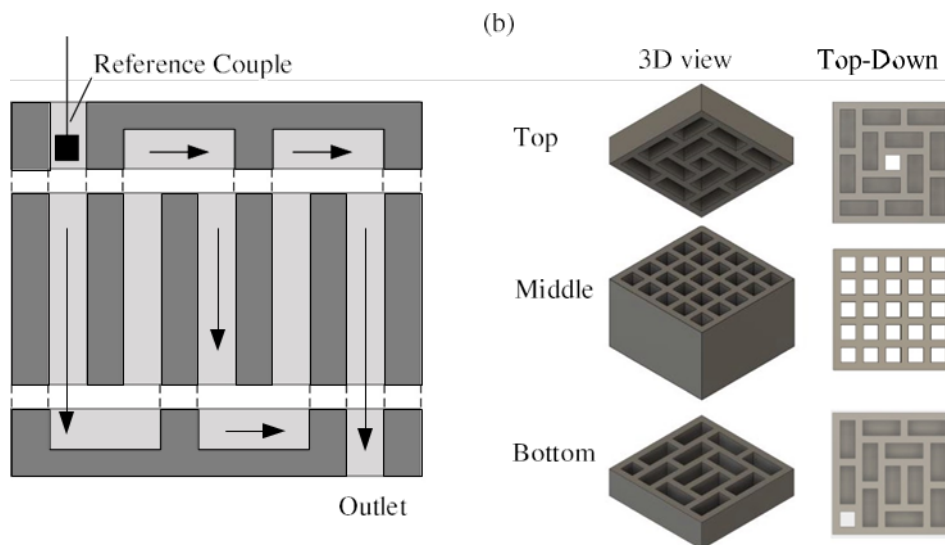


Figure 4-3. Reference electrodes design concepts based on long, serpentine fill channels produced by 3D printing and CNC machining. From Duffy et al.⁶⁰.

The results show that the longer channels maintain a constant potential for a longer period (Figure 4-4). While these experiments were carried on for < 240 days, the overall thought process could be beneficial to optimizing a reference electrode designed to implement into waste tanks.

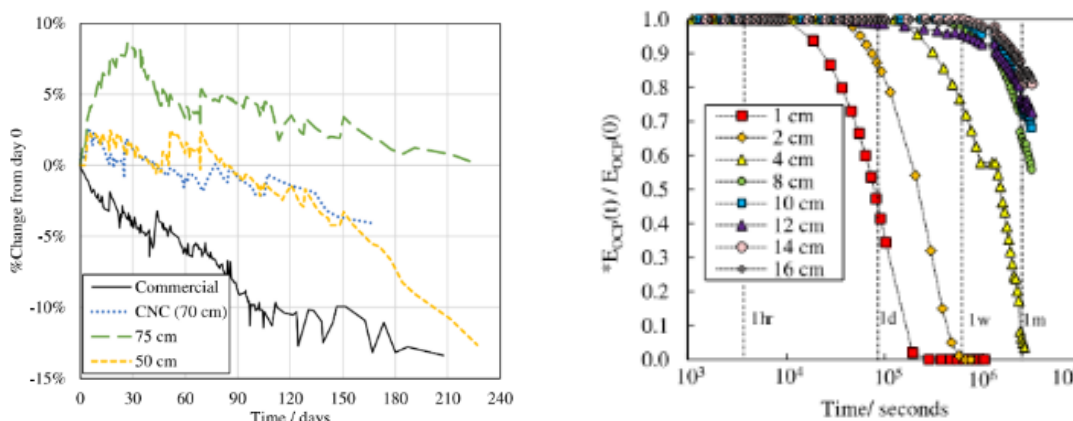


Figure 4-4. Experimental results showing change in percent over time with different lengths (left). Change in the OCP over time for the glass tube RE (right).⁶⁰

The concept of an increased diffusion length to extend electrode life is also being investigated through customized design modifications in a commercial Ag/AgCl reference electrode, manufactured by BORIN Manufacturing. The standard, off-the-shelf version of this electrode is 8.25-in. long x 1.25-in. diameter and feature a ceramic frit junction. The electrode body in the customized electrode design, is only one inch longer than the standard version. However, the diffusion path length between the junction and the Ag/AgCl element inside the modified electrode is 4 inches, which is about 8 times longer than the path length in the standard version.⁶¹ This modification is accomplished by compressing the coil-shaped Ag/AgCl element thereby increasing the distance between the ceramic junction of the electrode and the tip of the coil. Another advantage of the BORIN electrode design is that it contains a wet-solid fill consisting of gypsum saturated with NaCl. Diffusion of contaminating ionic species through the wet solid is expected to be slower than in liquid or gel fills that are found in other commercial reference electrode designs. The standard and customized Borin electrodes are currently undergoing long-term performance testing and evaluation at DNV in various Hanford waste simulants and in radioactive waste samples at the Hanford 222-S Laboratory.

4.2 Reference Electrodes with Improved Liquid Junction Designs

The junction or salt bridge in a reference electrode must maintain ionic contact between the external solution and the internal fill while having relatively low impedance. Free-flowing junctions that allow a small amount of fill electrolyte to stream out at a constant flow rate through a single leak path have the advantage of a constant and reproducible junction potential. However, these junction designs are impractical for field applications because the fill electrolyte needs to be periodically replenished. Additionally, a high flow rate from the junction can

⁶¹ S. Chawla, et al., DNV Test Plan & Status Report- 04102024, WRPS FY2024 Hanford Waste Chemistry and Corrosion Testing (10475418), Tank Integrity Expert Panel Corrosion Subgroup Meeting (Virtual), April 10, 2024.

contaminate the external environment, while too low a flow rate may make the junction susceptible to clogging by suspended matter resulting in erratic junction potentials.⁶²

Higuchi et al.⁶³ described a valve-actuator integrated Ag/AgCl reference electrode junction design to overcome these problems and provide a stable reference potential for pH measurement over long periods. This design incorporates a valve actuator based on a shape memory alloy wire to control the liquid junction, allowing it to open only during measurements, which helped in reducing the outflow of internal electrolyte. Figure 4-5 shows the operating principle of the intermittently opened liquid junction, the valve actuator design, and a schematic of the 70 mm long x 20 mm diameter pH probe assembly containing the valve actuator reference electrode, control circuit, and a battery.

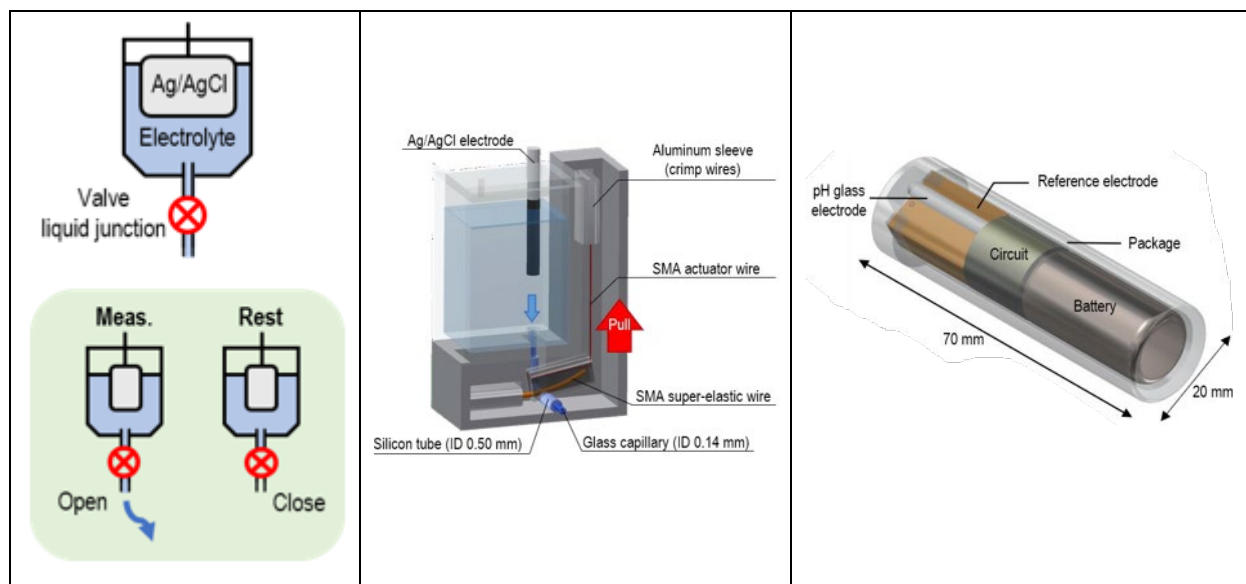


Figure 4-5. Left: Operating principle of valve-actuator reference electrode; Middle: Valve-actuator design using shape memory alloy wire; Right: Conceptual design of the valve-actuator integrated reference and pH electrode. From Higuchi et al.⁶³

The Ag/AgCl element was contained inside a small reservoir of KCl fill solution. A silicone tubing of 0.5-mm ID was connected to a bottom outlet in the KCl reservoir. The other end of the tubing was connected to a 0.14-mm ID glass capillary, which served as the liquid junction. The valve design was similar to a normally closed (NC) pinch valve. When no electrical current was flowing in the shape-memory actuator wire, the silicone tube was pinched, and the valve was in the NC position. The actuator wire contracted when a voltage was applied, which allowed the tubing bore to open and release a small amount of KCl through the capillary junction and enabled a potential measurement to be made with respect to the Ag/AgCl electrode. The valve-actuator reference electrode design exhibited stable potential values, with errors of 0.5 mV or less relative to the theoretical potential, and a response time of less than 0.083 seconds when

⁶² D.T. Sawyer and J.L. Roberts, *Experimental Electrochemistry for Chemists*, 1974, John Wiley & Sons.

⁶³ S. Higuchi, H. Okada, S. Takamatsu, and T. Itoh, *Valve-Actuator-Integrated Reference Electrode for an Ultra-Long-Life Rumen pH Sensor*, *Sensors* 2020, **20**: 1249; doi:10.3390/s20051249.

the liquid junction was switched open. The lifetime could be greatly extended by intermittent operation of the junction. Calculations showed that starting with an electrolyte volume of 500 μL in the valve and applying a differential pressure of 20 kPa inside the electrolyte container by injecting air before use, the reference electrode lifetime would be 2 years assuming that the valve was opened for 5 s every hour to make a measurement.

In practice, flow-restricted junction designs are more commonly used to minimize intermixing and contamination between the internal fill and external solution, especially in long-term potential monitoring. These junctions are typically made of porous glass, polymeric or ceramic frits, hydrophilic gels, membranes, capillaries, sealed quartz or asbestos fiber, or sealed Pt wire (see Figure 4-1).⁶² Improvements in the designs of salt-bridge reference electrodes include incorporation of nanoporous and capillary junctions. These bridge designs help maintain a stable reference potential by minimizing ion exchange and contamination of the electrode fill from the external test environment. Reference electrodes with nanoporous glass frits are commonly used in laboratory work. However, it was shown that the use of glass frits with very fine pore sizes (4-10 nm diameter) can introduce errors in the reference electrode potential due to electrostatic charge screening, particularly in low ionic strength solutions.⁶⁴ A later study by Anderson et al.⁶⁵ showed that increasing the pore size to 100 nm eliminates the charge screening effect. However, it was found that, even with a 100-nm pore size, the flow rate of reference electrode fill solution through the frit was low enough that diffusion remained the main transport mode through the frit. Therefore, cross-contamination of the fill and external solution could result from the diffusive exchange of ionic and neutral chemical species. It should also be noted that glass frits are incompatible with highly alkaline environments such as Hanford waste.

Polymeric frits made of Teflon and polyethylene generally exhibit low charge screening effects due to the absence of ionic surface groups but have relatively large pore sizes (1 to 10 μm) and pore walls that are hydrophobic, which make them electrically resistive.⁵⁹ It was shown that these problems could be overcome by using polymeric frits of these materials that had electrically neutral pore sizes of around 10 nm size and functionalizing the pore walls to improve wettability.⁶⁶ These frits exhibited very low leak rates of around $0.007 \pm 0.003 \mu\text{L/h}$.

Porous ceramic frits are commonly used in constricted-flow junctions of reference electrodes. Bosch et al.⁶⁷ investigated the porosity of magnesia-stabilized zirconia plugs for use in electrochemical sensors. The plugs were produced by cold isostatic pressing and sintering at various temperatures to achieve different porosities and pore sizes. High porosity and small pores were identified as key factors for optimal plug performance. It was found that the flow rate of electrolyte through the plugs, ranging from 0.2 to 25 $\mu\text{L/h}$, was controlled by the pore size.

⁶⁴ M. P. S. Mousavi, S. A. Saba, E. L. Anderson, M. A. Hillmyer, and P. Bühlmann, *Avoiding Errors in Electrochemical Measurements: Effect of Frit Material on the Performance of Reference Electrodes with Porous Frit Junctions*, *Anal. Chem.*, 2016, **88**: 8706–8713.

⁶⁵ E.L. Anderson, B.K. Troutdt, and P. Bühlmann, *Critical Comparison of Reference Electrodes with Salt Bridges Contained in Nanoporous Glass with 5, 20, 50, and 100 nm Diameter Pores*, *Anal. Sci.*, 2020, **36**: 187–191.

⁶⁶ E.L. Anderson, S.A. Saba, D.J. Loomi, P. Bühlmann, and M.A. Hillmyer, *Functionalized Mesoporous Polymers with Enhanced Performance as Reference Electrode Frits*, *ACS Appl. Nano Mater.* 2018, **1**(1): 139–144.

⁶⁷ R. W. Bosch, S. Straetmans, and S. Van Dyck, *Characterizations of porous ceramic plugs for use in electrochemical sensors*, *Journal OF Materials Science* 2002, **37**: 3973–3979.

For plugs with similar pore sizes, electrical conductance was higher for the plug with a higher porosity since it offered more electrolytic pathways.

Badr et al.⁶⁸ describe the preparation and evaluation of mesoporous glass–ceramic composite frits using low-cost materials like borosilicate and kaolin, sintered at relatively low temperatures (750–850 °C), for use in reference electrode junctions. Reference electrodes based on these composite frits exhibited flow rates as low as 0.002 ± 0.001 $\mu\text{L/h}$, improved potential stability, and reduced potential drift compared to existing reference electrodes based on glass or polymeric frits.

Suzuki et al.⁶⁹ developed a microfabricated liquid-junction Ag/AgCl reference electrode. The structure of the miniature liquid-junction Ag/AgCl reference electrode, shown in Figure 4-6, included a glass substrate with a 7 μm deep recess where the thin-film Ag/AgCl element was formed. A 4.5 μm thick polyimide layer was used as an intermediate layer to promote adhesion, and a 200 nm thick gold backbone layer was formed on top of the polyimide layer. A 300 nm thick silver pattern was then formed on the gold layer. The Ag/AgCl element was formed by chemically converting approximately 50% of the silver layer, in situ, to AgCl by immersing the chip in a 1.0 M FeCl_3 solution. The container for the internal electrolyte solution was formed by anisotropically etching a (100) silicon substrate using an SiO_2 mask and a 35 wt% KOH etchant. A rectangular groove for the electrolyte solution and a long narrow groove for a pin-hole liquid junction were etched into the silicon substrate. The glass and silicon substrates were aligned and bonded using a photocurable adhesive. The internal electrolyte solution, saturated with both KCl and AgCl, was introduced into the cavity by immersing the chip in the electrolyte solution and evacuating the chamber. Leakage of the electrolyte solution was also restricted by plugging the pin-hole liquid junction with cellulose acetate. The potential of the electrode was tested against a commercially available Ag/AgCl reference electrode in various KCl solutions. The electrode with an unrestricted pin-hole junction exhibited positive potential drift due to KCl effusion. The electrode with a cellulose-acetate-plug junction was insensitive to KCl concentration in the range of 10 mM to 1.0 M, maintaining a stable potential level within ± 1 mV for several hours. While such a design may not be suitable for a long-term potential monitoring application, it could be possibly used for a short-term potential measurement, e.g., when co-deployed with tank grab sampling equipment.

In considering the use of improved liquid junction designs and materials, such as those discussed above, for reference electrode in the Hanford tank application, the following are some general concerns: (1) long-term reliability of moving parts in active operation designs such as the intermittently actuated, free-flow junction, (2) compatibility of new polymeric or ceramic junction materials with the highly alkaline, radioactive waste environment, and (3) the possibility of plugging of nano-/meso-porous frit materials with nonconductive solids, leading to high electrode impedance.

⁶⁸ H. Ibrahim, A. Badr, and O. A. S. Rafea, *Evaluation of mesoporous borosilicate glass–ceramic composites as frits in reference electrodes*, RSC Adv., 2022, **12**: 28878–28885.

⁶⁹ H. Suzuki, T. Hirakawa, S. Sasaki, and I. Karube, *Micromachined liquid-junction Ag/AgCl reference electrode*, Sensors and Actuators B, 1998, **46**: 146–154.

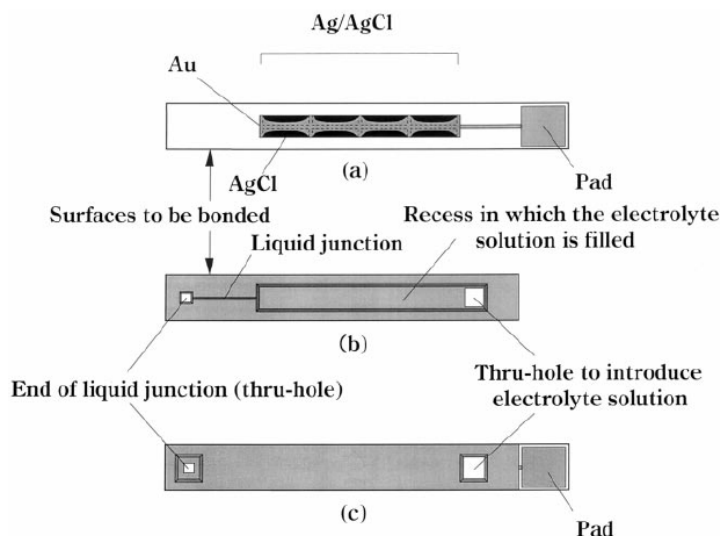


Figure 4-6. Structure of microfabricated liquid-junction Ag/AgCl reference electrode developed by Suzuki et al.⁵⁵

4.3 Ionic Liquid Reference Electrodes

Reference electrodes based on ionic liquids, also known as room temperature molten salts (RTMS), utilize these unique salts as the salt bridge component. Ionic liquids are nonpolar water-immiscible (lipophilic) organic compounds composed of a large organic cation and a smaller inorganic or organic anion and remain in a liquid state at room temperature. Morawska and Wardak⁷⁰ list the common types of cations and anions that form ionic liquids. The low melting points of ionic liquids are due to the size discrepancy between the cation and anion, which hinders the formation of a homogeneous crystal structure. Ionic liquids also have large ionic radii and low symmetry, with cation charge distributed over a large space.

An ionic liquid salt bridge maintains electrical neutrality by allowing ions to move between the reference electrode fill and the external solution being measured. Ionic liquids are chemically stable and have low volatility, which enhances the durability and reliability of the reference electrode.

Ionic liquid-based salt bridges avoid several deficiencies of conventional salt bridges, such as the need to replenish the bridge electrolyte and fluctuations of the liquid junction potential due to contamination. Physical robustness of the junction can be increased by incorporating ionic liquids into polymeric support membranes such as plasticized PVC, PMMA, fluoropolymers and silicones (see Trout⁵⁹ for cross-references). Morawska and Wardak⁷⁰ discuss the uses of ionic liquids as components of ion-selective membranes, both polymeric ones based on PVC and membranes in carbon paste electrodes. The liquids perform various functions in these membranes, including acting as lipophilic ionic additives, ionophores/ion exchangers, plasticizers, transducer media, and matrix components.

⁷⁰ K. Morawska and C. Wardak, *Application of ionic liquids in ion-selective electrodes and reference electrodes: A review*, Chem. Phys. Chem 2024, e202300818.

The transfer of sample ions into the ionic liquid phase can affect the phase-boundary potential, especially when the concentration of sample ions is high. Research by Kakiuchi et al⁷¹ focused on the phase boundary potential at the interface between ionic liquids and aqueous electrolyte solutions. They studied an RTMS mixture of 1-methyl-3-octylimidazolium salts of bis(trifluoromethylsulfonyl)imide and of bis(pentafluoroethylsulfonyl)imide that are immiscible with water. They found that ionic liquids can transfer, to some extent into the aqueous phase, resulting in an equilibrium distribution across the interface. This transfer does not significantly affect the interfacial phase boundary if other ions present do not transfer substantially into the ionic liquid phase.

Despite their potential benefits, ionic liquid reference electrodes have not seen widespread adoption due to challenges such as the purity of the ionic liquid and the complexity of their implementation.⁷²

4.4 Reference Electrodes with Flowless Junction Designs

Reference electrodes with flowless junctions differ from traditional reference electrodes by using a solid-state interface instead of a liquid junction, which makes them more robust and less prone to leakage or contamination. The solid junction is typically made of a hydrophobic polymeric or other solid conductive material, which is in direct contact with the electrolyte solution. Lindner et al.⁷³ discuss the materials used, which include polyvinyl resin, pressed Al₂O₃-PTFE, urea formaldehyde, poly methyl methacrylate-propylene carbonate, and polyester resin. The solid material is made ionically conductive by doping or dispersing an equitransferent salt such as KCl or lipophilic tetrabutyl ammonium tetrabutyl borate. These junction materials offer improved stability and reproducibility compared to liquid junctions. The solid junction design also makes the electrode more resistant to external pressure.

Diamond et al⁷⁴ discussed the performance and properties of an ionically conducting polymeric junction material, Refex™, highlighting its advantages over conventional materials. Refex (RepHex) was made of polyvinyl acetate with a high loading of KCl (1:1 ratio by weight of PVA to KCl) and designed for use in reference electrode junctions. Their studies showed that the Refex junction gave very stable potentials in buffer solutions in the pH 2 to pH 11.9 range, outperforming conventional ceramic frit junctions in terms of leakage rates. Impedance studies revealed that the high KCl loading in Refex results in low electrical resistance and efficient charge transfer, which are essential for stable potentiometric measurements.

⁷¹ T. Kakiuchi, N. Tsujioka, S. Kurita, and Y. Iwami, *Phase-boundary potential across the nonpolarized interface between the room-temperature molten salt and water*, *Electrochem. Commun.*, 2003, **5**(2): 159–164.

⁷² E. Lindner, M. Guzinski, T. A. Khan, and B.D. Pendley, *Reference electrodes with ionic liquid salt bridge: When will these innovative novel reference electrodes gain broad acceptance?* *ACS Sensors*, 2019, **4**(3): 549–561.

⁷³ P. Lingenfelter B. Bartoszewicz, J. Migdalski, T. Sokalski, M. M. Bucko, R. Filipek, and A. Lewenstam, *Reference Electrodes with Polymer-Based Membranes—Comprehensive Performance Characteristics, Membranes*, 2019, **9**, 161; doi:10.3390/membranes9120161.

⁷⁴ D. Diamond, E. McEnroe, M. McCarrick, and A. Lewenstam, *Evaluation of a New Solid-State Reference Electrode Junction Material for Ion-Selective Electrodes*, *Electroanalysis*, (1994), **6**: 962–971.

A recent study⁷⁵ by DNV evaluated the long-term performance of a commercially available Reflex Ag/AgCl electrode⁷⁶ in supernatant waste simulants of Tanks AY-101 and AW-101. This electrode is 4.7-in. long x 0.47-in. diameter and contains a fill of 2.8-M KCl (see photograph in Figure 4-7). The entire electrode barrel is made from the patented ionically conductive Reflex polymer. The Reflex electrode showed high stability at a potential near its theoretical half-cell potential of -37 mV(SCE) in the AY-101 waste simulant at room temperature, with a minimal positive drift of less than 5 mV over 6 months, compared to a 25 mV drift in a Van London electrode. While the Reflex electrode was promising in the AY-101 simulant, it failed by a large decline in potential after 6 weeks in the highly alkaline (5.76 M NaOH) AW-101 simulant. There was no perceptible damage or change in color of the Reflex electrode at the end of the 6-month test in AW-101 simulant. Subsequently, the electrode was immersed for 8 weeks in 4-M KCl, but the degradation was found to be irreversible as the electrode remained at a low potential near .175 mV(SCE).⁷⁷



Figure 4-7. Photograph of a commercially available Reflex Ag/AgCl reference electrode.

Another commercially available electrode with an ionically conductive polymeric junction that was evaluated at DNV in various waste simulants is the eDAQ Electrode. This Ag/AgCl electrode features a cylindrical body, 5.1 in. long x 0.47-in. diameter, made of PEEK and contains a fill of 3.4-M KCl. A proprietary conductive polymer plugs the bottom of the electrode barrel forming a flowless junction. These electrodes failed by exhibiting a large drop in potential after a few weeks of continuous immersion in various waste simulants. Investigation showed that the electrodes failed due to degradation of the conductive polymer junction, which allowed intrusion of the alkaline test solution into the electrode and attack on the Ag/AgCl element.⁷⁸

The main concerns with these flowless junction designs are the chemical and radiological compatibility of the polymeric junction materials with the waste environment and the lifetime limitations due to leaching of the ionic dopant (KCl) from the polymer matrix.

⁷⁵ S. Chawla, et al., RPP-RPT-64916, Rev. 0, FY2023 Hanford Waste Chemistry and Corrosion Testing Report, Prepared by DNV GL USA, Inc. for Washington River Protection Solutions, LLC, May 2024.

⁷⁶ Manufactured by REFEX Sensors Ltd, Part No. S8-5710-120.

⁷⁷ S. Chawla, et al., DNV Test Plan & Status Report- 03132024, WRPS FY2024 Hanford Waste Chemistry and Corrosion Testing (10475418), Tank Integrity Expert Panel Corrosion Subgroup Meeting (Virtual), March 13, 2024.

⁷⁸ S. Chawla, et al., RPP-RPT-64282, Rev. 0, FY2022 Hanford Waste Chemistry and Corrosion Testing Report, Prepared by DNV GL USA, Inc. for Washington River Protection Solutions, LLC, May 2024.

4.5 Solid-Contact Reference Electrodes

Efforts to address the challenges of traditional reference electrodes have led to the development of solid-state reference electrodes (SSREs) without an internal electrolyte and a liquid-liquid junction. Solid-state reference electrodes aim to eliminate liquid components, using materials like mixed ionic electronic conductors to maintain a stable potential. Collins⁷⁹ defines an SSRE as “any material in direct contact with the test solution that maintains a constant or predictable interfacial potential difference despite changing type and concentration of chemical species in the test electrolyte” and discusses practical limits and challenges in developing solid-state reference electrodes.

4.5.1 Electrodes with Solid Fills

Efforts to improve conventional reference electrodes include the use of gel-solidified electrolytes, which offer advantages like pressure resistance and position independence.⁵⁸ Other attempts include embedding the Ag/AgCl element in a solidified KCl melt inside a hollow casing with a porous ceramic frit at one end for making ionic contact with the external solution. Vonau et al.⁸⁰ described a sintered Ag/AgCl reference element embedded in a solidified melt of KCl, enclosed within a chemical-resistant, porous, ceramic cylinder, and sealed in a chemically resistive casing with a small opening (see Figure 4-8). The porous ceramic layer at the opening forms a junction to modulate ionic communication between the inner electrode and the analyte, limiting KCl dissolution into the analyte. Another design involved a second solid salt mixture added to the lower part of electrode to serve as a bridge electrode. While these designs improve potential stability and extend electrode lifetime compared to a conventional electrode, the use of a porous junction between the interior salt fill and the analyte allows dissolution of the KCl fill over time. In some designs, the electrode body is made of a conductive polymer, eliminating the need for a porous junction.^{79,80}

Kwon et al.⁸¹ described a solid-state Ag/AgCl electrode design that was fabricated by layering a silicone rubber film containing KCl on an AgCl surface, followed by a perfluorinated ionomer film, and finally a polyurethane-based membrane containing an H⁺-ion-selective ionophore, a lipophilic ionic additive, and a plasticizer. The electrode exhibited little potential variation even with the addition of very high concentrations of various salts and was stable over two years.

Lewenstam⁸² discussed two types of polymeric solid contact designs: those employing conducting polymers and those using redox polymers. Conducting polymers such as poly(pyrrole), poly(thiophene), and poly(aniline) are used in solid contacts due to their mixed conductivity and ability to support ion-to-electron coupling. Historical developments in solid contact technology include the use of poly(vinylferrocene) and composites like PMMA with modified graphite, as well as the introduction of carbon nanostructures.

⁷⁹ S. D. Collins, *Practical limits for solid-state reference electrodes*, *Sensors and Actuators B*, 1993, **10**: 169–178.

⁸⁰ W. Vonau, W. Oelßner, U. Guth, and J. Henze, *An all-solid-state reference electrode*, *Sensors and Actuators B*, 2010, **144**: 368–373.

⁸¹ N. Kwon, K. Lee, M. Won, and Y. Shim, *An all-solid-state reference electrode based on the layer-by-layer polymer coating*, *Analyst*, 2007, **132**: 906–912.

⁸² A. Lewenstam, *Handbook of Reference Electrodes*, 2013, Eds. G. Inzelt, A. Lewenstam, F. Scholz, Springer Heidelberg, New York, Dordrecht, London, 279–288.

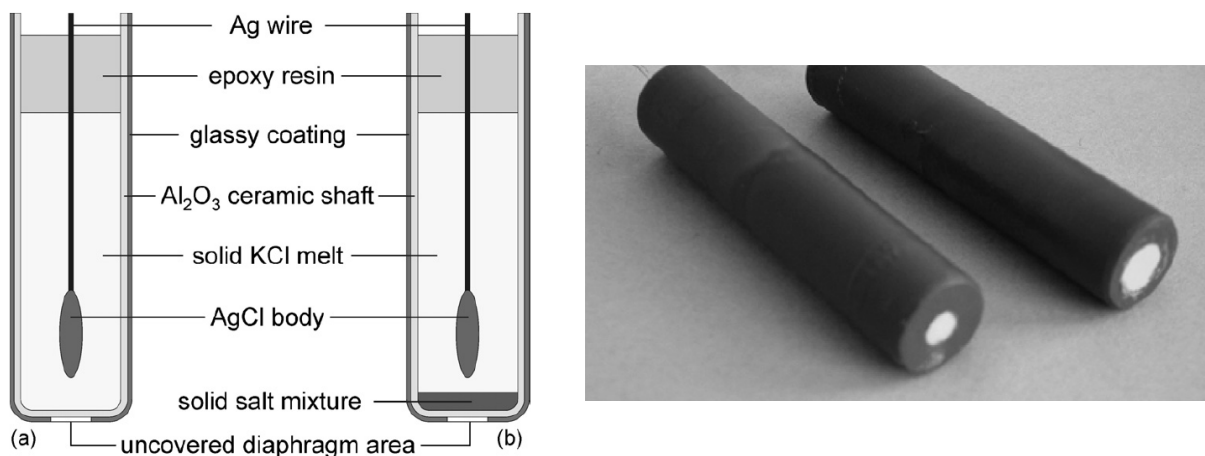


Figure 4-8. Left: Schematics of reference electrodes containing solidified KCl fill. Right: Photographs of electrodes prepared using Design (a). From Vonau et al.⁸⁰

Mousavi et al.⁸³ developed Ag/AgCl reference electrodes embedded in polyvinyl acetate (PVAc) loaded with KCl, which showed good potential stability across various analytes. However, these electrodes may have poor resistance to chemical and mechanical degradation in corrosive or abrasive environments.

In Patent WO 2018/201200 A1⁸⁴, Vepsalainen et al. describe methods for making an SSRE featuring an Ag/AgCl reference element within an electrochemically active composite. The composite includes a polymeric matrix loaded with a solid inorganic chloride salt. The matrix is a cross-linked vinyl polymer made from a copolymer of vinyl acetate and/or vinyl caprolactam and a cross-linking agent chosen from ethylene glycol di(meth)acrylate, poly(ethylene glycol) di(meth)acrylate, and glycerol propoxylate triacrylate.

Nolan et al.⁸⁵ developed solid state reference electrodes by dip coating Ag/AgCl wires with a solution of NaCl and polyvinylchloride (PVC) to create an immobilized electrolyte. They then coated the wire with a protective layer of permeable polyurethane or Nafion to prevent NaCl leaching into the analyte. However, these electrodes experienced significant drift due to low electrolyte loading and were not stable enough for many electrochemical applications.

Crisculo et al.⁸⁶ evaluated different fabrication strategies for solid-state Ag/AgCl reference electrodes, including membranes made of KCl- (or NaCl/KCl-) doped Agar, Polyvinyl Butyral (PVB), Polyvinyl Chloride (PVC), and Ionic-Liquid-doped PVC, for their stability in varying chloride concentrations and pH levels. The study found that PVC-based reference electrodes exhibited the highest stability with PVB and IL-PVC also showing promising results.

⁸³ Z. Mousavi, K. Granholm, T. Sokalski, and A. Lewenstam, *An analytical quality solid-state composite reference electrode*, *Analyst*, 2013, **138**: 5216–5220.

⁸⁴ International patent WO 2018/201200 A1, Solid state reference electrode, WIPO, 2018.

⁸⁵ M. Nolan, S. Tan, and S. Kounaves, *Fabrication and Characterization of a Solid-State Reference Electrode for Electroanalysis of Natural Waters with Ultramicroelectrodes*, *Anal. Chem.*, 1997, **69**(6): 1244-1247.

⁸⁶ F. Criscuolo; M. Galfione, S. Carrara; G. De Micheli, *All-solid-state Reference Electrodes for analytical applications*, 2019 IEEE 8th International Workshop on Advances in Sensors and Interfaces, 13-14 June 2019.

As discussed in Section 4.1, the commercially available BORIN electrode, that is currently undergoing testing at DNV and the Hanford 222-S Laboratory, contains a wet-solid fill consisting of gypsum saturated with NaCl. The use of a wet-solid fill reduces the diffusive loss of Cl⁻ ion from the fill and the diffusive contamination of the fill from extraneous chemical species, which improves the stability and longevity of the electrode.

4.5.2 Miniature Screen-Printed Reference Electrodes

Sophocleous⁸⁷ reviewed the significant amount of effort that has gone into the development of solid-state screen-printed microelectrodes, which are alternatives to conventional liquid- or gel-filled reference electrodes for use in potentiometric applications. Screen-printed Ag/AgCl reference electrodes consist of three functional layers: a conductor layer for electron transfer, an ion-to-electron layer (silver/silver chloride), and a KCl layer for controlling chloride ion concentration. Figure 4-9 shows some examples of screen-printed solid-state Ag/AgCl reference electrode configurations developed by various researchers. However, challenges remain in maintaining a stable chloride concentration around the Ag/AgCl element, cross-sensitivity, and lifetime. Researchers are trying to address these through innovative materials and fabrication techniques.

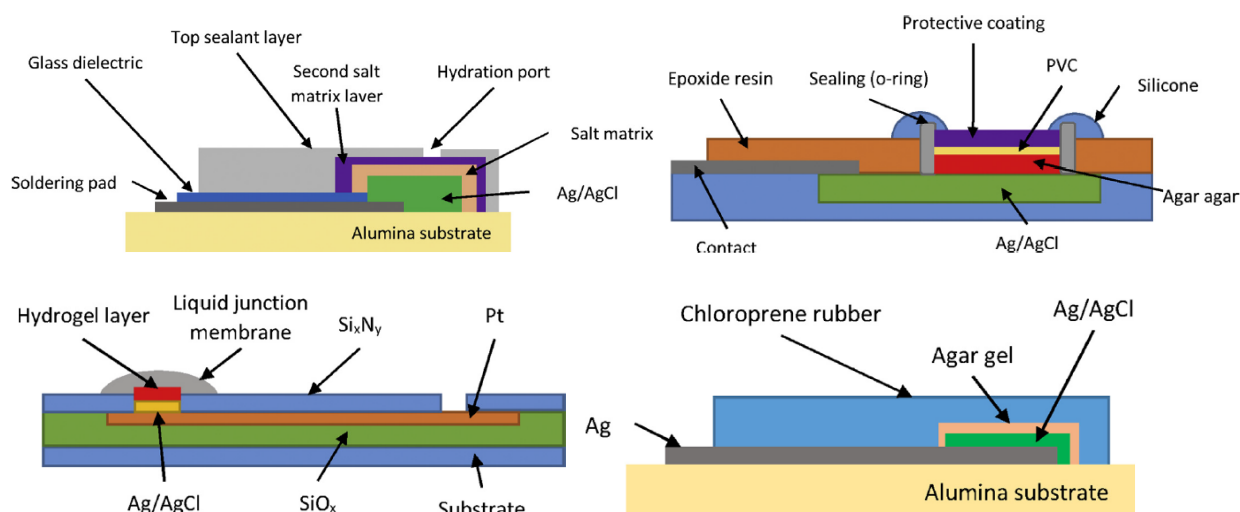


Figure 4-9. Some examples of screen-printed solid-state Ag/AgCl reference electrode configurations developed by various researchers. See Sophocleous⁸⁷ for details and cross-references.

The previously reported solid-state reference electrodes generally fail to provide a satisfactory balance of properties, particularly in terms of resistance to chemical and mechanical degradation, rapid conditioning and response, low impedance, and longevity. For long-term service in nuclear waste tanks, radiation stability of the solid contact materials is also

⁸⁷ M. Sophocleous and J. K. Atkinson, *A review of screen-printed silver/silver chloride (Ag/AgCl) reference electrodes potentially suitable for environmental potentiometric sensors*, *Sensors and Actuators A*, 2017, **267**: 106–120.

important.⁸⁸ There is an ongoing need to develop solid-state reference electrodes that offer an improved balance of these properties.

4.5.3 Perovskite-Based Electrodes

Gabel et al.⁸⁹ developed reference electrodes based on tungsten-substituted alkali molybdenum oxide bronzes that showed promising results for use as solid-state reference electrodes due to their stability and insensitivity to pH, Na⁺ concentration, and redox potential changes. The bronzes were synthesized via solid state reaction under inert conditions and had a perovskite-like structure with a composition, Li_xMo_{0.95}W_{0.05}O₃, where x = 0.3-0.4. Electrodes were made from polycrystalline samples of the synthesized bronze powders mixed with unsaturated polyester resin, cast into molds, and connected to a copper wire using electrically conductive adhesive, and the entire coated with epoxy for shielding. The electrical resistance of the electrodes fabricated this way was high (about 1–500 MΩ). Cyclic voltammograms for a Li_xMo_{0.95}W_{0.05}O₃ electrode in 0.1-M FeCl₂ showed no discernable oxidation-reduction peaks in comparison to a Pt electrode (see Figure 4-10). The behavior of the material could not be explained from the theory of cation exchange and intercalation and the exact mechanism of operation was unclear.

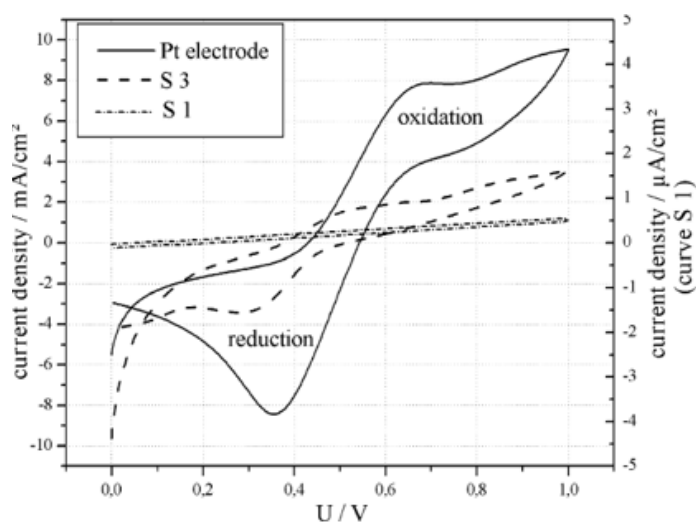


Figure 4-10. Cyclic voltammograms of a Na_{0.9}Mo₆O₁₇ (S 3) and Li_xMo_{0.95}W_{0.05}O₃ (S 1) in comparison to Pt in 0.1 M FeCl₂ (50 mV/s). From Gabel et al.⁸⁹

Lorant, et al.⁹⁰ studied an all-solid-state reference electrode using lithium lanthanum titanium oxide (LLTO) perovskite, Li_{0.3}La_{0.56}TiO₃, for electrochemical measurements in harsh environments, providing robustness, resistance to high temperatures and pressures, and no clogging (see Figure 4-11). The LLTO electrodes were manufactured using a dip-coating

⁸⁸ J. Savosina, M. Agafonova-Moroz, M. Khaydukova, A. Legin, V. Babain, P. Tolstoy, and D. Kirsanov, *On the Radiolytic Stability of Potentiometric Sensors with Plasticized Polymeric Membranes*, *Chemosensors* 2021, **9**: 214.

⁸⁹ J. Gabel, W. Vonau, P. Shu, U. Guth, *New reference electrodes based on tungsten-substituted molybdenum bronzes*, *Solid State Ionics*, 2004, **169**: 75–80.

⁹⁰ S. Lorant, C. Bohnke, M. Roffat, and O. Bohnke, *New concept of an all-solid-state reference electrode using a film of lithium lanthanum titanium oxide (LLTO)*, *Electrochim. Acta*, 2012, **80**: 418–425.

technique, followed by heat treatments, resulting in thick ceramic films on alumina substrates. The electrodes were tested in various pH buffer solutions, ranging up to pH 10 and demonstrated low impedance and stability over several days, as shown in Figure 4-11.

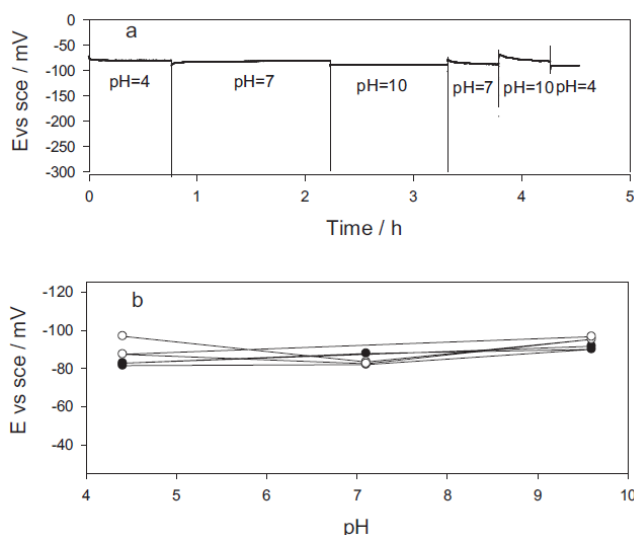


Figure 4-11. Potential of the solid state LLTO reference electrode as a function of time in buffer solutions of different pH at room temperature; and stabilized potentials of two LLTO electrodes as a function of pH. From Lorant et al.⁹⁰

Although the mechanism by which perovskite type materials maintain stability of potential in various environments remain unclear, these materials should be explored further to evaluate compatibility, potential stability, interference from common ions and redox-active species, and lifetime in alkaline waste simulants.

4.6 Field Effect Transistor (FET) Based Reference Electrodes

Various approaches to integrate reference systems with Field Effect Transistors (FETs) have been explored. These miniature FET-based reference electrodes, also called REFETs (Reference Field-Effect Transistors), are designed to provide a stable reference potential in potentiometric measurements. They are intended to be integrated with on-chip sensors for various applications such as medical diagnostics, environmental monitoring, and chemical analysis.

The basic architecture of the REFET is the same as a metal-oxide-semiconductor FET (MOSFET). Silicon is commonly used as a substrate for semiconductor devices, particularly in the creation of MOSFETs, which have three terminals: source, drain, and gate. The gate terminal, separated by a dielectric layer, modulates the current flow between the source and drain by applying a bias voltage. Various configurations of FETs exist, including back, top gate, dual gate, and electrolyte-gated FETs. REFETs typically consist of an FET with a reference

electrode material deposited on the gate. This material is chosen to be insensitive to the analyte of interest, ensuring a stable reference potential.

Comte and Janata⁹¹ first described the construction and performance of an integrated on-chip reference REFET used with ion-sensitive FETs (ISFETs) for pH and K⁺ measurements. To make a REFET, a small epoxy well was cast and cured around one of the ISFETs on the chip (see Figure 4-12). A buffered gel made of 1% agarose was packed into the well and a glass microcapillary was inserted into the gel to serve as an ionic conduit. The ion-sensitive gate of the second ISFET was used for ionic or pH measurements. The drain current of both transistors was measured with a differential current follower. The reference gate's performance was evaluated based on pH response, temperature, and noise sensitivity, demonstrating good stability and minimal drift.

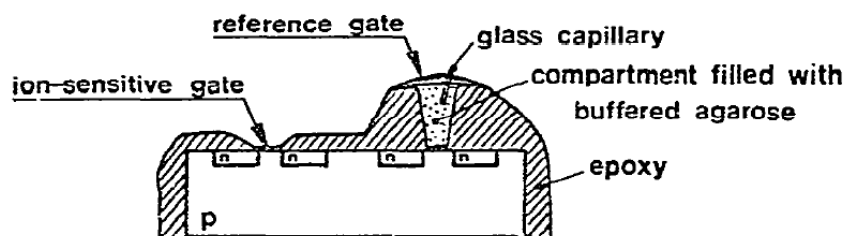


Figure 4-12. Schematic a chip with and ISFET and REFET. From Comte and Janata⁹¹.

Chudy et al.⁹² applied a membrane containing a highly lipophilic complex, which showed insensitivity to pH changes and various metal cations and chlorides, on the gate oxide surface of an ISFET. The response of this REFET was measured using an ISFET amplifier in a constant drain-current mode. The REFET demonstrated pH insensitivity over a range of pH 2 to 10 and maintained this performance over 100 days of continuous exposure to aqueous electrolyte. The REFET showed no significant response to sodium and potassium ions in specific concentration ranges, although higher concentrations of potassium cations did affect the sensor.

REFETs offer several advantages over traditional liquid-based reference electrodes, including improved stability, reduced size, and compatibility with microfabrication techniques. However, despite their advantages, REFETs face the same challenges as other solid-state reference electrodes such as drift over time, sensitivity to environmental conditions, and concerns about long-term durability.

5.0 Verification Protocols

During the development of the new reference electrodes, it will be critical to assess the performance of the prototypes. Electrochemical techniques have been utilized in the laboratory to assess the condition or performance of an electrode. Two of these methods, half-cell potential verification and electrochemical impedance spectroscopy, will be discussed below.

⁹¹ P.A. Comte and J. Janata, *A Field Effect Transistor as a Solid-State Reference Electrode*, *Analytica Chimica Acta*, 1978, **101**: 247–252.

⁹² M. Chudy, W. Wroblewski, Z. Brzozka, *Towards REFET*, *Sensors and Actuators B*, 1999, **57**: 47–50.

5.1 Half-cell Potential Verification

Reference electrodes that are commercially procured may come with a certificate of some type but there is no requirement or standardized practice in the industry for verifying the half-cell potential of manufactured reference electrodes. Most manufacturer certificates indicate that the reference electrode was checked versus another “Master” reference electrode (typically saturated calomel electrode) and they report the measured potential versus the expected potential and the acceptance criterion. However, there are typically no details on the manufacturer’s certificate to validate or justify the use of the master reference electrode as a trustworthy standard.

5.1.1 Master Reference Electrodes for Verification

It is common practice to check the potential of a reference electrode against an “in-house” master reference electrode before and after using it for laboratory or field measurements. The master reference electrode can be of any half-cell type (e.g., Ag/AgCl, Cu/CuSO₄, etc.), but generally speaking, the saturated calomel electrode (SCE) is considered one of the most stable half-cell chemistries that is readily available from most commercial vendors.

In order to maintain its status as master reference electrode, it should be kept and stored properly, and never used in experiments. Master reference electrodes should be replaced or verified every few years if possible.

5.1.2 Quinhydrone Electrode for Verification

Verification of a master reference electrode or any received batch of commercial reference electrodes can be accomplished with the quinhydrone electrode, which is based on the reversible redox system consisting of p-benzoquinone (quinone) and hydroquinone:



Under defined conditions, the quinhydrone electrode provides fast response times and highly reproducible potentials to within a few microvolts. Its main drawback is that it is less permanent than traditional glass electrodes such as SCE.

In addition to being highly accurate, the quinhydrone electrode has the advantage of being easily prepared in most laboratory settings. Quinhydrone can be readily procured as a reagent in equal molar ratio (1:1 complex) of hydroquinone and p-benzoquinone. By simply saturating pH 4 buffer solution with this 1:1 reagent and inserting an inert metal electrode, the quinhydrone redox half-cell can be established to serve as a verification potential. Nitrogen sweeping of the buffered solution is also recommended since hydroquinone is a reducing agent that undergoes aerial oxidation. Further details about the quinhydrone electrode and its limitations are thoroughly addressed by Ives and Janz⁹³.

⁹³ D.J.G. Ives and G.J. Janz, Reference Electrodes – Theory and Practice, 1961, Academic Press, Inc. (reprinted in 1996 by NACE International, Inc.).

5.2 Electrochemical Impedance Use for Functional Verification

Electrochemical impedance spectroscopy (EIS) is a powerful tool for characterizing electrical properties of materials and their interfaces with electronically conducting electrodes. It normally involves a small sinusoidal voltage excitation to the system at discrete frequencies while the resulting current response is measured. Alternatively, EIS measurements can consist of a sinusoidal current as the stimulus while the voltage response is measured. The frequency range that is typically surveyed in aqueous electrochemical systems is between 100 kHz and 1 mHz.

EIS data are commonly analyzed using an equivalent circuit to represent the physical system, which allows fundamental parameters such as electrolyte resistances, interfacial capacitances, and charge-transfer resistances to be obtained. However, the utility of these circuit models is restricted by the ability of the experimenter to construct an analog that is physically accurate. Despite the challenges of creating suitable circuit models, EIS still finds wide use in many applications where direct current (DC) techniques fall short of providing vital information. For example, EIS has been widely adopted in the evaluation of polymeric coating performance since it can resolve changes in the impedance as an electrolyte penetrates the coating. When EIS is used for ranking polymeric coatings, the low frequency impedance can be used as the primary figure of merit rather than trying to fit the data to an equivalent circuit.

In a similar way, EIS could be used as a diagnostic tool to detect or confirm when a reference electrode is experiencing degradation that compromises its ability to maintain a proper half-cell potential. The low frequency and high frequency impedances could simply be examined for magnitude changes rather than implementing an equivalent circuit approach to analyzing the data.

5.2.1 High Frequency (HF) Impedance Response

Performing impedance measurements on a reference electrode shifts its role to that of the working electrode, which introduces additional high frequency resistances beyond the electrolyte path between measurement electrodes. Namely, the internal fill resistance and junction resistance of the reference electrode become important factors in the high frequency domain. For reference electrodes with a double-junction construction, an additional junction resistance and fill resistance would also contribute to the measured impedances.

The high frequency impedance of a reference electrode is usually dominated by the resistance of its isolation junction(s), which is often a porous frit made of an inert material. This junction separates the reference electrode's internal filling solution from the test electrolyte. As previously discussed, a variety of junction types are used to construct reference electrodes, including ceramic frits, glass frits, polymeric frits, and asbestos threads. The Van Londen reference electrodes that are installed inside the Hanford double-shell tanks are of a single-junction construction and contain a polymeric (Kynar™) frit as the isolation junction. A slow flow of the filling solution through this junction is necessary for proper electrode operation. However, this slow flow creates a restricted flow path, which is why the junction often governs the HF impedance response of the reference electrode.

In a DNV study⁹⁴ involving the long-term performance of Van London reference electrodes in nonradioactive waste simulants, the high frequency impedance of the electrodes was monitored for approximately 1000 days. Figure 5-1 contains the potentials versus time (lower plot) and the high frequency impedances versus time (upper plot) of the reference electrodes that were exposed to various tank simulants. With the exception of one tank simulant (AW-105), it was found that the reference electrode potentials deviated significantly from the theoretical half-cell potential at some point during the test. Most of the electrodes “failed” by exhibiting a sudden, large drop in potential that that was hundreds of millivolts from the theoretical value. However, in the AY-101 tank simulant, the reference electrode deviation occurred in a more gradual manner in which the potential drifted upward with time.

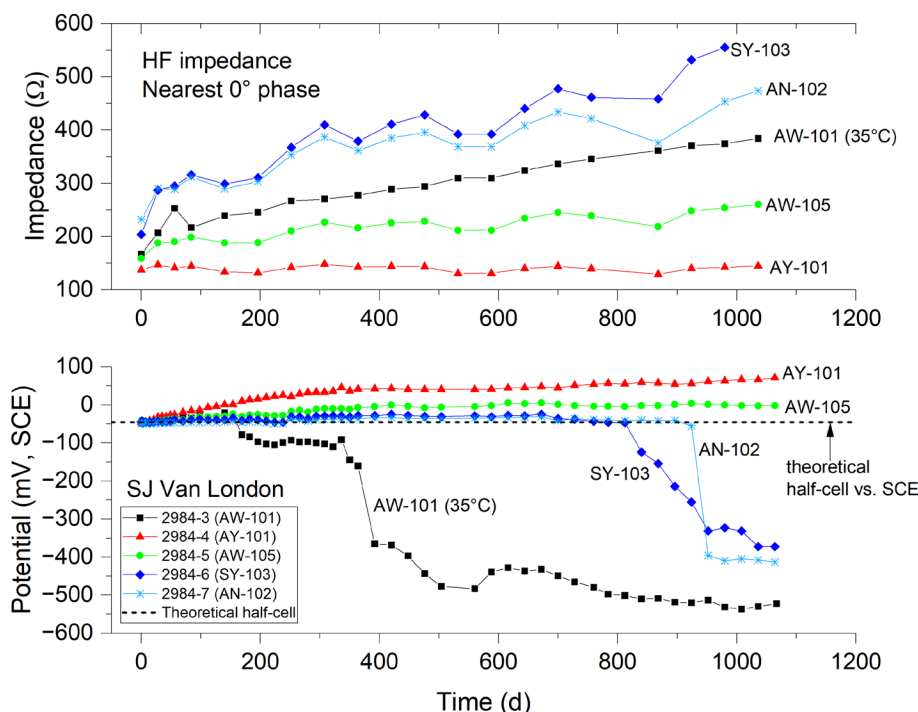


Figure 5-1. Results from 2018 study involving long-term exposure of Van London reference electrodes to various tank waste simulants: potentials vs. time (lower plot) and HF impedance vs. time (upper plot).⁹⁴

As shown in the upper plot of Figure 5-1, the HF impedance of the reference electrodes either remained flat or increased slightly with time. It was presumed that the increases in HF impedance were related to changes in the internal fill resistance, although increases in the frit resistance were not ruled out. Regardless of the exact cause, there were no correlations between HF impedance behavior and the timing of electrode failures. Despite these shortcomings, the HF impedance can still serve as a good diagnostic tool to verify that the reference electrode fill or frit is still functioning properly and providing adequate communication with the Ag/AgCl element.

⁹⁴ S. Chawla, et al., RPP-RPT-63781, FY2021 DST Chemistry Testing Report, Prepared by DNV GL USA, Inc. for Washington River Protection Solutions, LLC, May 2022.

5.2.2 Low Frequency (LF) Impedance Response

The low frequency response in most electrochemical systems consists of Faradaic processes, which involve charge-transfer resistances and mass-transfer resistances (Warburg impedances) at a conducting electrode interface. More specifically, for the Van London reference electrodes installed in Hanford double-shell tanks, the charge-transfer and mass-transfer resistances are associated with the Ag/AgCl wire element in contact with the internal fill. Since reference electrodes should ideally behave as non-polarizable electrodes, redox systems with facile kinetics or low charge-transfer resistances are desired. The Ag/AgCl redox system fulfills this characteristic by having low impedances at the low frequency end of the spectrum. Figure 5-2 shows an example of an impedance spectrum for an exemplar Van London electrode placed in 4 M KCl. The low frequency (2 mHz) impedance magnitude is around 2 k Ω , which is considered relatively small compared to the charge-transfer resistances associated with passive electrodes.

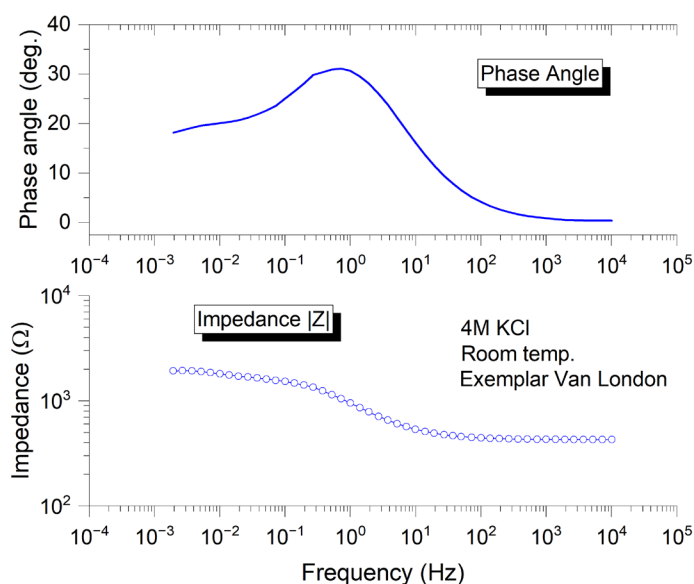


Figure 5-2. Impedance spectrum obtained on exemplar Van London reference electrode in 4 M KCl.

An increase in the impedance in the low frequency region has shown promise as a means of verifying reference electrode failure. This was demonstrated in a separate study⁹⁵ involving the long-term exposure of Van London reference electrodes in AW-101 simulant at 35°C. Figure 5-3 (*left plot*) contains the potential versus time data that were collected on a Van London electrode (SJ) immersed in AW-101 simulant for ~1000 days. After about 175 days of exposure, the reference electrode exhibited a large negative shift in potential to near -650 mV (SCE). A full-spectrum EIS scan was collected on the electrode after 529 days, which is also shown in Figure 5-3 (*right plot*). It is evident that the low frequency impedance was around 3 orders of magnitude higher compared to the exemplar electrode results. The large increase in LF impedance of the exposed reference electrode was attributed to the severe damage that was found on the Ag/AgCl wire during post-mortem examination. The wire showed major thinning and almost

⁹⁵ S. Chawla, K. Evans, S. Feng, and N. Sridhar, *Long-Term Performance of Reference Electrodes in Alkaline Radioactive Waste Storage Environments*, Corrosion Journal, 2024, **80**(5), 472-488.

complete loss of the AgCl layer, which was presumed to be due to interaction with the high hydroxide content of the waste simulant (calculated pH of 15.6).

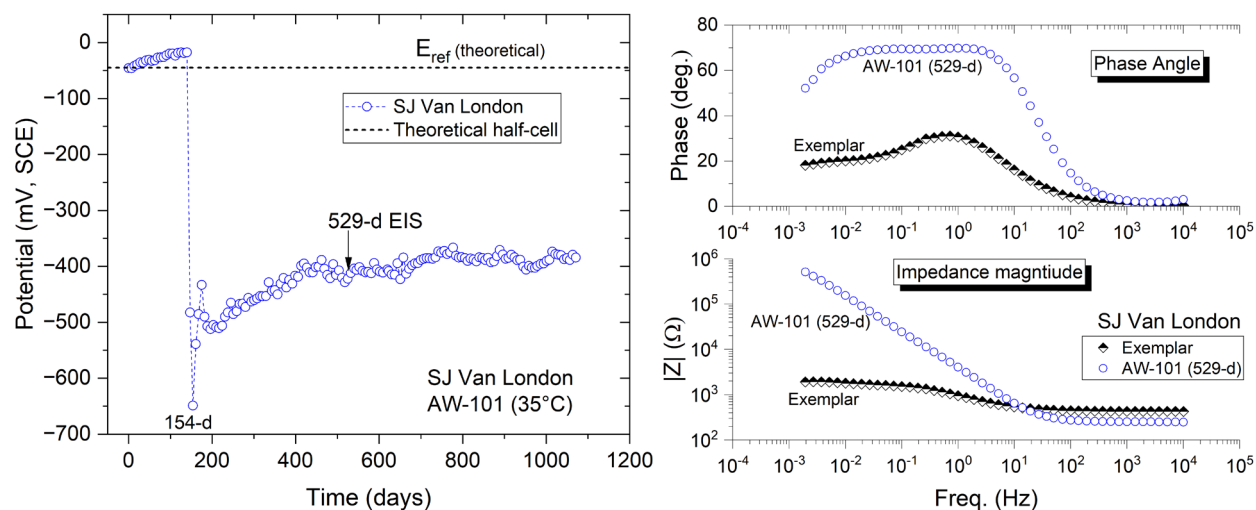


Figure 5-3. Long-term exposure of Van London reference electrode in AW-101 simulant at 35°C: Potential vs. time (left) and impedance spectrum of electrode after 529 days of exposure (right).⁹⁵

6.0 Summary

Tank corrosion and SCC can be monitored by using electrochemical techniques such as measurement of the OCP of the tank. Attempts to measure the OCP in waste tanks have been made at both Hanford and SRS. A reference electrode is typically utilized for these measurements. Failures of the reference electrodes in the chemically and radiolytically harsh environment have occurred after relatively short-term exposures. Therefore, DOE-EM has undertaken a research program to develop reference electrodes that are capable of surviving the waste tank environment for longer periods of time, such that there is increase confidence in the systems performance.

This literature review provides the following key observations about the utilization and testing of reference electrodes:

- Measurement of the OCP provides a fundamental basis for predicting long-term performance of a waste tank. This approach provides a conservative estimate of the likelihood of failure modes such as pitting corrosion and SCC.
- Key characteristics of an effective reference electrode system include: lack of sensitivity to redox species in the waste, lack of sensitivity to pH, non-polarizability, resistance to other chemical species, low impedance, electrolyte communication, chemical and radiation resistance of the electrode body, and mechanical integrity.
- Long-term (~3 years) testing of commercial Ag/AgCl under laboratory conditions show that the degradation/failure modes can be broadly classified into two types: (1) monotonic positive drift from the initial potential, and (2) a sharp drop to negative potentials after a period of relative stability. The degradation was attributable to diffusive intermixing of the internal fills of the Ag/AgCl reference electrodes with the external

simulant solutions over time through the porous frit junctions leading to extensive KCl depletion and contamination of the fills.

- The potential drift trends were correlated to Cl^- activity changes in the fill and the effects of various contaminant species originating from the waste simulants.
- Long-term studies on SJ Ag/AgCl reference electrodes in actual supernatant waste samples drawn from various DSTs also indicated that degradation of electrodes was found to be primarily due to the intrusion of aggressive chemicals causing clogging, physical and chemical degradation of AgCl, and alteration of the internal electrolyte. Radiation had less impact on electrode degradation compared to chemicals, although radiolytic species like H_2O_2 and HNO_3 could possibly have contributed to Ag wire degradation.
- Reference electrodes have been utilized at both Hanford and SRS in the past to make instantaneous measurement and for long term monitoring of the corrosion behavior of tanks. However, reference electrode failures have typically occurred within 2-3 years of installation. Trends in the potential drift that were indicative of failure of an electrode during laboratory tests correlate with those observed in the field.
- Electrochemical noise systems, another electrochemical technique, were also deployed in Hanford waste tanks to monitor for localized corrosion and SCC. Although, the technique had modest success, the utilization of the system was discontinued due to many issues related to interpretation of noise signals and interference from ambient electrical noise. Stainless steel materials for the system were robust, however, they tended to fail at EPDM gaskets. The use of a fiber re-enforced plastic body for the system also suffered significant degradation.

This literature review provides the following recommendations on materials, design and testing of future reference electrodes:

- Alternate materials of construction for the internal fill of the reference electrode include solid state Ag/AgCl CNT thread reference electrode and a solid state reference electrode using carbon nanotubes.
- Alternate materials of construction for the reference electrode frit include ion-conducting composite, porous polymer frits, and Teflon frits.
- Alternate materials of construction for the body of the electrode include polymer composites doped with sizeable amounts of high atomic number (high-Z) materials, epoxy resins, non-oxide and oxide ceramics, and carbides of transition metals.
- Additive manufacturing can use several different materials of interest for the development of the reference electrode such as ceramics, metals, and thermoplastics. It can potentially reduce the cost because it can consolidate multiple parts into one and minimize material usage by building objects up rather than cutting, molding, and combining materials.
- Various type of alternative design concepts for reference electrodes have been discussed in the literature to overcome the limitations of traditional reference electrodes. These can be broadly classified into the following categories: reference electrodes with extended diffusion lengths, reference electrodes with improved liquid junction designs, reference electrodes with flowless junction designs, ionic liquid reference electrodes, solid-contact reference electrodes, and Field Effect Transistor (FET) based reference electrodes.

- Reference electrode design development should focus on increasing the lifespan of reference electrodes by increasing the diffusion length of the internal and frit sections. Additive manufacturing may allow more flexibility and reproducibility to accomplish this objective.
- Testing protocols for the accuracy and functionality of the reference electrodes were presented. Electrochemical Impedance Spectroscopy (EIS) has been utilized in previous laboratory studies and may provide a baseline for comparison between the commercial electrodes and the newly developed electrodes.

Distribution:

SRNL

connie.herman@srnl.doe.gov
joseph.manna@srnl.doe.gov
morgana.whiteside@srnl.doe.gov
charles.james@srnl.doe.gov
pavan.shukla@srnl.doe.gov
bruce.wiersma@srnl.doe.gov
benjamin.barkai@srnl.doe.gov
kiana.sykes@srnl.doe.gov
junhua.jiang@srnl.doe.gov
camden02.chatham@srnl.doe.gov
drew.snelling@srnl.doe.gov
haley.jones@srnl.doe.gov
matthew02.williams@srnl.doe.gov
michael.stone@srnl.doe.gov

Records Administration (EDWS)

DNV

Sandeep.Chawla@dnv.com
nsridhar@mcconsult.com
John.Beavers@dnv.com
Kenneth.Evans@dnv.com
Kathleen.Sherer@dnv.com

DOE

em-labcall@em.doe.gov
ming.zhu@em.doe.gov
Kalee.Fenker@em.doe.gov

WRPS

jason_s_page@rl.gov
shawn_t_campbell@rl.gov
jason_r_gunter@rl.gov
kayle_d_boomer@rl.gov
melinda_r_fagundes@rl.gov